Pedro Tomás Martins Silva

BSc. Biology

Comparative Analysis of Locomotor Behavior and Descending Motor System Anatomy of Larval Zebrafish and Giant Danio

Dissertation submitted in partial fulfillment
of the requirements for the degree of

Master of Science in
Molecular Genetics and Biomedicine

Adviser: Michael Brian Orger, Principal Investigator, Champalimaud Foundation

Co-adviser: Adrien Paul Roger Jouary, Postdoctoral Researcher, Champalimaud Foundation

Examination Committee

Chairperson: Dr. Margarida Casal Ribeiro Castro Caldas Braga
Raporteur: Dr. André Guilherme Vilhena Valente Rodrigues da Silva
Members: Dr. Michael Brian Orger
Dr. Adrien Paul Roger Jouary

FACULDADE DE CIÊNCIAS E TECNOLOGIA
UNIVERSIDADE NOVA DE LISBOA

November, 2019

Comparative Analysis of Locomotor Behavior and Descending Motor System Anatomy of Larval Zebrafish and Giant Danio

This document was created using the (pdf)LaTeX processor, based in the "novathesis" template[1], developed at the Dep. Informática of FCT-NOVA [2].
[1] https://github.com/joaomlourenco/novathesis [2] http://www.di.fct.unl.pt

Acknowledgements

It was a pleasure and an honor to be part of the Champalimaud Research community for a full year. I want to thank Michael Orger, principal investigator of the Vision to Action Lab, for accepting me as a member of his lab and giving me the opportunity to develop such a challenging and ambitious project.

I wish to express my highest respect and gratitude to Adrien Jouary, Postdoctoral Researcher in the Vision to Action Lab, for all the support, guidance, and the constant teaching about the intricacies of behavioral neuroscience and Zebrafish. Most of what was achieved was thanks to him.

To all the other Vision to Action Lab members, thank you for everything.

A special thanks goes to the Fish Facility, whose members were tireless, always helping me with my requests. Another special thanks goes to the ABBE Facility, for helping me with the confocal imaging.

QuimTó provided hillarious laughs and random clowning, essential for a healthy mind.

Another special thanks goes for my bachelor's chemistry teacher, Ana Seca, for unending support since the first class she ever gave me.

Last but not least, thanks to my family for the support.

I wish I could have gone fishing more than I went. Fishing is the BEST! NEVER STOP FISHING!

Behavior set-ups were custom built by Adrien Jouary, with my help and always under his careful guidance.

Behavioral data analysis was done with the help of Adrien Jouary and Michael Orger.

Immunohistochemistry stainings were done with the help and guidance of Bernardo Esteves.

Image analysis and image registration was done with the help of Aaron Ostrovsky. The entire pipeline for achieving the brain template was devised by Aaron.

Backfills of reticulospinal neurons were done with help and guidance of Jens Bierfeld.

Head-restrained experiments were done with the help of Rita Félix and Elena Hindinger.

Alexandre Laborde, Adrien Jouary and Michael Orger provided the much needed coding support.

Abstract

A major challenge for comparative biology is understanding what aspects of an animal's locomotor repertoire represent general features of motor organization, versus specialized adaptations for its anatomy and ecological niche. In this thesis I investigate the Giant Danio larvae (*Devario aequipinnatus*) as a potential model for comparative studies with Zebrafish, a well-established animal model in neuroscience. To this end, I study the locomotor behavior of both species and how its differences are reflected in the underlying neural circuit structure. Initially, I compare the anatomy of the descending pathways controlling locomotion in Giant Danio to Zebrafish using retrograde labelling of reticulospinal neurons. I see a striking resemblance of the circuit in both species, with a roughly similar organization and the general division and number of cell clusters being very well conserved. Following, I compare visually guided behaviours in Giant Danio to different Zebrafish strains. Giant Danio show a stronger optomotor response than Zebrafish. The optomotor response of Giant Danio first appear around 4 days post fertilization and can be consistently and reliably evoked. During optomotor tracking Giant Danio show shorter interbout intervals and are able to track motion at higher speeds than Zebrafish. I also observe that the higher manoeuvrability of Giant Danio is also reflected during prey capture. Interestingly, Zebrafish strains derived from more recently wild-caught fish show more robust optomotor behaviour, closer to Giant Danio. Lastly, I demonstrate the suitability of using Giant Danio in a head-restrained preparation with a 3D virtual reality environment.

Combined with the potential for comparative approaches with Zebrafish, the faster development, larger neurons, and the rich behavioural repertoire of Giant Danio make it a promising model for neuroscience.

Keywords: Giant Danio; Zebrafish; Behavior; Reticulospinal neurons; Comparative approach

Resumo

Um grande desafio para a biologia comparativa é compreender que aspetos do reportório locomotor de um animal representam características gerais de organização motora ou adaptações especializadas para a sua anatomia e nicho ecológico. Neste trabalho, investiguei se o peixe *Devario aequipinnatus* (*D. aequipinnatus*) é um potencial modelo para estudos comparativos com o Peixe-zebra, um modelo bem estabelecido em neurociência. Para tal, comparei o comportamento locomotor e a estrutura neural subjacente das duas espécies, começando por estudar a anatomia das vias neurais descendentes que controlam a locomoção no *D. aequipinnatus*, usando uma marcação retrógrada de neurónios reticuloespinais. Verifiquei uma grande semelhança do circuito em ambas as espécies, tanto quanto à organização, como à divisão geral e número de aglomerados de células. Seguidamente, comparei comportamentos mediados pela visão no *D. aequipinnatus* com o de diferentes linhas de Peixe-zebra. O *D. aequipinnatus* mostrou uma resposta optomotora mais robusta do que o Peixe-zebra. Em relação à resposta optomotora do D. aequipinnatus, esta aparece aos 4 dias pós-fertilização e é provocada de forma consistente e confiável. No geral, a natação do *D. aequipinnatus* apresenta intervalos curtos entre cada movimento da cauda que lhe permitem seguir padrões de estimulação a velocidades mais elevadas que o Peixe-zebra. Observei também que a maior manobrabilidade do *D. aequipinnatus* se refletia durante o comportamento predatório. Linhas de Peixe-zebra derivadas de peixes capturados mais recentemente no seu habitat natural e, como tal, mais selvagens, mostraram maior robustez no comportamento optomotor, sendo a sua resposta optomotora mais parecida com a do *D. aequipinnatus*. Por fim, demonstrei que o *D. aequipinnatus* se adequa a utilização em experiências com preparações onde a cabeça é fixa e o peixe é colocado num ambiente tridimensional de realidade virtual.

Combinando o seu potencial para abordagens comparativas com Peixe-zebra, ao seu desenvolvimento mais rápido, neurónios maiores e um reportório comportamental rico, o *D. aequipinnatus* apresenta-se como um modelo promissor para a neurociência.

Palavras-chave: Devario aequipinnatus; Peixe-zebra; Comportamento; Neurónios reticuloespinais; Biologia comparativa

Contents

List of Figures

Acronyms

AF	Arborization fields.
BSA	Bovine serum albumin.
CMTK	Computational Morphometry Toolkit.
CNS	central nervous system.
CV	Coefficient of variation.
DMSO	Dimethyl sulfoxide.
dpf	days post fertilization.
EDTA	Ethylenediaminetetraacetic acid.
FPS	Frames per second.
HD	High Definition.
IBI	interbout interval.
ICI	intercapture interval.
IR	infra-red.
ISI	interstimulus interval.
LED	Light-emitting diode.

llf	lateral longitudinal fasciculus.
M-cell	Mauthner cell.
mlf	medial longitudinal fasciculus.
MW	Molecular Weight.
NGS	normal goat serum.
nMLF	nucleus of the Medial Longitudinal Fasciculus.
OKR	Optokinetic response.
OMR	Optomotor response.
PBT	Phosphate buffer solution with 0.25 % Triton.
PTU	1-phenyl 2-thiourea.
RGC	Retinal ganglion cell.
Ro	rhombomere.
SEM	Standard error of the mean.
STD	Standard deviation.
tERK	total ERK.
Tu	Tübingen.
ZBB	Zebrafish Brain Browser.

Chapter 1

Introduction

In this chapter I address fundamental aspects of this work. First, the importance of a comparative approach in neuroscience is detailed. This approach can expand our capacity to fully understand the significance of results in research. Next, an overview of the most common fish model organisms used in neuroscience is made, later focusing in the Zebrafish. Special attention is given to its visually evoked behaviors and locomotor repertoire. Finally, Giant Danio is introduced and the main goals and workflow of this project are described.

1.1 Comparative Approach in Neuroscience

When studying the neural basis of behavior, the traditional neuroethological approach was to identify the organism most suited to address the biological question of interest [1]. Usually this was an organism highly specialized in a particular task, for example, the study of prey localization in the barn owl [2], or auditory timing in the bat [3]. Such way of conducting research brought foundational discoveries upon neuroscience throughout the years [4]. For instance, *Aplysia* was used to study the learning and memory because of the easily identifiable and accessible neurons that mediate these behaviors [5], or the lamprey, which was used to study basic neural circuits that coordinate the generation of different patterns of motor behavior, known as central pattern generators [6].

With the advent of the genomic revolution there has been a clear convergence in the animal models used; the vast majority of neuroscience now focuses on what are now known as "standard model organisms"[4, 7]. These standard model organisms were originally chosen for their low maintenance costs and their breeding patterns, which were important for fields such as genetics and developmental biology, instead of being chosen for any specific behavioral trait or specialized function [8, 9]. The benefits of this led to

the rapid development of a wide range of tools that facilitate a detailed interrogation of neural circuits [4, 7]. But by converging on standard model species, it may not be feasible to address the diversity of mechanistic and functional adaptations present in even closely related species that may differ behaviorally [10]. Additionally, the generalization of scientific findings, derived from a set of standard model organisms, will require replication of the results beyond those species. And so, in the absence of comparative studies that harness comparative data, *"an entire field may be lead astray by observations that are either species specific or misinterpreted"* [4].

One of the longstanding goals in neuroscience has been to identify generalizable mechanisms that may shed light on functions and dysfunctions of the brain. On top of that, studying familiar functions across a diverse set of relevant species is a core concept of the comparative approach that could be embraced in order to achieve such generalizable mechanisms [7, 11]. Comparative studies are useful not just because of the potential diversity of behaviors that could be studied, but also because they allow us to discover what aspects of the system are fundamental, what is consistent across species versus specialized adaptations [12]. A good example of this is the jamming avoidance response in the electric fish *Eigenmannia sp.* and *Gymnarchus sp.* [13], which evolved their electric sense independently, but the neural circuits where the amplitude and phase information coding neurons lie turned out to have the same functional cell types and computations, even though in some cases they are localized in different brain areas; the jamming avoidance response consists on the modulation of the frequency of the produced electric signal, in order to avoid interference, leading to electrolocation inhibition, with another electric field produced by other fish. Besides allowing for the discovery of novel adaptations, with potentially bigger impact, the comparative approach also brings forth relevance when comparing systems across models of different complexity, and validity of major scientific statements made from standard model organisms [7, 10, 12, 14]. Additionally, the neuroscience community would benefit from the interplay between standard and nonstandard model organisms [4, 7]. Finally, for as many studies that use standard model organisms with great results achieved, resorting to a comparative approach could improve even further our capacity to fully understand the significance of the results.

1.2 Fish in Neuroscience

The most diverse class of vertebrates on Earth is the fish. Despite this diversity, and although there are increasing numbers of works done with fish, particularly with Zebrafish, fish still remain a largely untapped resource for comparative analyses of neural circuits and behavior, with the potential to bring new insights to questions about how the brain of vertebrates functions [12]. Considering the practical advantages that come with them – high throughput, fertility, developmental speed, amenability to genetic manipulations and relative simplicity of the nervous system – they did not go unnoticed in neuroscience. Studying fish also brought the opportunity to compare functions of neurological systems

in multiple lab strains [15].

The majority of the studies done with fish have been done on adult fish, and although the methods that exist now are amenable to larval fish, relatively little, outside of Zebrafish, is known regarding larval fish. In neuroscience, different fish models seemingly show up every day and are used for a variety of different questions. This diversity in model organisms provide rich research territories for those that are willing to go off the boundaries of the standard models and risk larger workloads for the chance of novel outcomes.

Here, I will discuss the fish models that are most used in neuroscience research. Besides Zebrafish, some common fish used in neuroscience are the Medaka (*Oryzias latipes*), Danionella (*Danionella translucida*) Three-spined Stickleback (*Gasterosteus aculeatus*), Tilapia (*Astatotilapia burtoni*), Mexican Cavefish (*Astianax mexicanus*) and the Goldfish (*Carassius auratus*). Medaka has been an important model for understanding the oculomotor function as well as neurotransmitter systems [16, 17]. Danionella is a highly promising emerging model; it owns the smallest known adult vertebrate brain and is transparent even as an adult making it especially useful for investigating vertebrate neural connectivity, brain function and behavior repertoire [18]. The Three-spined Stickleback has had major applications in behavioral neuroscience with regard to studying behavioral syndromes such as aggression-boldness [19, 20]. Studies on Tilapia are largely focused on behavioral neuroscience, in particular social hierarchy, social interactions, and aggression aspects of behavior, and just like Medaka, for understanding neurotransmitter systems [21, 22]. The Mexican Cavefish, also known as Mexican Tetra, has also been a model for behavioral neuroscience, where it was used to model neural bases of multiple behavioral changes, social behavior, and aggressiveness [23, 24]. Lastly, the Goldfish is one of the most used models. Goldfish have seen wide use as a model organism for both behavior – aversive conditioning, anxiety, fear and stress – as well as unravelling the retinal projections and neurotransmitter systems [15, 25, 26].

1.3 Zebrafish as a Model Organism

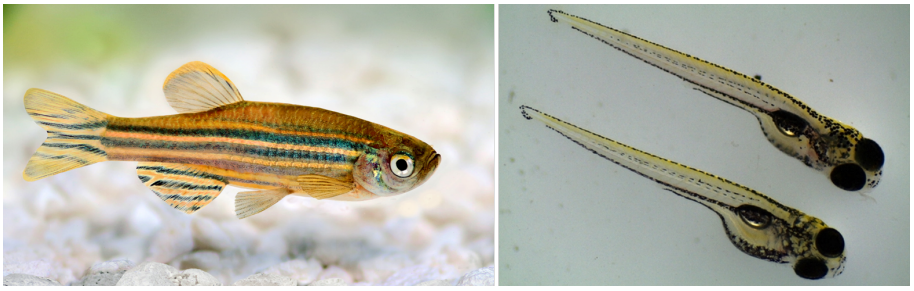

Figure 1.1: Left: Adult Zebrafish, Adapted from: Hines-UW, S (2014, November 12). *Timing can take the stripes off a zebrafish.* Retrieved from https://www.futurity.org/wp/wp-content/uploads/2014/11/zebrafish_1170.jpg ; Right: 4 dpf Tu Zebrafish larva.

Zebrafish (fig. 1.1), *Danio rerio*, is a small danionin (designation given to fish belonging to the danio and devario clades) teleost fish from the cyprinid subfamily Danioninae (Teleostei: Ostariophysi: Cypriniformes). Native to the streams of South-eastern Himalayan region [27], Zebrafish are pelagic and accustomed to living in slow-moving waters from rice paddies and slower reaches of streams, to rivers and lakes [28]. Because this small fish is easy to maintain in the laboratory, has low maintenance costs, low space requirements, a fast generation time and rapid reproductive cycle, produces clutches with over 100 embryos per mating pair with external development, and larvae transparency, it has been used for developmental and genetic studies since the late 1950s in a cost-efficient manner [29, 30]. By the 1980s, Zebrafish was already used as a genetically tractable organism [31–33]. Although Zebrafish stands far, phylogenetically, from humans (fig. 1.2), this species still shares 70% homology with human genes and have 10660 genes in common with chicken, mouse and human [34, 35]. Moreover, Zebrafish have a similar basic structure of central nervous system (CNS) morphology to other vertebrates, with all the major domains that are found in the mammalian brain. Additionally, its larval stages offer an unprecedented optical access to their CNS [35–38].

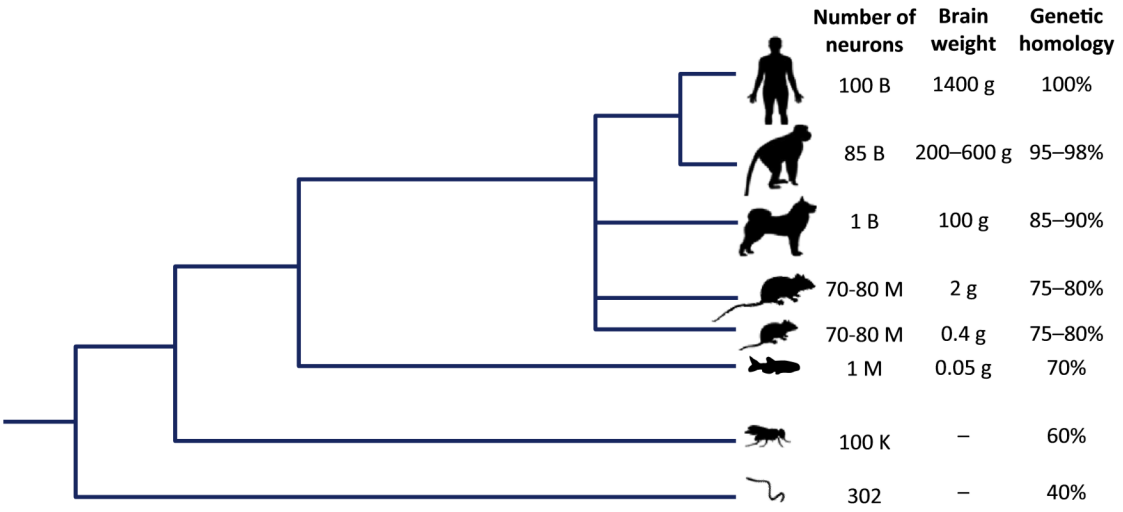

Figure 1.2: Although phylogenetically distant from humans, Zebrafish still shares 70% homology with human genes. Furthermore, its reduced brain size allows unprecedented optical access to their CNS in larval stages, while maintaining a similar basic structure of the CNS. Adapted from Stewart et al., 2014 [35].

Nowadays, with the most recent technical developments, including the ability to make precise genetic manipulations [39–41], the Zebrafish became an important tool for translational research [42]. The availability of large libraries of mutant and transgenic fish allow researchers to target specific cell types or provide vertebrate models of human neurological, neurodevelopmental and neurodegenerative diseases such as Alzheimer's, Parkinson's, epilepsy or autism [35, 38, 43–46]. Furthermore, larval Zebrafish, owing to their small brain size and optical transparency providing access to the CNS, has become an attractive model for optical imaging of brain development and function [47, 48]. Coupled with state-of-the-art optical imaging methods and optogenetic tools, Zebrafish

is growing as a vertebrate model for systems neuroscience as well. Some of the techniques that have been recently used include Two-Photon Scanning Microscopy, Selective Plane Illumination Microscopy, and Light-Field Microscopy. These approaches can simultaneously monitor brain activity over large regions, potentially even the whole-brain dynamics [49].

The currently available microscopy techniques, complemented by the continuously growing and extensive genetic modifications toolbox possible in Zebrafish, provide ways of reporting neuronal activity or directly controlling that activity with light. Optogenetic actuators such as channelrhodopsin induce or suppress neuronal activity in response to light, and upon expression in Zebrafish neurons, allow researchers to probe the causal role of neuronal activity in selected populations of neurons [50]. Similarly, optogenetic reporters such as GCaMP, a genetically encoded calcium indicator that changes its fluorescence properties in response to the binding of Ca^{2+}, can be expressed in selected populations of neurons in the fish's brain. Neurons fire action potentials, this opens voltage gated calcium channels that lead to large influx of Ca^{2+} into the cells. GCaMP's fluorescence increase upon calcium binding allows one to visually capture neuronal activity through the fluorescence changes in selected populations of neurons [51].

In contrast to other animal models such as mice or rat, these manipulations are performed in a non-invasive fashion, without the need for surgery or anesthesia, requiring only the larva to be head-restrained in agarose, leaving the eyes and the tail free to move [30]. Ultimately, the small size of the brain in comparison to the field of view of available imaging methods and optical accessibility paired with the ability to simultaneously monitor sensory and motor areas in the behaving larvae make Zebrafish an ideal model for the holistic approach on how the brain generates behavior [48]. From an ethological point of view, the zebrafish shows more advantages as an animal model to study behavior related questions. Those advantages are best seen in the larva's visually driven behaviors, as described in the next section.

1.4 Visually Evoked Behaviors in Larval Zebrafish

The visual system develops extraordinarily fast in the Zebrafish embryo. Considering the external embryonic development, there is a strong evolutionary pressure for rapid development of functional sensory systems [52]. In particular, vision is critical to their survival, allowing them to feed, navigate and avoid predators [53]. Innate visually guided behaviors begin to appear at just 3 days post fertilization (dpf), after Retinal ganglion cell (RGC) axons reach and innervate the tectal neuropil [54, 55]. These behaviors can be: phototaxis; two responses to visual motion, the Optokinetic response (OKR) and the OMR, where in the first they move their eyes and in the second they swim to follow a motion pattern; a visual startle response, prey capture and visually evoked escape.

Phototaxis represents one of the simplest forms of taxis behavior. In phototaxis, a fish will try to reach a desired location on the environment, according to the incidence

of light. Zebrafish larvae older than 3 dpf show phototactic behavior [52], seeking out lighter areas by adjusting their swimming behavior according to light variation and based on temporal and spatial cues [56–58]. Moreover, this phototactic response illustrates how a complex behavior transpires from simple behavioral rules. This phototactic behavior can be reproduced by a simple model in which the retinal OFF pathway, sensitive to the decay in lighting deploys contralateral turns and drives turning away from the darker side, and the ON pathway, active following an increase in light intensity and controlling the rate of approach by activating forward swims, stimulates approach [59].

The OKR first appears at 3 dpf [55] when a focused image can first be formed on the retina and the extraocular muscles have finished adopting their adult configuration, and persists throughout adulthood. Additionally, only at 3 dpf all 10 RGC Arborization fields (AF) are first innervated [60]. OKR is evoked by whole-field motion patterns, which give the perception of motion to the fish relative to fixed landmarks [54]. It is a robust visual stabilization behavior based on stereotyped tracking eye movements that are elicited when objects move across the visual field in order to reduce retinal image motion and thus obtain visual stabilization. It consists mainly of two components: a smooth pursuit (slow eye movements) followed by a fast saccade which resets the eyes once the object has left the visual field [55]. Also, the OKR requires circuits distributed throughout the brain involving connections from optic flow sensitive neurons in the pretectum to motor neurons controlling the eye muscles [61]. Due to its reliability, and the fact that larvae will perform it even when fully immobilized, the OKR is one of the more widely studied behaviors in zebrafish [62].

In larval Zebrafish, the OMR is present as early as 5 dpf, when the retina has developed enough to further support this behavior which requires the ability to see a pattern [52], and is maintained in adulthood [63]. Just like the OKR, the OMR is a visual stabilization behavior in response to whole-field motion, but in this case the fish will turn and swim in the direction of the perceived motion [64]. When presented with moving stimuli, Zebrafish larvae were seen to be able to adjust their average speed to match the stimulus [65], and even adapt their response gain based on visual feedback [49, 66]. The OMR consists of a set of basic motor components tuned to motion direction: the fish will perform forward swims driven by forward motion and turns driven by lateral movement [67]. Furthermore, it relies on contralateral relay of information from the RGCs to an arborization field in the pretectum, and from there ipsilaterally to reticulospinal neurons (which relay information form the brain to the spinal cord), in particular the nucleus of the Medial Longitudinal Fasciculus (nMLF), which in turn send direct motor response to the spinal cord through descending glutamatergic inputs [65, 68].

As in the OMR, in larval Zebrafish hunting and feeding starts at 5 dpf, when the retina has developed enough to support this behavior (allowing visual recognition) and their yolk supply has been mostly depleted [52]. Prey capture is a critical behavior for survival that relies on a complex sequence of movements. Initially, larvae have to do visual recognition of the prey. Following this recognition, two distinct phases take place

in prey capture behavior: an initial orientation and approach phase, during which the larva converges its eyes and maneuvers, through slow swims and J-turns (see Zebrafish Locomotor Repertoire section), in order to fit the prey into the newly formed binocular zone, and a capture phase, where a capture-swim is triggered once the prey is positioned at a correct location in front of the fish [69–71]. During prey capture, neurons in AF7 receive input from RGCs and project to the optic tectum, nMLF and the hindbrain [72]. Although in later larval stages larvae may use other sensory inputs to hunt [73], in early stages larvae mostly rely on vision to capture prey, as demonstrated by the dramatic decrease in the number of prey eaten in the dark [74].

The visual startle response has been described as first appearing around 3 dpf, when the larva is presented with sudden changes in illumination [54]. This response consists of an abrupt movement, often from a large angle turn, triggered from a change in the stimulus – illumination changes (i.e if it is changes in light intensity, or a dark flash) [57]. Turns evoked by light are kinematically indistinguishable from routine turns (see Zebrafish Locomotor Repertoire section), while those evoked by dark flashes appear to form a O-bend (see Zebrafish Locomotor Repertoire section) which was shown not to require the Mauthner cell (M-cell), distinguishing this response from the faster C-bend escape responses [62].

Visually evoked escape, in Zebrafish larvae, is an escape response to what, in a natural environment, would be a predator or any larger fish or object closing in that could represent a threat. This behavior can be elicited in a stereotyped manner with a looming stimulus, normally an expanding dark dot in a bright background [75–79] projected from below [76] or from the side [78]. This escape response is evoked when the stimulus has neared the fish to a point that it creates a "critical visual angle", with a fixed lag or waiting period, in relation to the looming stimulus critical visual angle [75, 76]. The escape motor circuits, based on the M-cell and its homologs, are then stimulated by tectal neurons capable of relaying information regarding the critical visual angle [76]. In terms of kinematics, the Zebrafish larvae performs a fast C-bend [78], characteristic of escape responses [62].

Through the presentation of different sets of stimuli, projected below, laterally or in 3D environments, these behaviors can be elicited in both freely swimming and head-restrained Zebrafish larvae. In those conditions, a reproducible set of larval swim types (locomotor repertoire) has already been identified and characterized [79]. That locomotor repertoire will be discussed more fully below.

1.5 Larval Zebrafish Locomotor Repertoire

Zebrafish larvae propel themselves through patterns of body undulations consisting largely of the curvature of the tail – tail oscillation – in the horizontal plane. In addition, the larva aids its swimming using rotations of the eyes and movements of the two pectoral fins. Freely swimming Zebrafish navigate in 3D environments, express their

behavior throughout the whole water column. But with Zebrafish larvae, experimentally reducing their behavior into a 2D plane, by confining them into shallow waters, allows for behavior to be easily recorded with a single camera without any stereoscopic vision tools.

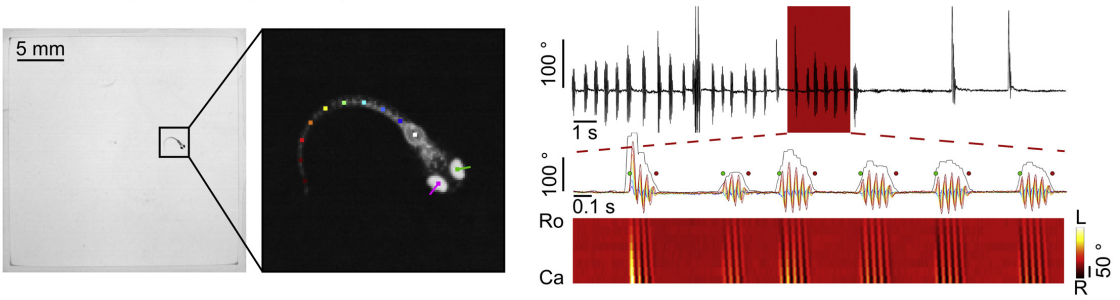

Figure 1.3: Zebrafish larvae locomotion can be divided into single events, the swim bouts, characterized by short bursts of tail movement that propel the larvae, followed by interbout periods where larvae move passively through the water. Left: Tracking of position, eyes and tail of Zebrafish larva. In order to be able to detect the bouts, it is necessary to track the larva; Right: Detection of the swim bouts from a tail end angle trace. Adapted from Marques et al., 2018 [79].

Once the larva has been confined to a movement in a single 2D plane, its movements can be segmented into elementary and discrete units that proceed through time. Zebrafish larva swim in a "burst and glide"fashion, characterized by swimming in short bursts of tail movement that propel the larvae, called swim bouts (fig. 1.3), followed by interbout periods where the larvae moves passively through the water [79]. These swim bouts can last between 80 to 400 milliseconds, with beat frequencies between 30 and 100 Hz [81]. Bouts follow an organization in sequence that enables larvae to carry out goals at longer timescales, including exploration of the environment [82] or precise control of speed [65]. And so, thanks to this discrete nature of locomotion, the quantification of behavior is greatly facilitated [83].

From 3 dpf to 4 dpf, Zebrafish larva go through a developmental switch, where their bouts change from isolated and long immature locomotor patterns, to shorter and more mature locomotor patterns with a short interval in between them [84] that allows the fish to sustain an active freely swimming behavior. Zebrafish larvae as young as five days post-fertilization already exhibit a rich repertoire of innate behaviors that enable them to explore the world [85, 86]. Observing the examples in Figure 1.4: (A) larvae can maintain their position in a changing environment with slow swims [64, 65]; (B) they can capture prey [69, 71]; (C) they avoid other larvae [79]; (D) and they escape from threatening stimuli [57, 76, 87, 88]. Furthermore, a total of 13 different bout types have been recently identified and characterized, acquired across a wide range of stimuli and related to different behaviors [79]. This rich behavior repertoire makes zebrafish larvae an attractive model organism to study in laboratory conditions.

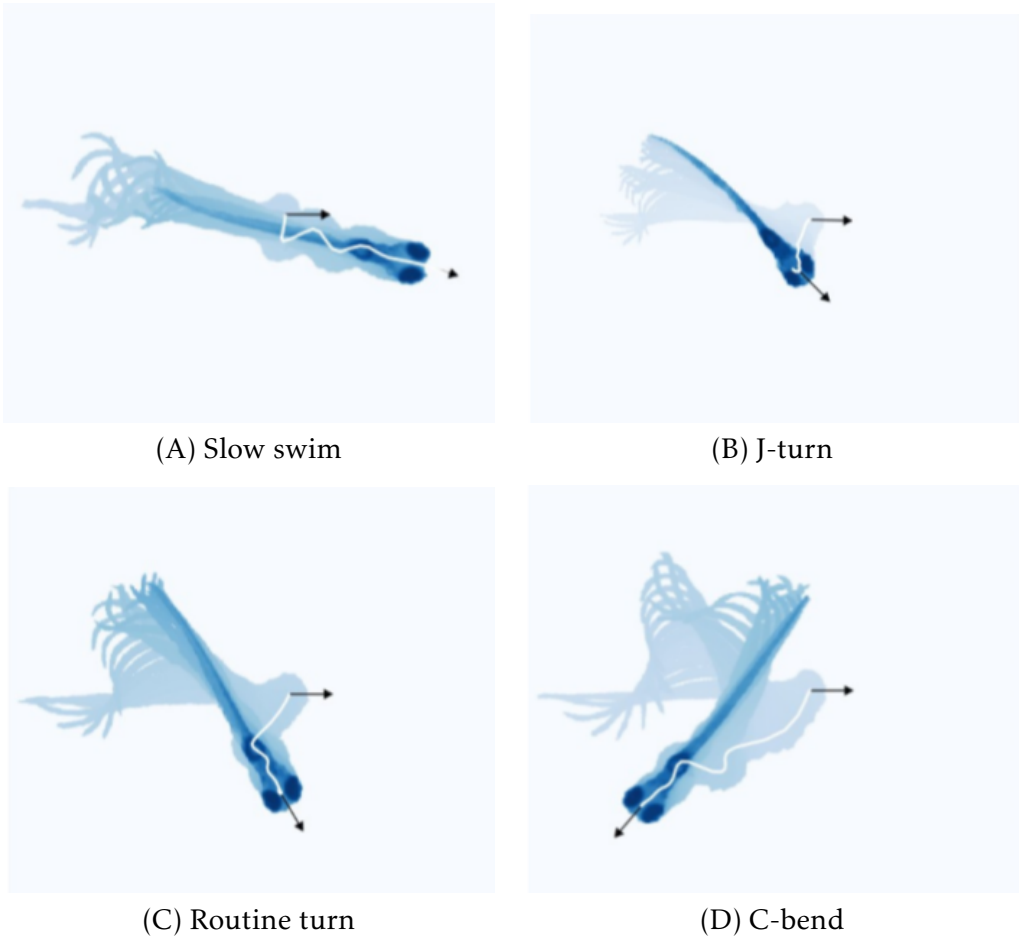

(A) Slow swim (B) J-turn

(C) Routine turn (D) C-bend

Figure 1.4: Example of a Zebrafish larva stereotyped swim bouts by super-imposing images of the larva's body as it moves. Head trajectory is shown by the white line and the orientation of the head at the beginning and end of the bout is represented by the black arrows. Adapted from Romano et al., 2015 [80]. (A) Low tail bend and beat frequency. (B) Fine reorientation turn achieved by a strong bend at the caudal region of the tail, associated with prey capture. (C) Reorientation turn characterised by its slow speed, large bend angle and, in most cases, unilaterality. (D) Turn associated with predator avoidance behaviors that relies on the Mauthner cells, characterised by its high-velocity and short duration. Named after the C shape the larva's body generates at the beginning of the movement.

1.6 The Giant Danio

Giant Danio (fig. 1.5), *Devario aequipinnatus*, is a danionin teleost fish from the cyprinid subfamily Danioninae (Teleostei: Ostariophysi: Cypriniformes) [89, 90]. Native to India, Nepal and Sri Lanka [27], and also found in Bangladesh [91], this species is pelagic and accustomed to living in small streams and rivers with fast water currents [28]. It is the largest of all the danionin species, displaying a size markedly greater than that of the Zebrafish, in which the adult can grow up to 15cm in length [92].

Following on the footsteps of the Zebrafish, Giant Danio also show some of the main advantages of a valuable research model as in being easy to maintain in the laboratory with low maintenance costs, a rapid reproductive cycle [93, 94], large clutches with over 2000 embryos per mating pair [95], external development, small larvae size and

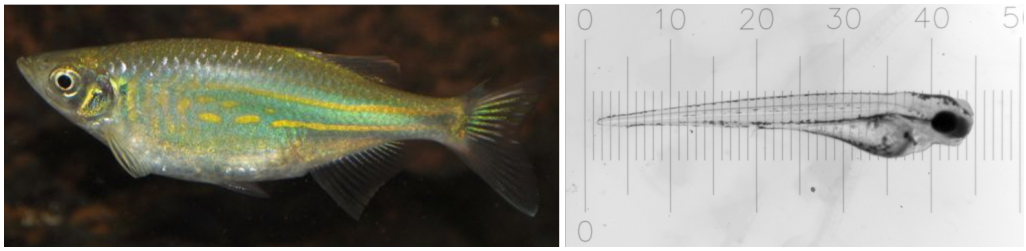

Figure 1.5: Left: Adult Giant Danio, Adapted from: Rudloff, K (2013, June). *Devario aequipinnatus*. Retrieved from https://www.biolib.cz/IMG/GAL/214411.jpg ; Right: 3 dpf Giant Danio larva, Photo credit: Champalimaud Research Fish Platform.

larvae transparency [96]. Furthermore, the phylogenetic proximity to Zebrafish make the Giant Danio a strong candidate not only for a valuable research model, but as well as for enabling comparative approaches with Zebrafish [28, 89, 90].

The Giant Danio has been used as a model for a multitude of different studies in various fields of research. The most recent works with this model encompass the fields of pharmacokinetics [97], ecotoxicology [98, 99], community ecology [100], developmental biology [94, 101, 102], conservation [103] and social behavior [104]. Other works that should be mentioned, with this species as model organism, covered major topics like electrophysiology, in retinal bipolar cell input mechanisms [105–107], and even research facilities management, specifically in the expansion of the *Pseudoloma neurophilia* known host range in different fish models kept in research facilities [108].

Considering the phylogenetic proximity to Zebrafish, the different body size and the fact that, although they may share habitat with Zebrafish, they are normally found in particular environmental conditions (faster water currents), the Giant Danio was chosen as a non-standard model organism for this comparative approach.

1.7 Objectives

Week-old larval Zebrafish (*Danio rerio*) already exhibit a diverse array of sensory driven behaviors that allow them to explore their environment, hunt prey and avoid predators. To study each one of these behavioral traits, the Orger Lab has developed an automated system for real-time behavior analysis at high spatial and temporal resolution. By using an unsupervised clustering method they identified 13 basic movements that the Zebrafish use when swimming [79]. Additionally, these movements are controlled by a stereotyped array of brainstem reticulospinal neurons. Understanding how generalizable the relationship between the behavior, the anatomy and the structure of the underlying neural circuits is in similar organisms, and in relation to what is known in Zebrafish, may provide foundations for future work in neuroethological research. Thus, in this work we followed a comparative approach and applied a systematic analysis to the behavior of a related fish species, the Giant Danio (*Devario aequipinnatus*), to try to answer three main questions: i) Do both species have similar locomotor characteristics? ii) Do Zebrafish and

Giant Danio have similar underlying motor system structure? iii) Will differences in the underlying motor system structure reflect differences in visually guided behaviors? To try and answer those questions, the following goals where set: Initially, i) characterize the descending reticulospinal neurons in the Giant Danio using retrograde labelling with dextran-conjugated dyes and confocal imaging, and identify identical/different structures from the Zebrafish; ii) record high-speed movements of Giant Danio and Zebrafish larvae and compare their locomotor performance in different behavior assays; lastly iii) apply the lab algorithms to the behavioral recordings data in order to identify basic swimming kinematics of the Giant Danio.

Chapter 2

Methods

In this chapter, all experimental procedures and sources of materials are presented. In brief, protocols for handling the animals, label spinal projecting neurons and do the imaging are detailed. Following, the different behavioral set-ups used, as well as the design of the behavioral assays and how the analysis of all acquired behavioral data underwent are described in detail. Lastly, how the larvae are tracked, while they swim during the experiments, and their bouts detected is briefly explained.

2.1 Experimental Models Rearing Conditions and Subject Details

Adult Zebrafish and Giant Danio were maintained by the vivarium platform at Champalimaud Research. These species are photoperiodic in their breeding and spawning tends to occur at the onset of daylight. Therefore, breeding pairs were set overnight the day before in a female-to-male ratio of 2:1 in breeding tanks. The following day, fish were returned to the system during the morning as soon as spawning was confirmed. Embryos were collected and reared at 28°C in E3 embryo medium (5 mM NaCl, 0.17 mM KCl, 0.33 mM $CaCl_2$ and 0.33 mM $MgSO_4$), with pH and salinity kept in physiological conditions [109]. Larval density was established at 15 Giant Danio or 20 Zebrafish per 90 mm petri dish. Larva were kept on a 14h/10h light/dark cycle. E3 embryo medium was changed daily until feeding started. Once feeding commenced, embryo medium was changed twice a day, always prior to feeding. Giant Danio were fed with rotifers (*Brachionus sp.*) after 4 dpf and Zebrafish after 5 dpf. From 8 dpf and 11 dpf, respectively, Giant Danio and Zebrafish were fed with *Artemia salina*. For experimental procedures where fish were raised past 8 dpf and up to 14 dpf, larger 150 mm diameter petri-dish were used.

Despite their similarities, Giant Danio have some small differences from Zebrafish

when it comes to optimal rearing conditions. Those differences were mostly reflected in small changes on conductivity values [95] from Zebrafish. While efforts were made to optimize the breeding conditions for the Giant Danio larvae during our experiments, larvae from both species were raised in the same embryo medium and we did not observe any problems with growth and viability of Giant Danio larvae under these conditions.

Three Zebrafish strains were used: Tübingen (Tu), Anju and 5D. Rearing conditions were the same for all strains. These strains were chosen so that the behavior of a commonly used inbred strain (Tu) could be compared, performance-wise, to Zebrafish strains derived from more recently wild-caught fish. These strains derived from more recently wild-caught fish could potentially show more robust behavior responses.

For experiments involving the growth trajectories of the larvae, both Tu Zebrafish and Giant Danio larvae were reared in the same conditions but kept at a density of 4 per petri-dish. For backfills and confocal imaging with Giant Danio, the E3 embryo medium was changed to a 0.003 % w/v solution of PTU (1-phenyl 2-thiourea) in E3 embryo medium 8 to 9 hours post fertilization to prevent the development of pigmentation. The PTU solution was then changed daily; other rearing conditions were kept the same.

All experimental procedures and animal handling were approved by the Champalimaud Foundation Ethics Committee and the Portuguese Direção Geral de Alimentação e Veterinária and were performed according to the European Directive 2010/63/EU.

2.2 Fish growth

To measure larvae growth throughout development, larvae of each species were raised in sets of 4 until they were 14 dpf. A total of 8 larvae from Giant Danio and Tu Zebrafish were raised for growth measurements. From 4 dpf onwards, pictures of each larva were taken daily, for a total of 10 images per fish. Pictures were taken from above with a custom-made high-resolution imaging set-up, using an infra-red (IR) sensitive camera (MC1362, Mikrotron). The larvae swam freely in a custom-made acrylic transparent circular arena (Annex I.1) with a 25 mm diameter and 2 mm depth, illuminated by a custom-made 10x3x10 cm Light-emitting diode (LED) backlight (850 nm) placed below the larvae arena. The fish were imaged between 12:30h and 13:30h on each day. Image analysis and total length measurements were made using a custom MATLAB (Mathworks, USA) script (Annex I.6). All daily measurements were then averaged in order to plot a growth curve including the Standard deviation (STD). In order to compare total length variation in both species, the Coefficient of variation (CV) for every age was calculated.

2.3 Retrograde Labeling of Reticulospinal Neurons in Giant Danio

Retrograde labeling (backfills) of the reticulospinal neurons in Giant Danio was performed following a protocol adapted from Ma and colleagues [110] and Lu and colleagues [111]. 5 dpf larvae were put on a 5 % agarose base and excess medium was removed to restrain larvae movement. A 1 % w/v solution of Texas Red-Dextran conjugate (3000 MW, Lysine Fixable, Invitrogen) in Zebrafish external solution (134 mM NaCl, 2.9 mM KCl, 2.1 mM $CaCl_2$, 1.2 mM $MgCl_2$ and 10 mM HEPES glucose, pH 7.853) was pressure injected with a micro-manipulator into ventral spinal cord, targeting descending axon tracts at the fifth and seventeenth myotome level, transecting the cord and overlaying muscles dorsal to the notochord (fig. 2.1). Dye application was done through a needle made from a GC100F-10 glass capillary (Harvard Apparatus) using a micropipette puller P-2000 (Sutter Instrument). After the injection, larvae were left in E3 embryo medium at 28°C overnight to allow retrograde filling of reticulospinal neurons. On the following morning, 6 dpf larvae were screened for positive labeling of the reticulospinal neurons under an Axio Zoom.V16 fluorescence microscope (Zeiss). The specimens with the most extensive labeling were selected for fixation. Larvae were sacrificed with tricaine 1.6 mg/ml, followed by fixation in 4 % paraformaldehyde during two hours at room temperature and finally washed in Phosphate buffer solution with 0.25 % Triton (PBT) [112].

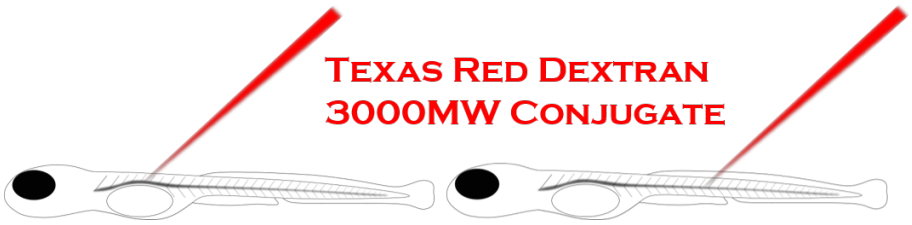

Figure 2.1: Representation of the Giant Danio backfills. A solution of Texas Red-Dextran conjugate (3000 MW) in Zebrafish external solution was pressure injected into the ventral spinal cord. Injections were done in two different places, one more rostral (left side), near the 5^{th} myomere, and one more caudal (right side), near the 17^{th} myomere.

2.4 tERK immunohistochemistry staining

After fixation, retrogradely labelled Giant Danio larvae with extensive labeling were processed for whole-mount immunohistochemistry staining. The protocol was adapted from Randlett and colleagues [113].

Whole larvae were subjected to heat-induced epitope retrieval by treatment with TrisHCl 150 mM pH 9 at 70°C for 15 min and then permeabilized in 0.05 % Trypsin-EDTA for 5 min on ice. After incubation in blocking buffer (PBT + 1 % Bovine serum albumin (BSA) + 2 % NGS + 1 % Dimethyl sulfoxide (DMSO)), samples were incubated with a mouse anti-tERK (4696S, Cell Signaling Technology) antibody. The anti-tERK was

used as a whole-brain counterstain, as it labels the cytoplasm of neurons. Then, samples were washed in PBT and incubated with the appropriate secondary antibody, an Alexa Fluor 633 conjugate (Invitrogen). All antibodies were diluted 1/500 in PBT + 1 % BSA + 1 % DMSO.

2.5 Confocal Microscopy

For imaging the stained tissues, samples were mounted in low-melting agarose (1.5 % in PBS) directly on a glass coverslip (thickness of 0.17 ± 0.005 mm). Fish larvae were positioned dorsal side up and as straight and close to the coverslip as possible, with the help of forceps. After being surrounded by a grease well filled with PBS, the microscope slide was added and the sample was imaged [112].

Fish were imaged using an upright confocal Zeiss Laser Scanning Microscope 710 coupled with a 25x/0.8 NA multi-immersion objective (Zeiss). A diode-pumped solid-state 561 nm laser and a HeNe 633 nm laser unit were used to excite the Texas Red Dextran conjugate fluorophore and Alexa Fluor 633 conjugate, respectively. As immersion medium, Immersol-W (Invitrogen) with refractive index n=1.334, matching the refractive index of water, was used. The imaging volume was selected manually and acquisition parameters (pinhole size, pixel dwell time, digital gain, digital offset and laser power) were optimized for optimal dynamic range and signal-to-noise ratio. To image the whole brain a tiling configuration was used where two adjacent tiles (one of the forebrain and optic tectum, a second of the cerebellum and hindbrain) with 15 % overlap were acquired and stitched together (see image analysis). Each tile was imaged with a zoom factor of 0.6x at 2428x2428 pixels with 16bit depth, for an effective voxel size of 0.23x0.23x1.0 310 μm. After stitching, the field of view of each image was approximately 1045x570x350 310 μm.

2.6 Image Analysis

Confocal images analysis was done using the open source software Fiji [114]. Image tiles were stitched together using the 3D Stitching plugin [115], and raw full stacks were generated. To build the Giant Danio reference brain, a method adapted from Marquart and colleagues was followed [116]. Imaged individual brains were examined, and the individual with the greatest extent of the brain in the field of view was chosen as the initial seed. Each individual brain was then registered to the seed using an affine and non-rigid warping algorithm implemented in Computational Morphometry Toolkit (CMTK) (see `http://www.nitrc.org/projects/cmtk/`). Each registration was checked to ensure that the alignment was good for each brain, and then a shape-averaged brain was generated using CMTK's *avg_adm* function. This average brain then served as a template for two subsequent rounds of registration and averaging (fig. 2.2). In order to assess the precision of the registration, eight landmarks were selected in the template image, and the X, Y, and Z of each were recorded. These eight landmarks were then identified in each of the four

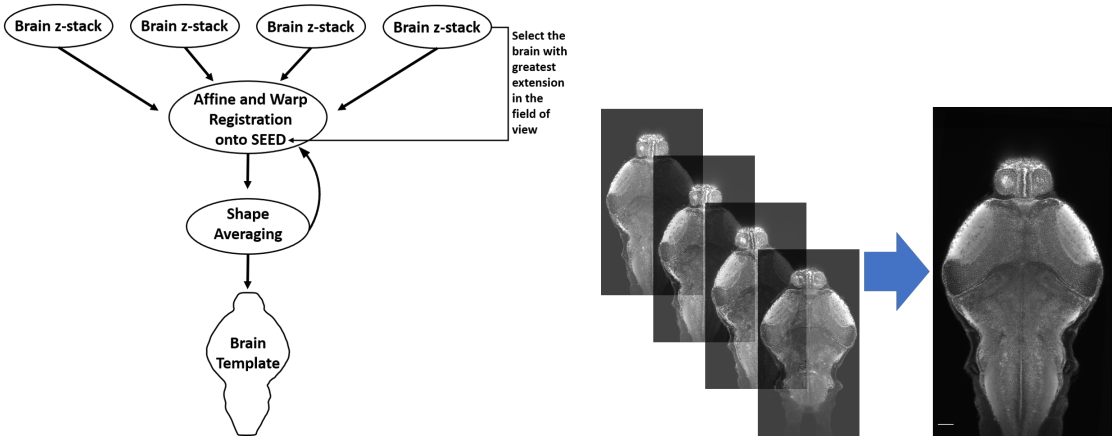

Figure 2.2: Simplified cartoon of brain registration process. Left: Registration pipeline scheme. Initially the individual with greatest extent of the brain in the field of view is chosen as the initial seed. Then, individual brains are registered to the seed using an affine and non-rigid warping algorithm implemented in CMTK. Following, a shape-averaged brain is generated using CMTK's *avg_adm* algorithm, which then serves as a template for two subsequent rounds of registration and averaging to obtain the final shape-averaged brain or brain template. Right: Example of registration of four confocal brain stacks to generate a shape-averaged brain.

original (un-registered) individual confocal stacks, and their locations were noted. These landmarks were used to calculate the Euclidean distance to the corresponding landmark in the template space, with the following formula:

$$d(p,q) = \sqrt{\sum_{i=1}^{3} (p_i - q_i)^2}$$

The landmarks of the individual brains were then transformed into the template space using 3D warping registrations carried out on the corresponding tERK channels and the *"streamxform"* function of the CMTK package. The same two calculations of distance were performed as above on the newly transformed points.

To anatomically identify and characterize the reticulospinal neurons in the Giant Danio, stacks from multiple samples were compared to Zebrafish reticulospinal neurons labeling from previous literature [110, 111, 113, 117–121] using the open source software Fiji [114]. Because neurons overlap one another in the z-dimension, a 3D analysis was required to distinguish them.

For presentation purposes, max intensity z-projections with inverted lookup table values and standard deviation z-projections were made from the stacks of the chosen samples.

2.7 Behavioral set-ups

2.7.1 Low-Resolution Behavior set-up

The low-resolution behavior set-up was used to run circular Optomotor response (OMR) experiments with both Giant Danio and all three Zebrafish strains. Freely swimming

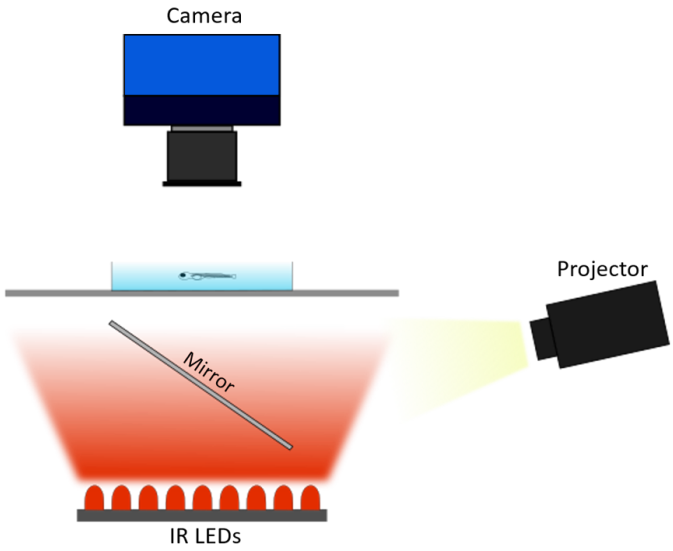

Figure 2.3: General organization of a set-up used in behavioral experiments. Illumination is done from below with an LED backlight, and image acquisition is done with an IR sensitive camera from above. Stimulation is done using a projector and projecting onto a cold mirror placed between the IR LED backlight and the arena.

larvae were recorded in a custom-made acrylic arena consisting of a 10 mm wide circular track that had a 140 mm outer diameter, 120 mm inner diameter and 8 mm depth (Annex I.2). Images were recorded from above at 3 Frames per second (FPS) using an IR sensitive camera (Chameleon3 USB3 CM3-U3-13Y3M-CS, Flir), coupled with an HD Vari-Focal Fujinon CCTV lens (YV2.8X2.8SA-2, Fujifilm) and a 790 nm long pass filter. To optimize the field of view in this set-up it was necessary to trade off spatial resolution, so it was only possible to track the fish's position, but no to record fine tail kinematics. This set-up was therefore limited to tracking the position of the larva. Illumination was provided from below by a custom-made 130x25x110 mm IR LED array backlight (850 nm). Visual stimuli were projected by a ML750e projector (Optoma) onto a cold mirror (Edmund Optics) placed between the IR LED backlight and the arena, allowing simultaneous illumination of the larva and presentation of the visual stimuli (fig. 2.3).

Visual stimulation and behavioral recordings were controlled by software custom-written in MATLAB (Mathworks, USA).

2.7.2 High-Resolution Behavior set-up

The high-resolution behavior set-up was used to run virtual open loop OMR and prey capture experiments with both Giant Danio and Tu Zebrafish. Recording of behavior of freely swimming larvae was done using three different custom-made acrylic concave arenas. Arena dimensions were proportionally increased to use with larvae in different developmental stages. Zebrafish larvae from 4 dpf to 6 dpf were recorded in a 50 mm diameter arena with a 4 mm depth; 8 dpf to 14 dpf Zebrafish larvae and 4 dpf to 8 dpf Giant Danio larvae were recorded in a 66 mm diameter arena with a 5.3 mm depth; and 9

dpf to 14 dpf Giant Danio larvae were recorded in a 88 mm diameter arena with a 7 mm depth (Annex I.3). Images were recorded from above at 700 FPS using an IR sensitive high-speed camera (MC1362, Mikrotron), coupled with an Apo-Xenoplan 2.0/24 (Schneider) lens and a 790 nm long pass filter. 948x948 pixel images were acquired, with the number of microns per pixel varying according to the size of the arena used. This high spatial and temporal resolution enabled the tracking of the tail and acquisition of the kinematic parameters of even the fastest movements executed by the larvae. Illumination and visual stimulation were performed in the same way as in the low-resolution behavior set-up (fig. 2.3).

Visual stimulation and behavioral recordings were controlled by software custom-written in Visual C# (Microsoft).

2.7.3 Head-Restrained Behavior set-up

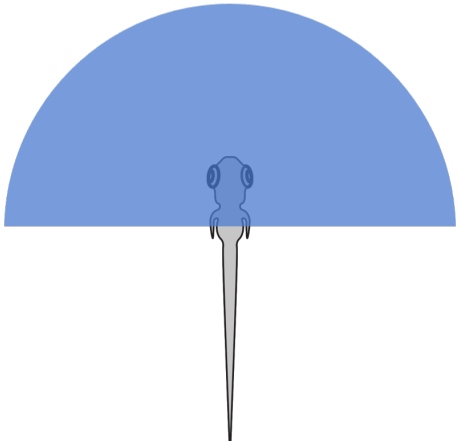

Figure 2.4: Tail-free head-embedded, or head-restrained, larva preparation. Embedding is done with low-melting agarose (1.6 % in E3 embryo medium). This preparation was used in the Head-Restrained Closed Loop Virtual Reality Optomotor Response assay experiments.

The head-restrained behavior set-up was used to run closed loop OMR experiments with Giant Danio. Tail-free head-embedded larvae (fig. 2.4) were recorded in a custom-made acrylic cylindrical arena with a 36 mm diameter and a 25 mm depth (Annex I.4). Images were recorded from above using the same IR sensitive high-speed camera used in the high-resolution behavior set-up described above, coupled with an Apo-Xenoplan 2.8/50 (Schneider) lens and a 790 nm long pass filter. Illumination was provided from below by a mounted IR LED (M780L3, Thorlabs) backlight. Visual stimulation was projected by a ML750e projector (Optoma), through a plano-convex lens (LA1172, Thorlabs), onto one cold mirror and two first-surface mirrors (Thorlabs), the cold mirror placed in between the mounted IR LED backlight and the arena, and one first-surface mirror on each side of the arena located left and right in relation to the fish position (fig. 2.5). In this set-up, tracking of the tail and acquisition of the kinematic parameters was also done during the recordings.

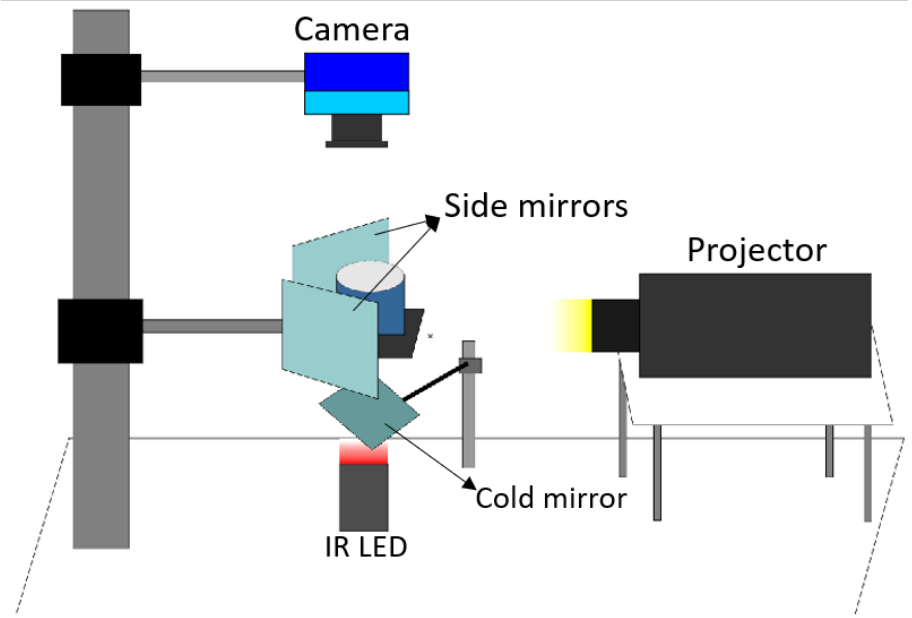

Figure 2.5: Schematic representation of the head-restrained set-up. This set-up is considerably different from the remaining, since there is a need to create a 3D virtual environment. The main difference remains in the mirrors used and their location. In order to create the 3D virtual reality environment, visual stimulation needs to be projected below the fish and sideways, creating the "illusion"of full retinal flow. To achieve this, one cold mirror is placed in between the mounted IR LED backlight and the arena, and two first-surface mirrors are positioned on each side of the arena, located left and right in relation to the fish position when head-restrained in the arena.

As for the high-resolution behavior set-up, visual stimulation and behavioral recordings were controlled by software custom-written in Visual C# (Microsoft).

2.8 Behavioral Assays

The behavioral recordings were performed in acrylic transparent arenas that varied in shape, size and depth, according to the set-up, the behavior assay that was performed, and the age of the larva. All behavior assays were performed with a single larva at a time. Experiments lasted from 15 min to 2 hr depending on the duration of the stimuli protocol used for each assay. The visual stimuli protocols used in all set-ups were projected on a diffuser screen placed 5mm below the larva.

Larvae were tested with four different assays: Circular Optomotor Response, Virtual Open Loop Optomotor Response, Prey Capture and Head-restrained Closed-Loop Virtual Reality Optomotor Response.

2.8.1 Circular Optomotor Response

The three Zebrafish strains and Giant Danio larvae, from 4 dpf to 14 dpf, were tracked freely swimming in the low-resolution circular track described above. A total of four larvae were recorded per day.

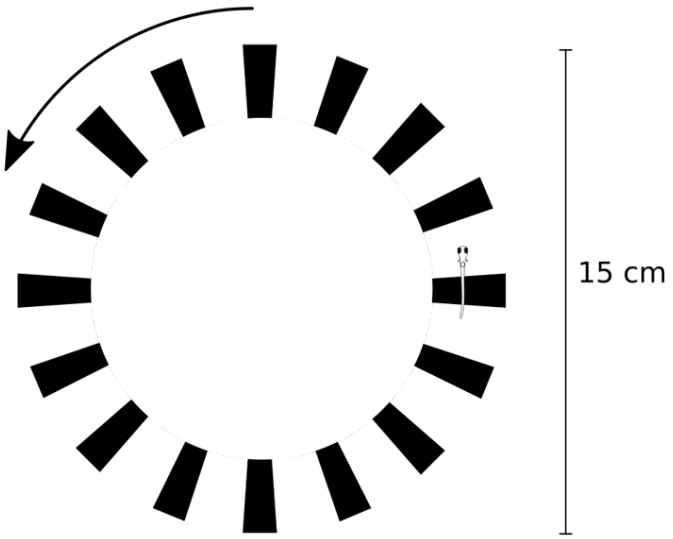

Figure 2.6: Schematic representation of the radial gratings used for visual stimulation in the Circular Optomotor Response assay. Image credit: Adrien Jouary.

The visual stimuli consisted of a radial grating with a spatial period of approximately 9° (fig. 2.6), which is equivalent to a 10 mm spatial period at the center of the track; the grating was displayed at maximum contrast and drifting at different speeds. A total of nine speeds were tested: 0 mm/s, 2 mm/s, 4 mm/s, 7 mm/s, 10 mm/s, 15 mm/s, 20 mm/s, 30 mm/s and 40 mm/s (speed is defined for the center of the track). Before starting an experiment, larvae were placed in the arena for a 10 min habituation period. During an experiment larva were presented with 10 sets of visual stimuli. Each set, which lasted a total of 12 min, consisted of the nine speeds presented in random order. Each speed was displayed for 1 min followed by an interstimulus interval (ISI) of 20 s during which the grating was static. Whenever there was a new drifting speed the direction of the grating was reversed.

2.8.2 Virtual Open Loop Optomotor Response

Tu Zebrafish larvae at 4 dpf, 5dpf, 6dpf, 8dpf, 10dpf, 12dpf and 14dpf, and Giant Danio larvae at 4 dpf, 5 dpf, 6 dpf, 7 dpf, 8 dpf and 10 dpf, were recorded freely swimming in custom-made concave arenas using the high-resolution behavior set-up, as mentioned above. Up to 18 larvae were recorded per day.

Visual stimuli consisted of a rectangular grating with a spatial period of 10 mm at the maximum contrast, drifting at different speeds and directions relative to the position and orientation of the larva. The tested speeds were the following: 0 mm/s, 3 mm/s, 5 mm/s, 8 mm/s, 10 mm/s, 15 mm/s, 20 mm/s and 30 mm/s. Along with the speeds, the directions of the gratings were 0°, 45°, 90°, 135°, 180°, 225°, 270° and 315°, always in relation to the fish orientation (fig. 2.7). The gratings were projected in an experimental closed loop, in other words, translating and rotating the stimulus to cancel the larva's own motion. Thus, the larva's swimming would have no effect on the visual feedback.

For example, if a larva viewing a forward motion grating accelerated, the stimulus would also increase in speed in the same direction so that the larva continued to experience the forward motion at the same speed as it would be if the larva was stationary (fig. 2.8). This was done by tracking the larva position and heading in real time during an experiment. Every larva went through a 10 min habituation period in the arena before starting an experiment as for the circular OMR experiment. During an experiment, larvae underwent a total of 720 trials. One trial, which lasted a total of 5 s, consisted of the projection of one speed in one direction. Each speed at every direction was repeated 15 times, in a fully randomized order.

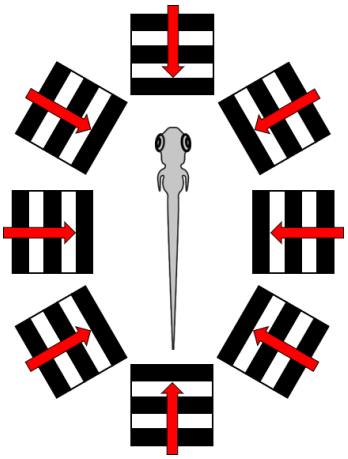

Figure 2.7: Schematic representation of the eight directions of the rectangular gratings used during the Visual Open Loop Opotmotor Response assay. The directions of the gratings were 0°, 45°, 90°, 135°, 180°, 225°, 270° and 315°.

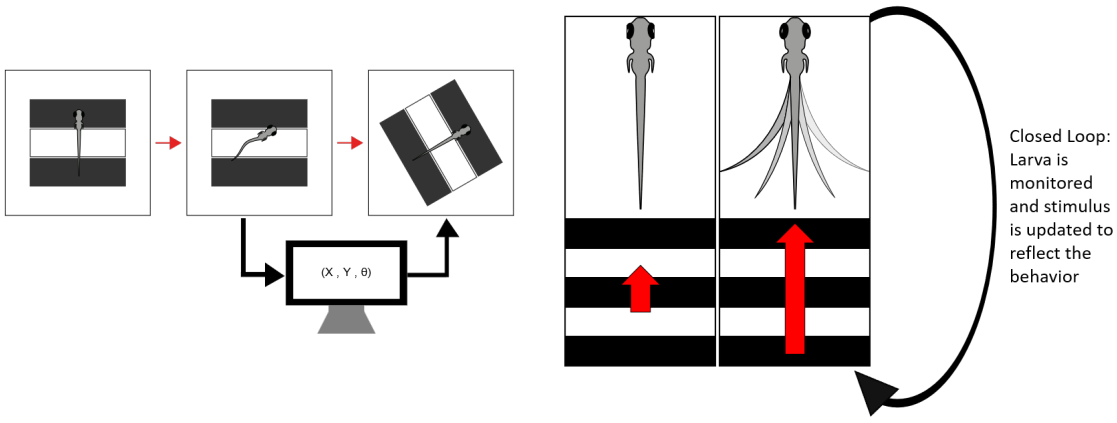

Figure 2.8: Schematic representation of how a virtual open loop, a kind of experimental closed loop, works. Left: Whenever the larva turns, the stimuli is updated and rotated to cancel the larva's own motion ; Right: When there is forward motion (red arrow - size represents speed of the grating), if the larva swims the gratings increase their speed in the same direction so that the larva continued to experience the forward motion at the same speed as it would be if the larva was still stationary.

2.8.3 Prey Capture

To assess prey capture behavior, Tu Zebrafish and Giant Danio larvae, at 6 dpf and 5 dpf, respectively, were recorded freely swimming in a custom-made 19 mm diameter 3 mm deep acrylic concave arena (Annex I.5). Images were recorded at 10 FPS using the high-resolution behavior set-up. Although no tail tracking was used in these experiments, the high-resolution set-up was necessary in order to be able to see the rotifers and identify hunting events. Before starting the experiment, larvae were put in the arena and habituated for 3 min. After the habituation period larvae were fed 50-200 live rotifers and were allowed to hunt for 15 min. At the end of the experiment, the resulting video was analyzed in order to count the number of rotifers eaten. Analysis of the video was done manually, going through the 9000 frames one-by-one, identifying whenever a rotifer was eaten.

2.8.4 Head-Restrained Closed Loop Virtual Reality Optomotor Response

This assay was adapted from Portugues and Engert (2011)[66] and used as a "proof of concept". It was necessary to see if the Giant Danio larvae behaved and performed OMR when head restrained to prove that it is in fact a valuable model with potential for functional imaging and neuronal recordings.

Giant Danio larvae at 4 dpf and 5 dpf were recorded head-embedded using the head-restrained behavior set-up. Embedding was done in low-melting agarose (1.6 % in E3 embryo medium) on top of a sylgard (Dow Corning) cone. After embedding, the tail was freed to move, keeping only the head stationary in agarose. The cone was then put inside the cylindrical arena (Annex I.4).

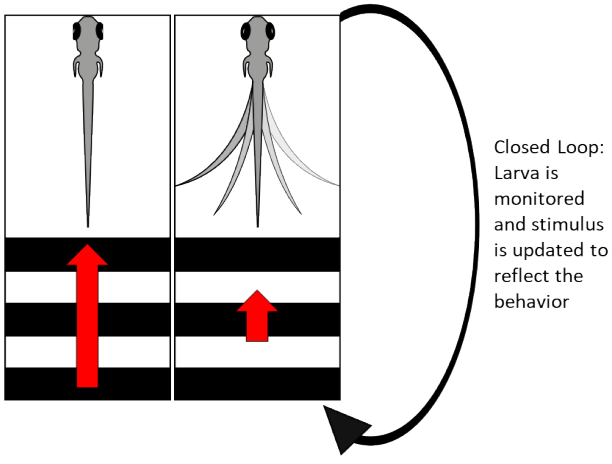

Figure 2.9: Schematic representation of the closed loop used during the Head-Restrained Closed Loop Virtual Reality Optomotor Response assay experiments. If a larva viewing a forward motion (red arrow - size represents speed of the grating) grating tried to swim forward, the stimulus decreased in speed so that the larvae perceived itself moving forward.

Visual stimuli consisted of a set of black and white stripes, projected laterally (from both sides, left and right relative to the fish position) onto the curved walls of the arena,

with anamorphic perspective, so they appeared to extend on an infinite horizontal surface, and a linear gratings pattern, projected from below. Both patterns were presented with a spatial period of 10 mm and with maximum contrast. Stimuli were updated in an experimental closed loop according to the larva's swimming. This was designed to create a 3D virtual reality environment through which the fish could swim. In this case, the translation and rotation of the stimulus was updated in a way to simulate the effect of the larvae's intended motion. For example, if a larva viewing a forward motion grating tried to swim forward, the stimulus decreased in speed so that the larvae perceived itself moving forward (fig. 2.9). Stimuli were presented drifting at different speeds: 0 mm/s, 3 mm/s, 5 mm/s, 8 mm/s, 10 mm/s, 12 mm/s, 15 mm/s, 20 mm/s, 25 mm/s and 30 mm/s. Every larva went through a total of three trials, each lasting a total of 8 min and consisting on the projection of each speed in a random order for 30 s followed by an ISI of 20 s during which the grating was static.

After experiments, head embedded larvae were left embedded overnight to look at survival rates in agarose.

2.9 Behavior Analysis

Behavioral assays tracked data was always analyzed quantitatively using a custom MATLAB (Mathworks, USA) scripts. Data that was not acquired through tracking the larva in any assay was partially analyzed manually and again with custom MATLAB (Mathworks, USA) scripts. A qualitative analysis was done for comparing the prey capture behavior between Giant Danio and Zebrafish, to look at bout traces from both species and at tail end angles from head-restrained Giant Danio larvae.

2.9.1 Circular Optomotor Response

Circular OMR tracking data was analyzed using custom-written MATLAB (Mathworks, USA) scripts. All acquired data went through a pre-processing script, in order to get rid of tracking mistakes during the experiments and compute speed during spontaneous movements (no stimulation) and during trials. To compute speed, the minimum bounding circle of all data points was calculated in order to define the center and radius of the circle. From there, the angular speed during each stimuli speed in all trials, for positive directions (swimming in the direction of the stimuli) and negative directions (swimming against the direction of the stimuli), was calculated and the spontaneous speed during ISI was extracted. These calculations were done per fish and per stimuli speed. Every strain of fish was saved independently, keeping all data regarding Tu Zebrafish, Anju Zebrafish, 5D Zebrafish and Giant Danio separated.

After pre-processing the data, a new script was used to analyze the already pre-processed data. To look at the improvement of the speed of Tu Zebrafish and Giant Danio larvae during OMR with age, average speed was calculated by splitting frames

into 2 s windows of time and averaging only the positive values, where the larvae was swimming in the direction of the gratings. A linear regression analysis was run on the calculated average speed to compare the development of the obtained slopes as a way to clearly state if the larvae was showing a response or not. For the purpose of looking at the probability distribution of the larvae speed during all trials per stimuli speeds, average speed of each strain during stimulations, dissociating the behavioral states that lead the larvae to track or not track the stimuli (tracking state vs non-tracking state); the average speed of each larva per stimuli speed was calculated by splitting frames into 2 s windows of time. Following, the average speed per stimuli per strain was calculated averaging the full distribution of speed values. STD was calculated per stimuli speed and was further used to calculate the Standard error of the mean (SEM) per strain.

In order to compare the tracking state and non-tracking state of the larvae, the average time spent following the stimuli (tracking state) and average time spent stationary (non-tracking state) between Giant Danio and Zebrafish, the pre-processed data from all Zebrafish strains was pooled together and then used to do the same calculations mentioned above. This data was then compared for significance using the Wilcoxon Rank-sum test coupled to a Bonferroni correction, by multiplying each p value obtained by the total number of tests run, considering the result of that operation to infer the true significance (if p remained < 0.05 then it was considered significant and null hypothesis was rejected).

2.9.2 Virtual Open Loop Optomotor Response

Data acquired during the virtual open loop OMR experiments was analyzed with a custom MATLAB (Mathworks, USA) script previously developed in the lab. With this MATLAB script, data regarding bout duration, interbout interval (IBI), and bout traces was extracted. In order to make interpretation easier, all data regarding bout duration and IBI from fish of the same developmental stage were pooled together and represented as probability density functions. To facilitate qualitative analysis, bout traces were manually cut into smaller fragments of 20 s, where the bout onset and bout offset were clearly identified and labelled.

2.9.3 Prey Capture

The resulting videos from the prey capture experiments were analyzed in order to verify that the larva was successfully eating the prey, count the number of rotifers eaten and look at the intercapture interval (ICI). Analysis of the video was done manually, going through the 9000 frames one-by-one, identifying whenever a rotifer was eaten. The number of the frames where rotifers where captured were then inserted into a custom MATLAB (Mathworks, USA) script, separated into species, Giant Danio and Zebrafish. After, an average for the cumulative number of eaten rotifers and ICI was calculated for each species. Lastly, STD was calculated and further used to calculate the SEM, per

species. To see if the difference in the number of eaten rotifers between both species was significant, a Wilcoxon Rank-sum test was run on the data.

2.9.4 Head-Restrained Closed Loop Virtual Reality Optomotor Response

Head-Restrained Closed Loop Virtual Reality Optomotor Response data was analyzed with a custom MATLAB (Mathworks, USA) script. For the purpose of looking at the probability distribution of the larvae intended speed during all trials per stimuli speeds, the intended speed was calculated by splitting frames into 2 s windows of time. Considering that the larvae are restrained and cannot move, the algorithm predicts the amount of displacement a larva would create with each bout it performs, and that displacement is what is defined as being the intended speed. Number of bouts and length of the IBIs performed by the larvae during stimulation were analyzed, in a qualitative manner, from the tail end angle trace given by the tail tracking applied to the larvae during the experiments.

2.10 Fish Tracking, Tail Segmentation and Bout Detection

Most of the defining features of the Zebrafish larvae's locomotion can be found on its tail, as such, studying the behavior of the Zebrafish or Giant Danio larvae requires recording the changes in tail conformation over time as the animal moves. In addition, because the larvae move by producing sudden bursts of activity, it is necessary to use a high spatial and temporal resolution camera to capture data fast enough to acquire key kinematic parameters of fish locomotion. Moreover, because the stimuli presented to the fish works on the visible part of the spectrum of light, it could be recorded by the camera, which in turn would interfere with the image acquisition and data analysis. And so, a camera that can record data in other parts of the light spectrum, as the infrared, is necessary to record the behavior without interference from the stimuli. Considering all the above mention constraints, in this work the IR sensitive high-speed camera (MC1362, Mikrotron) was used in the head-restrained and high-resolution behavior set-ups.

Tracking was done by a custom-written program following previously published work [79]. In brief, the tracking algorithm starts by doing a background subtraction in order to isolate the larva from the rest of the arena (fig. 2.10 - 1). This is done by subtracting the current image with a model for the background. The background model was acquired by calculating the mode for each pixel across multiple frames over a short time interval. This is done to ensure that during that time interval the larva moves between the frames, avoiding its incorporation in the background model. Then the fish is found by locating one of the eyes through the identification of the darkest pixel in the image. A search along a circle, centered on the first eye, whose radius is an approximate distance between the eyes is then used to find the second eye (fig. 2.10 - 2). After finding both eyes, a middle point between them defines the larva's head position (fig. 2.10 - 3). The direction of the tail is acquired by performing a search on a circle centered on the middle

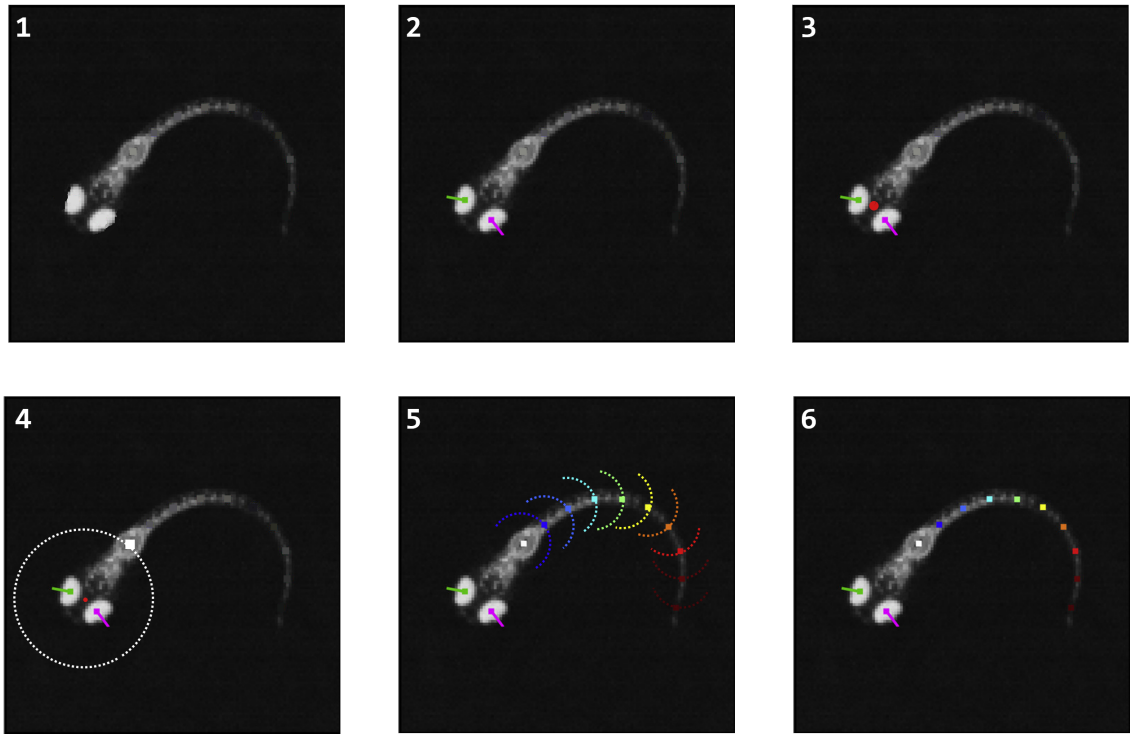

Figure 2.10: Steps of the tail tracking algorithm. 1) Background subtracted image. 2) Locating the position of the eyes. 3) Calculating midpoint between the eyes. 4) Determining tail direction by searching for a recognizable body landmark. 5) Consecutive arc search to find segments along the tail. 6) Tracked larva.

point that defined the head position and with a radius of 450 µm, which is the usual distance to a recognizable body landmark (the swim bladder) (fig. 2.10 - 4). Once the direction of the tail is found, its curvature can be calculated by segmenting it in up to 10 equally distant consecutive segments, 300 µm apart. Starting from the swim bladder, each segment is marked by a point, with the first tail segment starting 300 µm from the swim bladder center point. Points along a 120° arc around the previous tail segment are used to calculate the rotation of the next tail segment (fig. 2.10 - 5). The direction of the rotation is calculated through the center of mass of the intensity of the pixels around the arc. Although all 10 segments could be used to track the fish tail movement and analyze kinematic parameters from, normally only the first 7 segments were used, since the last three segments often have a lower signal-to-noise ratio.

Bout detection was done using a custom-written program according to a method published by Marques and colleagues [79]. In brief, a smoothing function is applied to the tracking output of every tail point in order to remove background noise. Then, the change in tail curvature for every individual tail point is calculated. Finally, the cumulative sum of this value along the tail is acquired and the absolute value of this measure summed over the length of the tail is calculated. A threshold on this value is used to define the bout onsets and offsets.

Chapter 3

Results

The results of the experimental work undergone during this project are shown in this chapter. I will start by addressing anatomy-related data, followed by the behavioral data. First, the growth throughout development for larvae of both species is analyzed, since it was the most basic and fundamental analysis necessary to develop the rest of the project. Next, a careful evaluation of the precision of the registration process to construct the brain template is made, as well as a characterization of the labelled reticulospinal neurons anatomy from the Giant Danio backfills, in order to allow a comparative analysis between the brain structure and underlying motor circuits of both species. Lastly, a description and comparison of the locomotor performance of both species in different behavior assays with different experimental conditions is made. Those behavior assays, with different experimental conditions, were designed in a way that would allow the comparison of the larvae performance, as well as tracking them for acquisition and analysis of kinematic parameters. The behavior assays were focused on two specific visually evoked behaviors – the optomotor response and prey capture.

3.1 Anatomy

3.1.1 Growth throughout development

Giant Danio have an overall faster development than Zebrafish. Hatching in Giant Danio happens around 1 dpf, swim bladder inflation happens between 3 – 4 dpf and feeding starts at 4 dpf. Zebrafish takes approximately 2.5 – 3 dpf to hatch, while inflation of the swim bladder happens between 4 – 5 dpf and feeding only commences at 5 dpf. Although they lay smaller eggs, Giant Danio are already bigger than Zebrafish at hatching. To assess larva total length, measurements were made from the pictures taken daily from 4 dpf to 14 dpf, using a MATLAB (Mathworks, USA) script (see algorithm I.6). The measurements

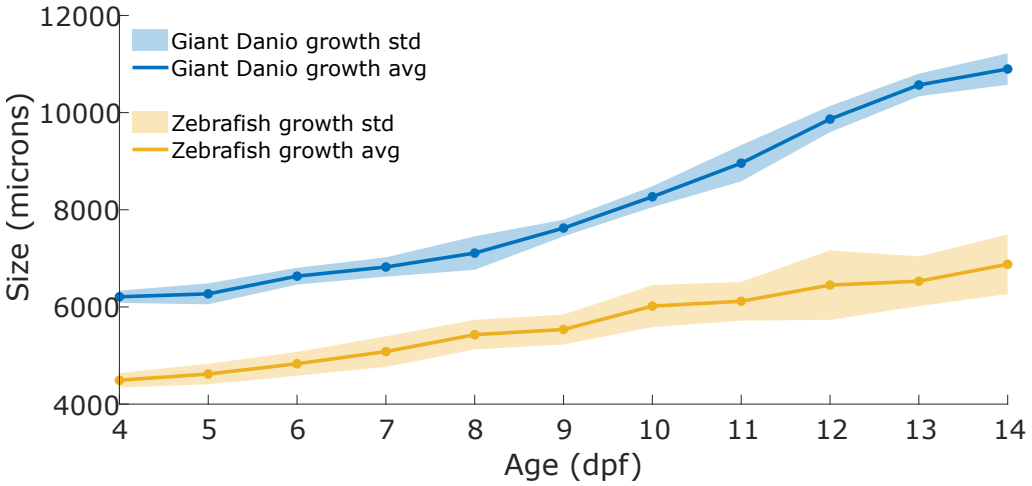

Figure 3.1: Growth curves of Giant Danio and Zebrafish larvae, from 4 dpf to 14 dpf.

were made for three primary reasons: 1) to have a clear idea of their growth rate, 2) to better define the developmental stages during which I wanted to study behavior, and 3) to design and build arenas for behavior assays accordingly. With these three things in mind, I would then be able to do a fair comparative analysis between species. From the images acquired during the different growth stages, a growth curve for Giant Danio and Zebrafish was constructed. Analyzing the growth curves of each species (fig. 3.1), Giant Danio at 4 dpf (N=8) were already almost 40 % bigger than Zebrafish (N=8), with an average size of 6.2 mm (STD ±126 µm), while the latter only measured an average size of 4.5 mm (STD ±148 µm). At 7 dpf, the Giant Danio entered a period of accelerated growth, where growth rate increases considerably to the point where fish grew more than half a millimeter a day. This sudden increase in growth rate could be linked to the fish exhausting most of its yolk nutrient reserves and starting to feed independently. The same was not seen in Zebrafish, which kept a more linear growth. Furthermore, total length variation in Giant Danio larvae (CV values ranged from 0.02 to 0.05) was less evident than in Zebrafish, for which big size variations could be seen throughout development (CV values ranged from 0.032 to 0.111). At 14 dpf, Giant Danio larvae measure an average of 10.9 mm (STD ±324 µm) while the Zebrafish measure an average of 6.9 mm (STD ±615 µm), more than 50 % difference in size for the Giant Danio at this development stage. The faster development of the Giant Danio, coupled with a larger size and the fact that they start hunting one day sooner than the Zebrafish, raised the possibility for an earlier onset of visually guided behaviors in this species.

3.1.2 One for All – The Brain Template

To facilitate a comparative analysis of different structures and brain regions in the Giant Danio, and between Giant Danio and the Zebrafish, I constructed a shape averaged brain template of the anti-tERK immunohistochemical stainings in Giant Danio (fig. 3.2). The purpose of this template was to be able to analyze the overall anatomy of the Giant

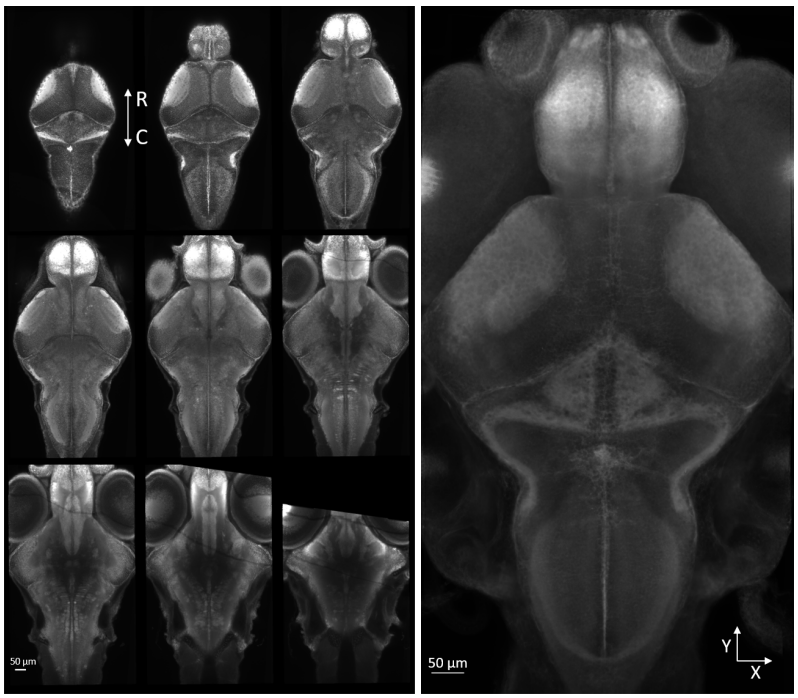

Figure 3.2: tERK Giant Danio shape averaged brain template. Left: Montage of multiple z-slices of the tERK Giant Danio reference brain. Dorsal part of the brain represented on the upper left slice and most ventral part of the brain acquired in the bottom right slice. R - rostral, C - caudal ; Right: Standard deviation z-projection of the Giant Danio reference brain.

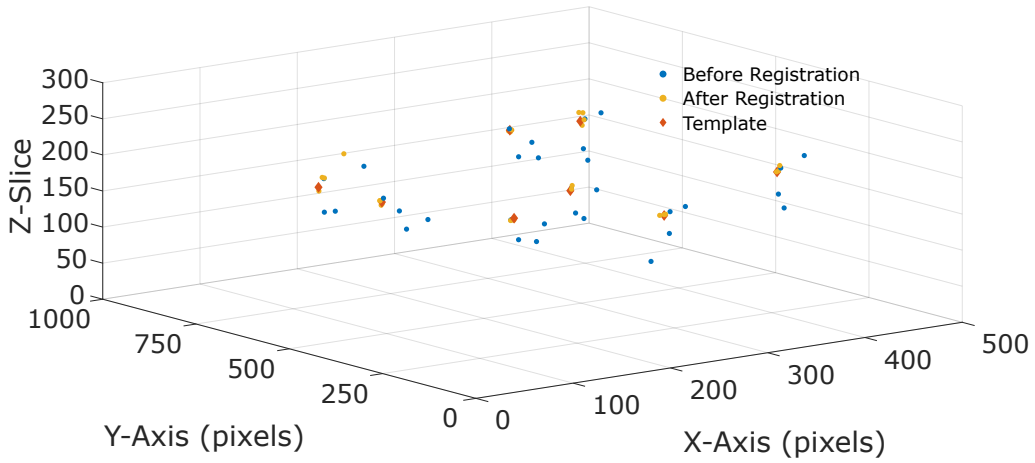

Figure 3.3: Evaluation of the registration precision. The position of eight landmarks was compared, before and after registration of the four individual brains used to make the template brain. The selected landmarks are spread out before registration and after registration they mostly overlap with themselves and the template.

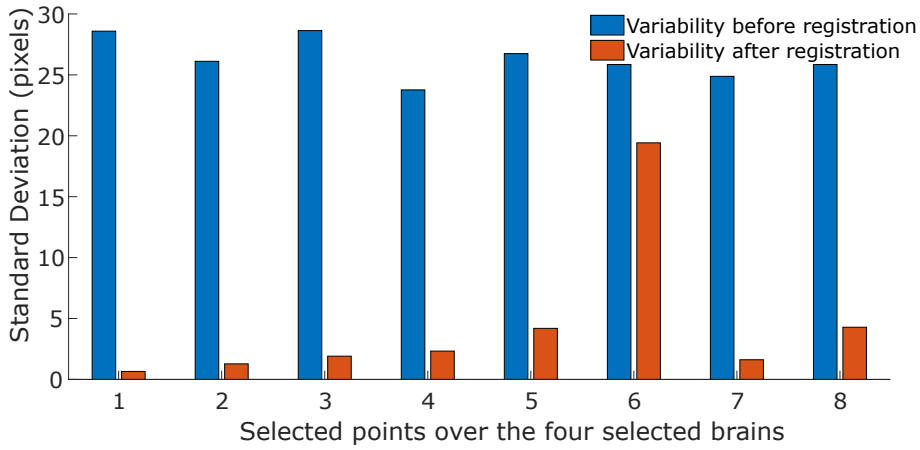

Figure 3.4: Average variability of the position of eight landmarks over the four selected brains before and after registration.

Danio brain, so that it could be bridged to a Zebrafish template and further support the comparative approach. To make the template, brain registration was done with four Giant Danio immunohistochemical tERK stained brain confocal stacks. In short, each individual brain was registered into a common space by rigid, affine, and non-rigid registration using the CMTK library. A shape average image was then generated using the *"avg_adm"* function from CMTK. The new average was then used as the target for another round of registrations. This process was carried out over 3 iterations. This final template was used in further analysis as the template or reference image of the Giant Danio.

In order to assess the precision of the registration, eight selected landmarks (see Methods) were used to calculate the Euclidean distance to the corresponding landmark in the template space. The same calculation of distance was performed as above on the transformed points as well.

With these four measures, the standard deviation of the Euclidean distances, before and after registration, for each one of the eight selected points over the four selected brains, was calculated. The average variability for each one of the eight selected points over the four selected brains was also calculated. By observing the groups formed by the points before registration and after registration (fig. 3.3), and the variability in the calculated Euclidean distances of each set of four points for each of the eight landmarks (fig. 3.4), a simple interpretation regarding how well the registration process went can be made.

Analyzing the sets of four points for each of the eight landmarks, before and after registration, in relation to the position on the template, it becomes clear that, with the registration, all points are brought closer to the same space and to the template, demonstrating the precision of the process. Furthermore, considering that after all the registration steps it is expected for all the points in the same landmarks, over different brains, to be brought to the same biological space, the variability (fig. 3.4) for every set of points was considerably reduced after registration, revealing a good level of precision of the process.

The only group of points where no big improvement was seen with registration was the set of points relative to the 6th (fig. 3.4) landmark selected. This sudden change in the variability from the other sets of points is probably due to the landmark chosen itself, which was in an area of the fish brain that could have been tilted or suffered some deformation during the mounting process for confocal imaging. Therefore, the variability could be due to errors in accurately selecting the landmark across different fish, rather than an error in the registration; alternatively, the error could be due to the registration not performing well in regions that are highly variable. The small variability seen in the other sets can be due to simple biological variability, which places an upper limit on registration precision. Even so, the overall variability, after the registration, was approximately 4.5 µm, which is similar to the size of a cell body. It is worth noting that this level of precision is comparable to what is seen in published Zebrafish registrations. Lastly, upon close observation of the shape-averaged brain template stack obtained, no noticeable distortions or artefacts were found, further supporting the registration quality.

In summary, I have shown that the tERK immunohistochemical staining works in Giant Danio with the same protocol applied to Zebrafish, supporting the idea that tools developed for Zebrafish can be easily adapted to this model. Furthermore, it was the first time a brain template was made for this model. Using this template, a bridging registration to already existing Zebrafish standard atlases can be made, further allowing the anatomical, functional, and molecular insights from Zebrafish to be tested in Giant Danio. Finally, with the template done, the aim was to analyze the underlying motor circuits of the larvae, using a retrograde labelling technique.

3.1.3 Anatomy of spinal projection neurons

After observing the shape-averaged brain template, it was necessary to have a more in-depth analysis of the underlying circuit structure of the descending motor system. Therefore, I made multiple backfills of the Giant Danio reticulospinal neurons. The purpose of the backfills was to be able to analyze and characterize the overall anatomy of the Giant Danio reticulospinal neurons and to confirm if the underlying motor circuit organization of the model was conserved in relation to the Zebrafish or not. To do that, a Texas Red-Dextran conjugated (3000 MW, Lysine Fixable, Invitrogen) dye was pressure injected with a micro-manipulator into ventral spinal cord of the Giant Danio, followed by confocal imaging of the positive labelled larva in the next morning.

Analyzing the Giant Danio backfills (fig. 3.5), the labelled reticulospinal neurons are organized in a total of 7 clusters. These clusters are arranged bilaterally, remaining approximately symmetrical in relation to the midline of the brain. The first and largest cluster lies in the nucleus of the Medial Longitudinal Fasciculus (nMLF), located in the midbrain. In the hindbrain, reticulospinal neurons clusters are periodically spaced along the neuraxis. Three of those clusters are present in the rostral hindbrain (rhombomere

(Ro) 1 (Ro1), 2 (Ro2) and 3 (Ro3)) and three are present in the medial hindbrain (rhombomere 4 (Ro4), 5 (Ro5) and 6 (Ro6)). In the caudal level of the hindbrain (rhombomere 7 (Ro7)) no clear cluster of cells was found.

All labelled cells are in positions that are reproducible in the different backfills, although not all backfills achieve a complete labelling of all reticulospinal neurons. It is also clear that the arrangement and morphology of cells varies considerably according to the location of the soma, either in the midbrain or hindbrain. For these reasons, it was not feasible to get accurate cell counts on the multiple clusters. More backfills would have to be acquired and analyzed, in order to get an accurate total cell count. No single-cell identification techniques were used, so any direct cell comparison with Zebrafish is speculation based on anatomical features.

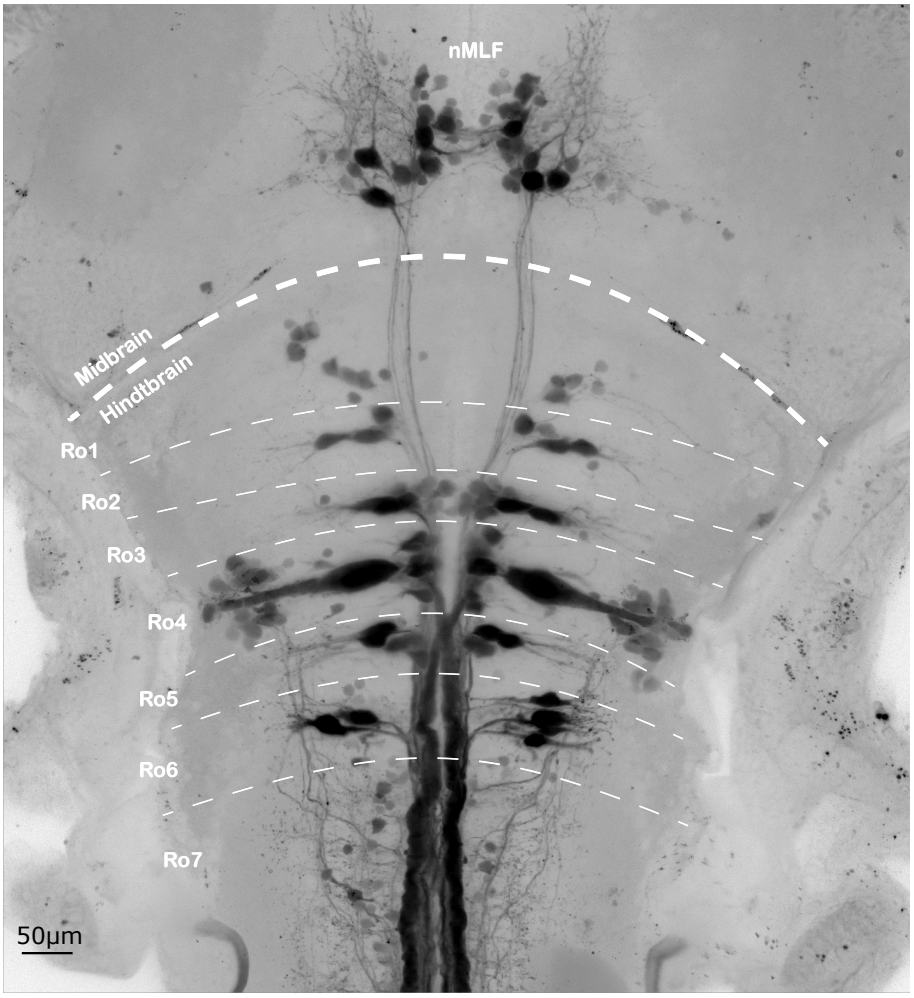

Figure 3.5: Max intensity z-projection of a Giant Danio backfill. The general division and major cell clusters can be clearly identified. nMLF - nucleus of the medial longitudinal fasciculus; Ro - rhombomere; R - rostral; C - caudal.

3.1.3.1 Cluster 1, nucleus of Medial Longitudinal Fasciculus

Starting to analyze the clusters along the rostral-caudal axis, the first and most rostral group of cells is a large midbrain cluster that sits in the nMLF in the midbrain. Their axons rise from caudal aspects of the soma, later forming a caudally directed bundle and projecting ipsilaterally down, forming the medial longitudinal fasciculus (mlf), and their dendrites project mostly laterally and rostrally. This cluster can be separated into two sub-clusters representing a division of the nMLF, one dorsal and one more ventral. The first sub-cluster, lying more dorsally, is characterized by a group of cells spread mediolaterally and rostrocaudally, where a set of big cells resembling the MeL cells (MeLm, MeLr and MeLc in Zebrafish) can be found, although in a different arrangement. The more caudal of the big cells, resembling MeLc, has a dendrite that projects contralaterally. The second sub-cluster, more ventral and with less cells, lies more rostrally and medially in relation to the dorsal cluster. In this sub-cluster, some cells have contralaterally projecting processes, with three cells, one of them resembling the MeM1 cell in Zebrafish, clearly showing these contralateral projections.

3.1.3.2 Cluster 2, Rhombomere 1

In the hindbrain, the neurons present a diffuse and regularly spaced arrangement. The first cluster lies in Ro1; the cluster can be distinguished into a sub-cluster located more rostral and lateral in relation to the midline, also lying more dorsally, and another more caudal and medial, lying more ventrally. These sub-clusters resemble the RoL1 and RoM1 cells in Zebrafish, respectively. The lateral and more dorsal cluster is composed of mostly round shape cells that show ipsilateral projections from the caudal aspect of the soma, forming the lateral longitudinal fasciculus (llf). One cell from the cluster shows a projection coming from a more medial aspect of the soma that goes in the direction of the midline, but it is unclear whether it projects to the ipsilateral mlf, or if it projects to the contralateral mlf. The medial and more ventral cluster is composed of a group of rounded cells and one fusiform cell. These cells have axons projecting ipsilaterally from the medial aspect of the soma into the mlf, and dendrites that project ventrolaterally, with some projections clearly branching near the wall of the brain in the ventrolateral column of neuropil, as observed previously in Zebrafish preparations [117].

In between the Ro1 and Ro2, in Zebrafish, the mlf starts to split into a dorsal mlf and a ventral mlf [119]. In the Giant Danio backfills the same was expected. The division of the mlf was observed in 9 fish out of the total 13; based on this limited dataset, establishing where in the circuit the division happened is not possible. The fish where this division was not seen was due to overall bad staining. From this, I concluded that there is in fact a division of the mlf into the dorsal mlf and ventral mlf.

3.1.3.3 Cluster 3, Rhombomere 2

In Ro2, there is a cluster of medially located cells. This cluster can be divided into a dorsal and ventral sub-cluster. The dorsal sub-cluster is mostly composed of fusiform cells that resemble the RoM2 cells in Zebrafish, showing axons projecting ipsilaterally from a medial aspect of the soma through the dorsal mlf and dendrites projecting dorsolaterally from a lateral aspect of the soma. Some of these dorsolateral projections branch near the wall of the brain in the dorsolateral column of neuropil, while the other go more caudally, but it becomes unclear where they branch. The ventral sub-cluster cells are mostly rounded with axons projecting ipsilaterally from the caudal aspect of the soma through the ventral mlf, and with dendrites projecting from a lateral aspect of the soma that extend to the llf and to the ventral column of the neuropil. One big round cell, the most ventral one of the cluster, shows an axonal projection that extends ventromedial and contralaterally to the cluster found on Ro3, although it was unclear if those projections descend to the mlf or not.

3.1.3.4 Cluster 4, Rhombomere 3

The next cluster lies in Ro3. This is a close-packed cluster that extends dorsoventrally in a medial position near the mlf. The cluster can be divided into a dorsal and a ventral region, based on the cells' morphology and location. Starting dorsally, predominantly fusiform cells, resembling the RoM3 cells in Zebrafish, can be found projecting ipsilaterally from the medial aspect of the soma down the dorsal mlf and with dendrites that project dorsolaterally, some to the llf and across it, some to the vestibular nucleus, and some branching near the wall of the brain in the neuropil area. Ventrally, fusiform cells start to give way to more rounded cells, resembling the RoV3 cells in Zebrafish, that are more medially located and that will form the ventral region. This region lies underneath the mlf and is composed of round shaped cells. These cells show ventrolaterally projecting dendrites and ipsilaterally descending projecting axons from a medial aspect of the soma, likely with projections to the ventral mlf. There are at least two ventrally located cells that almost lie on top of the medial line. These cells seem to have contralateral projections to the opposite cluster.

3.1.3.5 Cluster 5, Rhombomere 4

In the medial region of the hindbrain, in Ro4, a cell cluster can be found ventromedially, and dorsally to this cluster there are the prominent Mauthner cell (M-cell). Laterally, although not belonging to the reticulospinal neurons, the closely packed vestibulospinal cells of the vestibular nucleus can be clearly seen. The M-cell is located dorsally in relation to the ventromedial cluster. It shows a descending contralateral large axon projection from the medial aspect of the soma to the dorsal mlf. The lateral dendrite projections and branching are obscured in most of the analyzed confocal stacks due to the presence

of labeled vestibulospinal cells. The ventromedial cluster that is present can be further divided along the dorsoventral axis. The dorsal section, located medial and slightly ventral to the M-cell, is made of tightly packed round cells, resembling the MiM1 cell in Zebrafish. These cells have ipsilaterally projecting axons from the medial aspect of the soma caudally on the dorsal mlf and, based on very faint labels, they also show laterally projecting dendrites that extend almost to the vestibular nucleus, although the branching was not possible to trace. The ventral section of the cluster has more cells than the dorsal one and presents a rostrocaudal organization of close-packed cells, resembling the MiV1 cells in Zebrafish. These cells show, in most cases, ipsilaterally projecting axons from the medial aspect of the soma down on the ventral mlf, and dendrites projecting ventrolaterally and branching bellow the vestibular nucleus, near the wall of the brain. Also, some of these ventral cells appear to have projections that cross the midline, but the traces are inconclusive.

3.1.3.6 Cluster 6, Rhombomere 5

Two clusters can be identified in Ro5, a dorsal cluster and a ventromedial cluster. The dorsal cluster encompasses round-shaped cells, resembling the MiD2 cells in Zebrafish. At least two cells show axons projecting from the medial aspect of the soma contralaterally through the dorsal mlf while the remaining are inconclusive whether their axons project ipsilaterally or contralaterally, since they become obscured by the axons of the M-cells. Most of the laterally projecting dendrites branch in the lateral neuropil area, while some project across the llf. The ventral cluster has more cells than the dorsal one, similar to Ro4. These cells are round with axons projecting from the medial aspect of the soma ipsilaterally down on the ventral mlf and dendrites projecting ventrolaterally to the ventrolateral column of neuropil, with some projections seemingly reaching down to the llf. This cluster strongly resembles the MiV2 cells in Zebrafish.

3.1.3.7 Cluster 7, Rhombomere 6

Still in the medial region of the hindbrain, is where the last and most dorsal cluster of cells in the hindbrain is found, specifically in Ro6. This cluster had higher variability in soma location, although never to the point of changing the overall location of the cluster. It is composed of a mix of fusiform and round cells, resembling the MiD3 cells in Zebrafish. The most dorsal cells of the cluster send axons from the medial aspect of the soma contralaterally down in the dorsal mlf. Ventral to the MiD3 homologous cells, there are two cells projecting their axons from the medial aspect of the soma contralaterally down on the dorsal mlf. For the remaining cells in this cluster it is unclear whether their axons cross the midline. Overall, all the cells in this cluster present dendrites projecting ventrolaterally past the llf and branching in the ventrolateral column of neuropil.

3.1.3.8 Rhombomere 7

In the caudal region of the hindbrain, Ro7, no clear cluster of cells was found. All the backfills analyzed show a multitude of small rounded labelled cells scattered rostrocaudally in this region and spreading dorsoventrally from the dorsal mlf level to bellow the ventral mlf. These cells show neurites projecting from medial and lateral aspects of the soma, although it was not possible to trace those projections. In a few backfills, isolated larger cells were found with axons projecting through the mlf, although it is not possible to say if they projected ipsi- or contralaterally. Lastly, in the most caudal part of the hindbrain it is possible to see the ventral and dorsal divisions of the mlf merging.

Altogether, the retrograde labelling worked in the Giant Danio with positive results, using a protocol and technique adapted directly from the Zebrafish. Furthermore, after a detailed analysis of the reticulospinal neurons, there is a clear similarity to the Zebrafish circuit, already described in depth in the literature [117, 119, 122], with the general division and number of clusters being very well conserved. Such anatomical similarities could be complemented at the behavior level. And so, different behavior assays were used with both species in order to carefully analyze if similarities at the behavior level were indeed present.

3.2 Behavior

3.2.1 Optomotor Response

The Circular Optomotor Response behavior assay was used in order to look at four main aspects: 1) the ontogeny of the Optomotor response (OMR) in the Giant Danio and Zebrafish, 2) to analyze if there is an improvement in the OMR performance with age, 3) to look for evidence of tracking vs non-tracking states during stimulation and, 4) to look at the speed tuning while performing the OMR at different speeds.

The first two points arose from the questions of when in development is the onset of the OMR and if, with development, fish would improve or perform the OMR better, trying to better match their speed to the stimuli being presented. Furthermore, to look at the OMR at different developmental stages would allow to identify, approximately, the onset of the response in both species. Using the newly developed Circular Optomotor Response behavior assay and bearing in mind that the fish could follow the stimuli without any barrier stopping it, Giant Danio and Tu Zebrafish larvae, from 4 to 14 dpf, were subjected to gratings stimuli at different speeds. We aimed to understand how well the fish performs the OMR and tunes its swim speed in relation to the stimuli speed. With this, I was able to confirm that the OMR in the Giant Danio was consistently elicited one day earlier than in Zebrafish. From the linear regression analysis, at 4 dpf Giant Danio performed the OMR, with the slope being significant for all ages, while the Tu Zebrafish only showed an OMR at 5 dpf, since the slope at 4 dpf was not significant (fig. 3.6). Examining the average speed at different ages and for every stimuli speed in both species (fig. 3.7), no

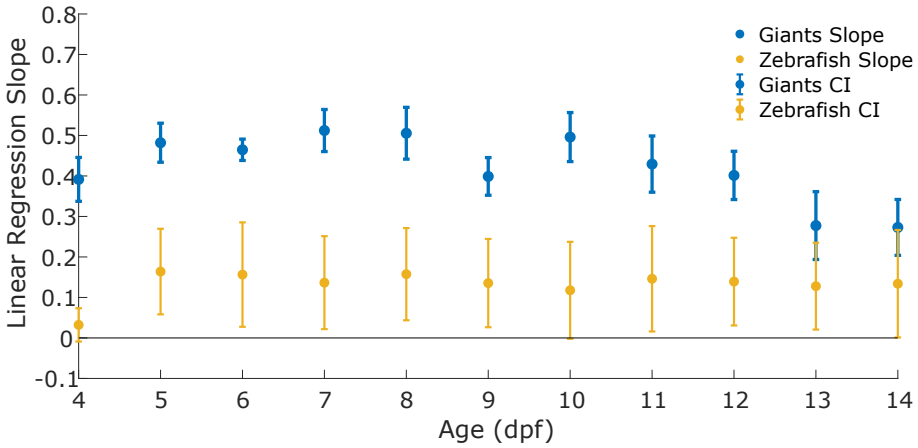

Figure 3.6: Comparison across developments of the slopes of the linear regression analysis of the average speed of Giant Danio and Zebrafish larvae. A slope of 0 is equivalent to a larvae not changing its speed according to the stimuli speed, and a slope of 1 would be a larvae perfectly tracking the stimuli. Giant Danio larvae performed the OMR even at 4 dpf, with the slope being significant ($p<0.05$) for all ages. Tu Zebrafish only performed the OMR from 5 dpf onwards, since the slope at 4 dpf was not significant. Error bars show 95% confidence interval.

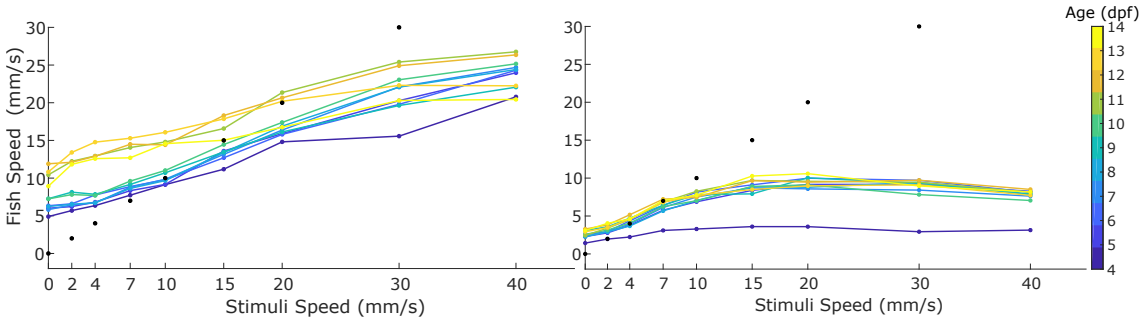

Figure 3.7: Average speed per stimuli speed for every age. Left: Giant Danio larvae show an onset of the OMR at 4 dpf and an increasing average speed with the increase of the stimuli speed while performing the OMR, although not with a gain of one. This increase is seen in larvae from 4 dpf up to 12 dpf. At 13 dpf and 14 dpf, Giant Danio larvae track the increasing stimulus speed up to 30 mm/s, without further increasing their average speed afterwards; Right: Tu Zebrafish show an onset of the OMR at 5 dpf. At all ages where the OMR is clear, an increase in the average speed is seen with stimuli speeds up to 20 mm/s, and from there the larvae reach a plateau, without further increasing the average speed. From 5 dpf onwards there is no apparent improvement of the average speed with age, since the average speed varies little with the age of the larvae. Black dots represent a gain of 1.

OMR in Tu Zebrafish larvae at 4 dpf can be seen, while in Giant Danio, with the increase of the stimuli speed, there is a clear OMR that increases its speed with the stimuli speed, although not with a gain of one.

In Tu Zebrafish larvae there was no apparent improvement with age from 5 dpf onwards, with the average speed varying little with the age of the larvae (fig. 3.6, 3.7). Furthermore, in all ages from 5 dpf to 14 dpf, an increase in the average speed can be seen with stimuli speed up to 20 mm/s, and from there the larvae reach a plateau, without further increasing the average speed with the increase in the stimulus speed.

In the case of the Giant Danio, the larvae are able to increase their swimming speed in response to increases in stimuli speed (fig. 3.7). This increase is seen in larvae from 4

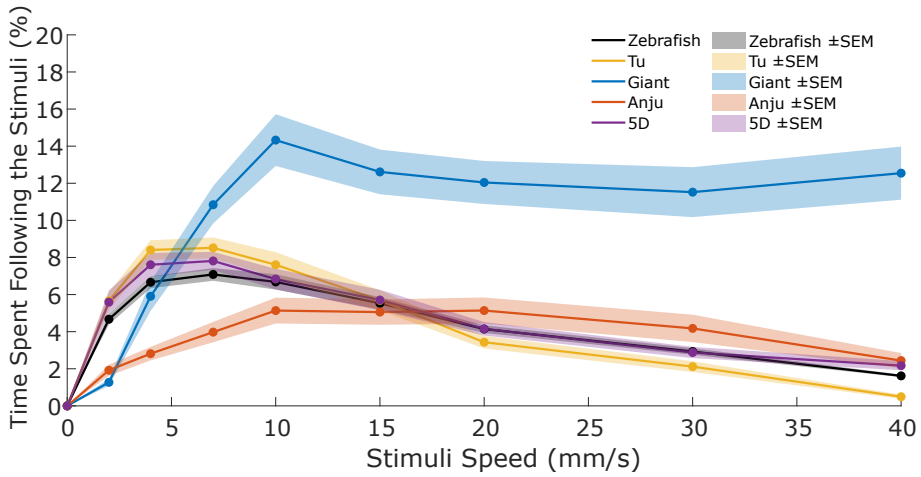

Figure 3.8: Time spent following the OMR stimuli. There is a significant difference in the tracking state for all but one stimulus speed, 7 mm/s, in the time spent following the stimuli for Giant Danio and Zebrafish. Zebrafish larvae spend more time in a tracking state for lower stimulus speeds, especially for 7 mm/s, while Giant Danio larvae spend more time in a tracking state for speeds above 7 mm/s. Shaded regions represent the SEM.

dpf up to 12 dpf. At 13 dpf and 14 dpf, Giant Danio larvae track the increasing stimulus speed up to 30 mm/s, not further increasing their average speed afterwards, which is equivalent to reducing their performance, although still doing the OMR. Following these results, it was necessary to understand how well the larvae were tracking the stimuli, and which speeds elicited the best results, more than just how fast were they swimming on average in relation to each stimuli speed presented.

Observations regarding the evidence of the tracking vs non-tracking states during stimulation were done in order to dissociate the effects of behavioral state that lead the fish to track at some times but not at others, from the actual response gain when tracking. The analyzed larvae ages, from 5 to 8 dpf, were selected according to the most commonly used ages in Zebrafish, as well as the best ages when it comes to performance (age interval where no further improvement was seen after), and ages that matched the best sizes to work with.

Comparing both species, including multiple Zebrafish strains, by speeds, excluding 0 mm/s, Tu and 5D Zebrafish larvae spent more time following stimuli at 7 mm/s, spending an average of 8.5 % (SEM ±0.6) and 7.8 % (SEM ±0.5) of the time following the gratings while performing the OMR, respectively (fig. 3.8). Anju Zebrafish spent more time following the stimuli, 5.1 % (SEM ±0.7) of the time, at 20 mm/s. Contrasting with Tu Zebrafish, both Zebrafish wild-derived strains, Anju and 5D, swam more at higher speeds. Differently, Giant Danio larvae spent more time following stimuli at 10 mm/s, at which they spent an average of 14.3 % (SEM ±1.4) of the time following the gratings while performing the OMR. In general, Giant Danio were significantly different from Zebrafish (in general – all strains pooled together), except for one stimulus speed, 7 mm/s.

The time spent stationary is expected to follow the opposite trend to the time spent following the stimuli.

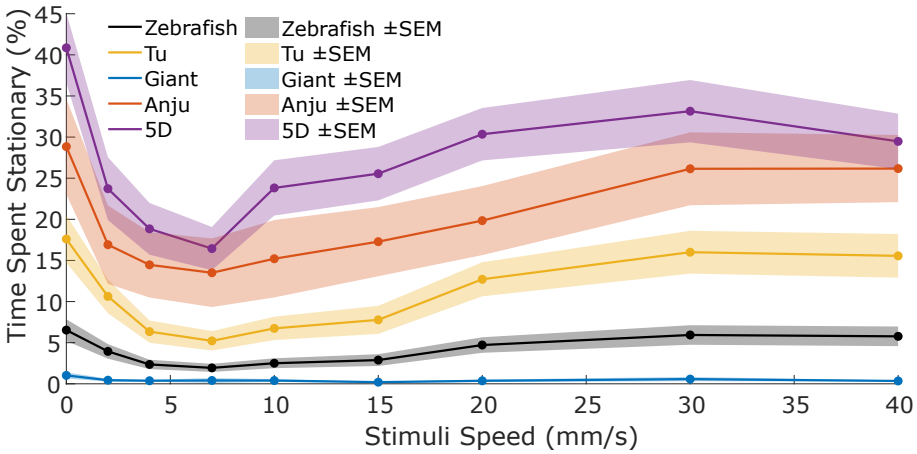

Figure 3.9: Time spent stationary during stimulation. The time spent stationary, in a non-tracking state, of the Zebrafish larvae follow an opposite trend to what is seen in the time spent following the stimuli during a tracking state. This is conserved in all three Zebrafish strains. Giant Danio do not show a clear stationary non-tracking state. Shaded regions represent the SEM.

Tu and 5D Zebrafish larvae spent more time stationary at 30 mm/s, 16 % (SEM ±2.6) and 33.1 % (SEM ±3.8) of the time, while at 7 mm/s larvae spent the shortest percentage of time stationary, 5.2 % (SEM ±1.2) and 16.4 % (SEM ±2.6) of the time, respectively (fig. 3.9). Anju Zebrafish spent more time stationary at 40 mm/s, 26.2 % (SEM ±4.1), while at 7 mm/s, like the other two strains of Zebrafish, spent the least time stationary, 13.5 % (SEM ±4.2) of the time. Furthermore, as the stimuli speed increased above 7 mm/s, so did the percentage of time the larvae of the three strains spent stationary. Giant Danio larvae, on the other hand, never spent more than 0.6 % (SEM ±0.3) of time stationary, which was spent at 30 mm/s. Surprisingly, when looking at Giant Danio and Zebrafish (in general – all strains pooled together), the difference between both species for the time spent stationary was not significant for any of the stimuli speed . Once the difference between both species was clear, in time spent following versus stationary in relation to the stimuli speed, it was imperative to look at the full distribution of data and the speed tuning of the fish during each stimuli speed.

The speed tuning analysis, in both species, was done in order to understand the tracking capacity at different speeds and limitations of the OMR in each species, as well as to understand what was happening whenever the larvae were not following or stationary during stimulation. This data was addressed with the use of violin plots. These, although similar to box plots, offer more information than the basic summary statistics. The violin plot shows the full distribution of data in a probability density function. The whole length of the violin plot shows all possible results, while the inside area will define the probability of that result. The larger the area, the higher the probability of having that result. Looking at the full distribution of the data from 5 dpf to 8 dpf in the violin plots, positive values mark when a larva is swimming in the direction of the gratings, negative ones mark the opposite and near zero or zero values mark when larvae were stationary. By carefully observing the violin plots for Giant Danio and the Zebrafish strains (fig. 3.10),

differences in OMR performance between both become clear. Tu, Anju and 5D Zebrafish larvae performed OMR and were able to track the gratings well up to a stimuli speed of 20 mm/s. However, they show higher probability of tracking the stimulus at lower speeds. Although larvae also tracked stimuli speeds above 20 mm/s, the amount of time they performed the OMR at speeds above 20 mm/s was reduced, with the big majority of the larvae that swam in the direction of the grating not matching the grating speed. The exception comes with the Anju Zebrafish, where these have a higher probability of performing the OMR at 20 mm/s, and even at higher stimuli speeds, in comparison with the other two strains. Moreover, at a stimuli speed of 20 mm/s, the larvae reach a plateau in terms of performance. In fact, like mentioned above, if we look at the average speed of the Tu, Anju and 5D larvae for all the stimuli speeds in the same developmental period, even though the fish do not show an average gain that matches the stimuli speed, that plateau becomes clear and the increase in performance, that was seen from the 2 mm/s up to the 20 mm/s, ceases for higher speeds (fig. 3.7).

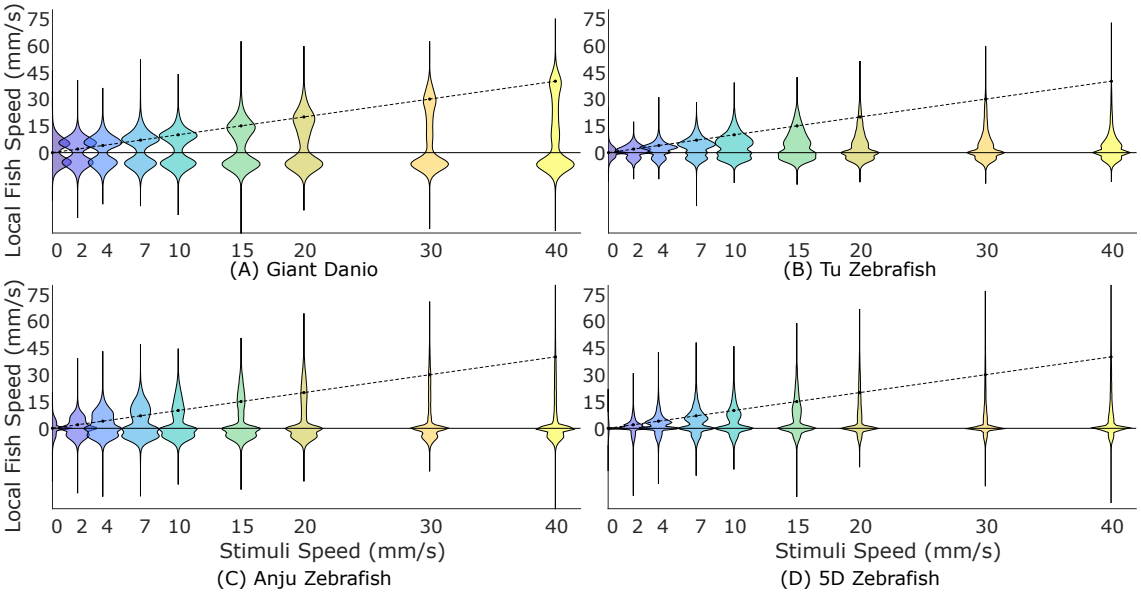

Figure 3.10: Full distribution of the data for the speed tuning analysis from 5 dpf to 8 dpf larvae. Positive values mark when a larva is swimming in the direction of the gratings, negative ones mark the opposite and near zero or zero values mark when larvae were stationary. (A) - Giant Danio perform the OMR while tracking the projected stimuli at stimuli speeds above 7 mm/s. At stimuli speeds lower than 7 mm/s, the larvae show much less probability of matching the gratings speed, almost always swimming at a "basal" swimming speed that is higher than the stimuli speed; (B) - Tu Zebrafish performed OMR and were able to track the gratings well up to a stimuli speed of 20 mm/s. However, they show higher probability of tracking the stimulus at lower speeds; (C) - Anju Zebrafish, like Tu Zebrafish, performed OMR and have higher probability of tracking the stimulus at lower speeds. But comparing with the other two Zebrafish strains, Anju have a higher probability of performing the OMR at 20 mm/s, and even at higher stimuli speeds; (D) - 5D Zebrafish, just like Tu Zebrafish, performed OMR and were able to track the gratings well up to a stimuli speed of 20 mm/s, although they show higher probability of tracking the stimulus at lower speeds. Black dashed line and dots represent a gain of 1.

Giant Danio larvae (fig. 3.10), at stimuli speeds above 7 mm/s, were able to perform the OMR while tracking the projected stimuli, even at the higher speeds. In contrast, at stimuli speeds lower than 7 mm/s, the larvae show much less probability of matching the

gratings speed, almost always performing an OMR at a "basal" swimming speed, similar to what is seen for a stimuli speed of 0 mm/s where the larvae mostly swim at an average of 6 mm/s. By analyzing the average speed of the Giant Danio larvae (fig. 3.7) while performing an OMR at different stimuli speeds, there is a clear constant increase in their performance without reaching a plateau. Although they never really show an average gain that matches the stimuli speed, there is a constant increase in the average speed of the larvae with the increasing speed of the stimulation.

Whenever the larvae swam in the opposite direction of the gratings, they show a higher probability of swimming always at identical speed against the gratings, resembling a basal speed, instead of varying it a lot or performing an anti-OMR (matching the gratings speed while going in the opposite direction). This event was independent of the stimuli speed being projected, considering that different stimuli speeds show no apparent effect on the speed at which larvae swam against the gratings. This trend was seen in both species, although the speed at which they most frequently swam may differ (fig. 3.10).

Overall, the Giant Danio showed an OMR with earlier onset than the Zebrafish larvae. Not only did they perform the OMR more constantly and consistently, but also did it at higher speeds. Furthermore, when assessing the average speed, the Giant Danio show a clear increase in performance, while Zebrafish reached a plateau. Also, it is worth mentioning that, in the case of the wilder Zebrafish strains, the Anju and 5D strains, although they stayed stationary for longer than Tu, they performed the OMR at higher speeds as well as they showed a higher average speed. Specially in the case of the Anju strain, they show a higher probability of performing the OMR at the stimuli speed than the other two strains. Seeing how well Giant Danio performed in comparison with all Zebrafish strains, it was necessary to look at the swimming kinematics of both fish.

3.2.2 Virtual Open Loop Optomotor Response

In order to look at the swimming kinematics of the Giant Danio and Tu Zebrafish, a set-up that allowed to track the tail of the fish was necessary, coupled to a behavior assay, the Virtual Open Loop Optomotor Response, capable of eliciting different types of swims in the fish. In total, 302 experiments were run, using Giant Danio larvae with 4 dpf, 5 dpf, 6 dpf, 8 dpf and to 10 dpf, and Tu Zebrafish larvae with 4 dpf, 5 dpf, 6 dpf, 8 dpf, 10 dpf, 12 dpf and 14 dpf. Building the data set itself was already an important step, since it lays the foundation for future work and more complex analysis that could not be done during the time being. Furthermore, it allowed to analyze bout traces, bout duration and interbout interval (IBI) from a large number of Giant Danio (N= 136) and Zebrafish (N= 152). The remaining fish (from the 302) that were not used for the swimming kinematics analyzed were fish that were excluded from the analysis due to tracking mistakes.

Observing the example bout traces from both Giant Danio and Tu Zebrafish (fig. 3.11), in the same interval of time, Giant Danio performs almost twice as many bouts as the Tu Zebrafish, with shorter IBIs. Furthermore, from 4 dpf to 10 dpf, Giant Danio larvae

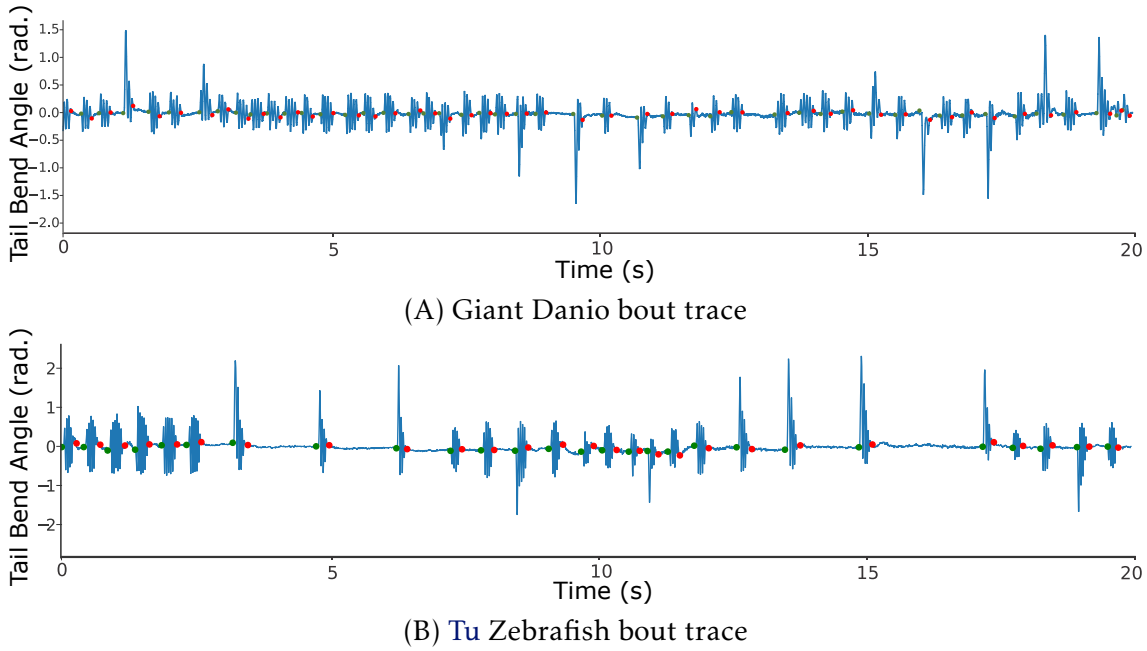

(A) Giant Danio bout trace

(B) Tu Zebrafish bout trace

Figure 3.11: 20 s section of bout traces from Giant Danio and Zebrafish larvae. Green dots - bout onset; Red dots - bout offset

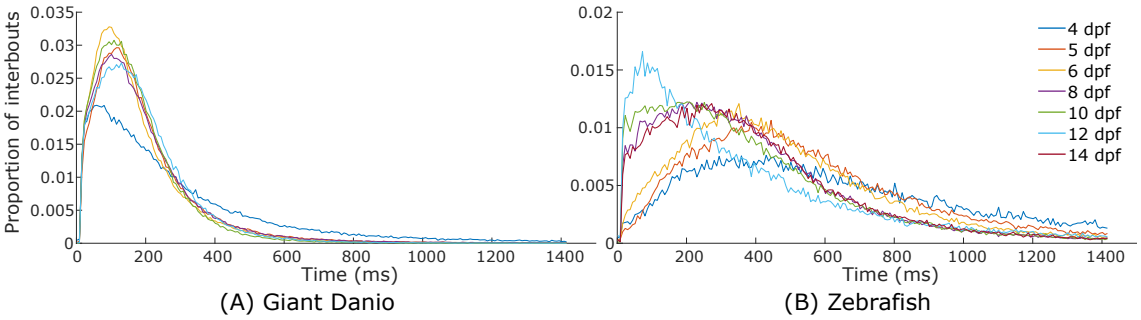

(A) Giant Danio

(B) Zebrafish

Figure 3.12: Interbout Interval over different developmental stages. (A) - Giant Danio larvae show very little variability of their IBI, increasing only the probability of performing IBI below 200 ms from 4 dpf onwards, from which the IBI remains identical up to 10 dpf; (B) - Tu Zebrafish larvae reduce their IBI with age. From 4 dpf to 6 dpf, they have higher probability of performing bouts with IBIs above 350 ms, and from 8 dpf onwards, they have higher probability of performing bouts with IBIs reduced to values between 200 and 300 ms.

show a shorter IBI than Tu Zebrafish larvae, with high probability of performing bouts with less than 200 ms IBI (fig. 3.12). Tu Zebrafish larvae show a reduction of the IBI with age, with higher probability of performing bouts with IBIs above 350 ms from 4 dpf to 6 dpf, and from 8dpf onwards, there is higher probability of performing bouts with IBIs reduced to values between 200 and 300 ms. Additionally, Giant Danio larvae, aside from 4 dpf larva, do not show much variability in their bout duration, remaining identical from 5 dpf to 10 dpf (fig. 3.13). In the case of Tu Zebrafish, as the fish develops, there is a clear shift, with bouts becoming shorter. In the end, both species have a similar bout duration.

The fact that Giant Danio larvae swim in a more continuous fashion, by performing more bouts with shorter IBI, could aid the larvae maneuverability while executing

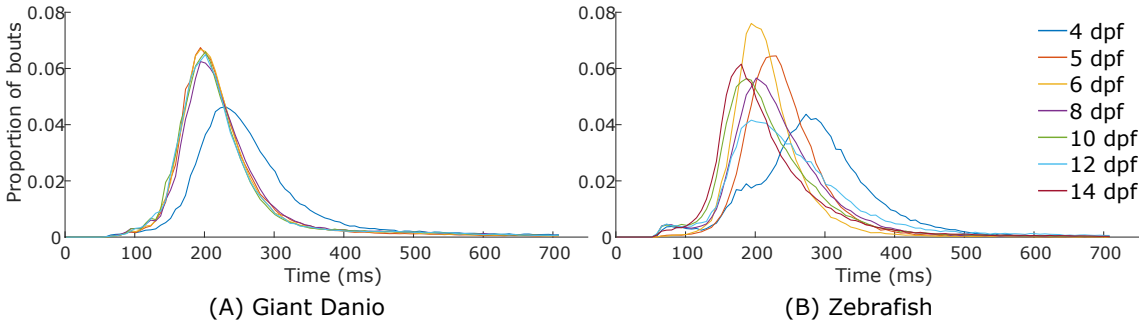

Figure 3.13: Bout Duration over different developmental stages. (A) - Giant Danio larvae show a reduction in their bout duration from 4 dpf to 5 dpf. From 5 dpf onwards, the bout duration remains identical; (B) - Tu Zebrafish show a clear shift in the bout duration as the fish develops, with bouts becoming shorter.

behaviors essential for its survival, especially prey capture.

3.2.3 Prey Capture

Prey capture is a critical behavior for the survival of larvae. Hunting and feeding has to start when their yolk supply has been mostly depleted. In Giant Danio, prey capture starts at 4 dpf, while on Zebrafish it starts one day later, at 5 dpf. To assess prey capture behavior, Tu Zebrafish and Giant Danio larvae, at 6 dpf and 5 dpf respectively, were recorded freely swimming while hunting rotifers, a common lab food for Zebrafish larvae. The developmental stage of the larvae to experience with was chosen so that all larvae had already been fed once, avoiding experimenting with naive larvae. Larvae were recorded freely swimming, one at a time, hunting live rotifers for 15 min. At the end of the experiment, the resulting video was analyzed manually, going through 9000 frames one-by-one, identifying whenever a rotifer was eaten.

Similar to the Zebrafish [71], in the Giant Danio every hunting event was initiated with the eye convergence response (both eyes rotate nasally), with high vergence angle, to locate a potential prey. Following eye convergence, the larvae maneuvered in relation to the rotifer with orienting turns similar to J-turns, coupled with pectoral fin movements. To complete the capture, in most cases larvae approached the rotifers and, once at striking distance of the rotifer, sucked the rotifers in. Movements resembling the Zebrafish larva capture-swim were rarely performed by Giant Danio larva. The few cases where the movements resembled the Zebrafish larva capture-swims, the full motion of the movement was not fully captured due to the short acquisition speed of the camera, and it was unclear if the larva actually captured the rotifer. This leads us to believe that, instead of performing capture-swims, which are based in a feeding strategy combining ram and suction feeding to be able to successfully capture and swallow the rotifer [69], they rely more on a feeding strategy closer to suction feeding. Like the Zebrafish, Giant Danio larva maintained a high eye vergence angle even some time after the rotifer was captured.

Analyzing the number of rotifers eaten (fig. 3.14), on average, per fish, Giant Danio ate 11 rotifers, while Zebrafish ate 7. In fact, in 15 min, Giant Danio ate approximately

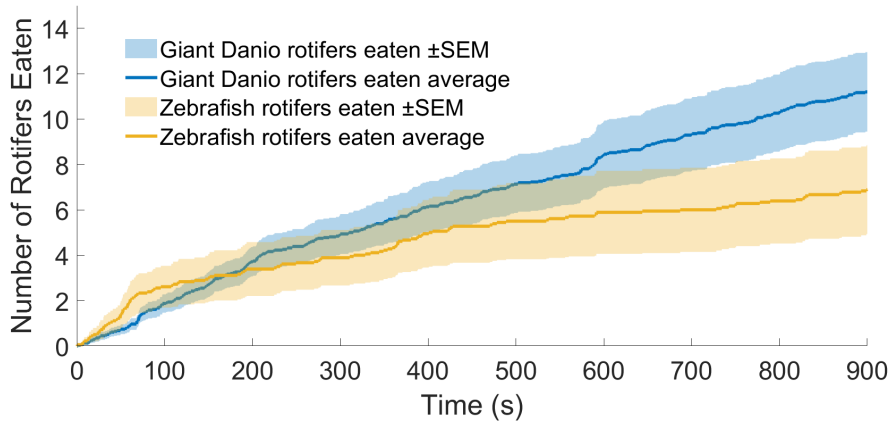

Figure 3.14: Average cumulative number of rotifers eaten per Giant Danio and Zebrafish larvae.

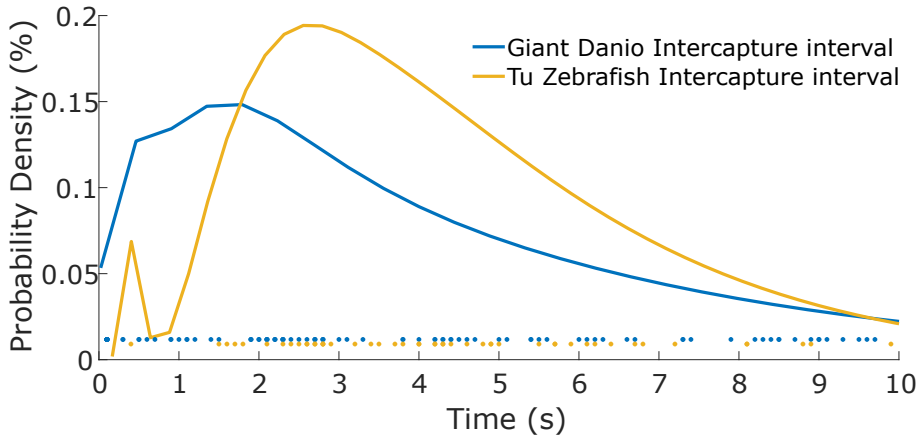

Figure 3.15: Giant Danio and Zebrafish larvae ICI. Giant Danio larvae manage to capture rotifers with ICI lower than 1 s, while Tu Zebrafish larvae never managed to capture rotifers with an ICI smaller than 1.5 s, with exception for one isolated case.

36 % more rotifers than Zebrafish. Even so, this difference was not significant (p=0.07). Furthermore, from the beginning of the experiments, Zebrafish showed more activity and captured more rotifers in the first 170 s of the experiment. After that, although Zebrafish kept on capturing rotifers, the number of captured rotifers did not increase greatly with time. The Giant Danio kept capturing rotifers throughout the experiment, without showing any clear variation in the level of predatory activity.

Examining the intercapture interval (ICI) (fig. 3.15), while Zebrafish larvae never managed to capture rotifers with an ICI smaller than 1.5 s, with exception for one isolated case, the Giant Danio larvae managed to capture rotifers with ICI lower than 1 s. Such short ICI could reflect a higher maneuverability of the Giant Danio larvae in early stages or could be related to the simple fact that they swim more continuously than Zebrafish larvae. Besides, the hunting method used by Giant Danio larvae which is more similar to a suction-feeding style, in comparison to the more common capture-swim of the Zebrafish larvae, could lead to Giant Danio larvae capturing rotifers with shorter ICIs. Additionally, when observing Giant Danio in a larger petri dish, they appeared to hunt more vigorously

raising the possibility that their behavior is inhibited in the confined arena used during the recordings.

Besides starting to capture prey one day earlier than Zebrafish, Giant Danio eat more rotifers and can capture them in shorter ICIs. After these results that further support how well Giant Danio perform different behaviors freely swimming, we were interested to test whether they can perform and show behavior traits in a partially restrained preparation suitable for in vivo physiology. Confirming that would allow us to move on to different behavior assays, and structural and functional imaging for neural recordings.

3.2.4 Head-Restrained Closed Loop Virtual Reality Optomotor Response

The Head-Restrained Closed Loop Virtual Reality Optomotor Response assay was used as a "proof of concept". Considering the wide application of head-restrained preparations and virtual reality environments with model organisms in neuroscience, especially with Zebrafish, it was of the utmost importance to see if the Giant Danio would show behavioral responses under such preparation and in a closed loop 3D virtual reality environment. The head-restrained condition of the fish was paired with the OMR in this assay, since the OMR is an innate behavior and previously was reliably elicited in freely-swimming Giants.

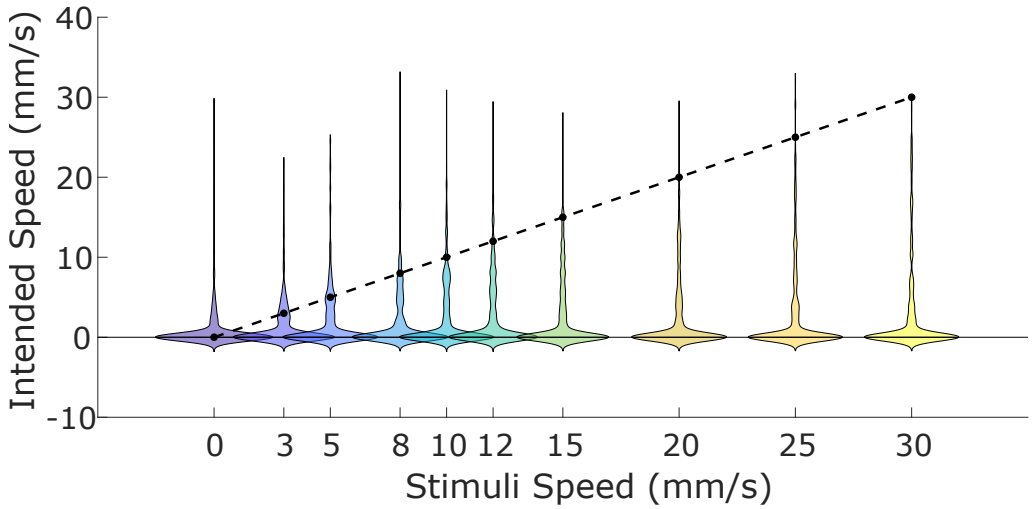

Figure 3.16: Full distribution of the Giant Danio larvae intended speed at each stimuli speed. Most of the larvae did not reliably perform a speed tuning to the stimuli speeds or performed the OMR. As the stimuli speed increases up to 15 mm/s, the larvae still show an intended swimming speed at the stimuli speed. At higher speeds, even though some larvae may have performed a speed tuning at those speeds, there is a higher probability of not having the larvae performing the OMR at such speeds. Black dots and dashed line represent a gain of 1.

Giant Danio larvae at 4 dpf and 5 dpf were recorded head-embedded, using the head-restrained behavior set-up. This was done to check if the larvae would perform the OMR and if the swimming kinematics, IBI, and number of bouts of the response would reflect what was observed in freely swimming fish. Lastly, larvae were left head-restrained overnight to see if they survived and or showed any signs of being affect by the

head-embedding.

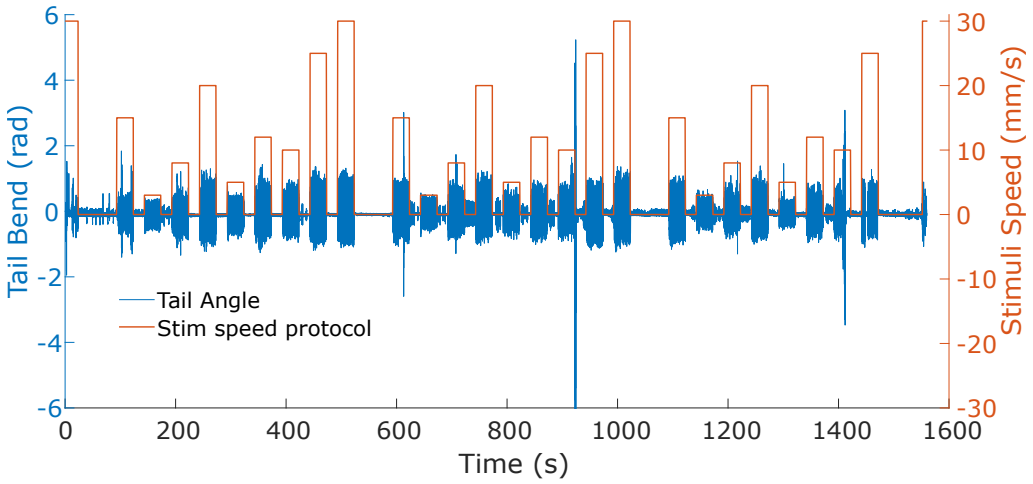

Figure 3.17: Example of a single tail end bend angle trace from a full head-restrained experiment where the larva closely tracks the changes in stimulus speed.

Soon after being head-embedded and having their tails freed, Giant Danio larvae showed signs of behaving under this preparation. Spontaneous swimming was observed before starting any experiment. Larvae performed the OMR when head-restrained, although not as consistently as in freely swimming fish. Observing the full distribution of the larvae intended speed at each stimuli speed in the violin plot (fig. 3.16), it becomes clear that most of the larvae did not reliably speed tune to the stimuli speeds or performed the OMR. While the highest probability is for larvae to be stationary, as the stimuli speeds increase from 3 mm/s to 15 mm/s, some still show an intended swimming speed at the stimuli speed. At higher speeds, although larvae still tracked the stimuli, the probability of having a larva swimming at speeds above 15 mm/s was reduced in comparison to lower speeds. Furthermore, observing only the tail end bend angle traces of the larvae during the whole experiment showed that, for those larvae that swam during stimulation, many times that there was no stimulation, the larvae remained stationary. A good example of an almost optimal response from a larva during an experiment is seen in the presented tail end bend angle trace (fig. 3.17), where the larva swam mostly only during stimulation and remained stationary during many of the ISI and the three 30 s stimulation repetitions of 0 mm/s stimuli speed.

Next, I want to see if some basic swimming kinematics, like the IBI or the number of bouts performed, varied with different stimuli speeds of the gratings presented. With the increase in the stimuli speed, larvae shortened their IBI and performed more bouts during the stimulation period of 30 s (fig. 3.18). This matches the swimming kinematics that were observed for freely moving larvae during the virtual open loop OMR assay (data not shown).

After the experiments, all larvae that were left head-restrained overnight survived and, once freed from the agarose, begin swimming without showing any signs of perturbation from being head-embedded (data not shown).

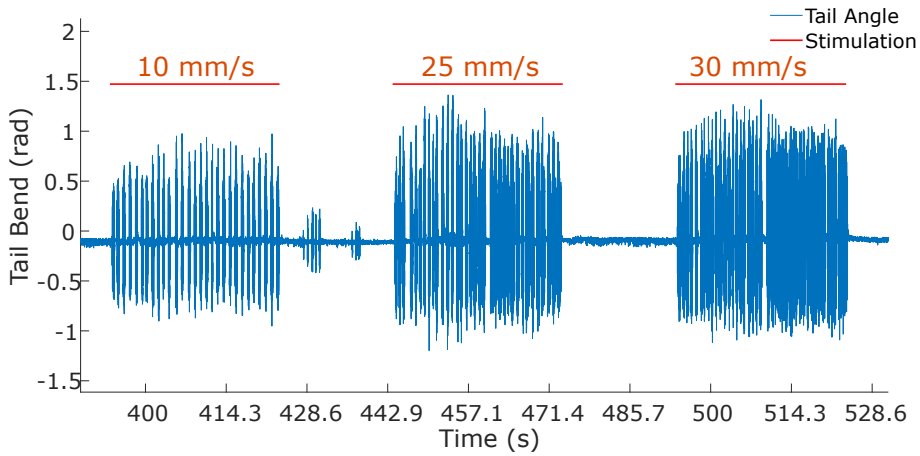

Figure 3.18: Single tail end bend angle trace during a sequence of three stimulation trials. With the increase in the stimuli speed, larvae shorten their IBI and perform more bouts during the stimulation period.

Overall, it was possible to get larvae showing swimming kinematics identical to what would be expected from freely swimming larvae, as well as showing good responses during stimulation. These observations validate this assay while at the same time showing the potential that the Giant Danio larvae hold in head-restrained preparations, coupled or not with closed loop virtual reality environments.

Chapter 4

Discussion

Throughout history, neuroscience research has relied on a wide range of animal taxa. Recently, this diversity of resources has been funneled down to a set of so-called standard model organisms, risking losing all that diversity has to offer in a comparative approach. Through comparative studies of non-model species, research based on standard model organisms could be complemented in such a way that would grant more refined results and improve our capacity to fully understand their significance. Plus, allying fish to neuroscience, given their diversity and wide use in research, brings the potential to unveil new insights on neural circuits and behavior, and how the vertebrate brain functions.

From all the fish models used in neuroscience, Zebrafish is considered to be among the standard model organisms and has a wide range of tools developed to use in research. As larvae, Zebrafish rely a lot on their vision during their development and show clear visually evoked behaviors: two responses to visual motion, the Optokinetic response (OKR) and the Optomotor response (OMR), a visual startle response, prey capture and visually evoked escape. Furthermore, Zebrafish larva show a very stereotyped and reproducible set of larval swim types (locomotor repertoire). The characterization of the Zebrafish locomotor repertoire in the existing literature revolved around identifying kinematically distinct categories of swim bouts [57, 69, 70, 79, 85, 88, 123–125]. Those works culminated, recently, in the classification of 13 types of swim bouts performed by Zebrafish [79]. This, together with the fact that larvae can be confined to shallow waters to reduce their behavior to a 2D plane, allows for a detailed and rich quantification of behavior.

Here, the Giant Danio, a phylogenetically close fish species to Zebrafish, is being introduced as a potential model for comparative studies with Zebrafish. The larvae of both species were compared for growth and tested with different behavior assays in order to compare the behavioral responses and swimming kinematics of both. Also, a brain template was made for the Giant Danio and the anatomy of the descending pathways

controlling locomotion was compared in both species. To do so, a systematic analysis to the different behaviors was applied to behavioral recordings; labelling techniques like retrograde labelling and immunohistochemical staining, coupled to confocal imaging, were used to study the anatomy of the descending pathways controlling locomotion and create the brain template; and computational algorithms developed by the lab were used to look at swimming kinematics. The results obtained during this project, as well as the methods applied to obtain them, will be further discussed within the frame of current knowledge and recent literature.

4.1 Anatomy

4.1.1 Growth

Larval total length was measured to have a clear idea of their growth rate of larvae from both species. This allowed to better define the developmental stages during which I wanted to study behavior, and to design and build arenas for behavior assays scaled according to the expected size of the larvae. Measurements were made from pictures taken daily, from 4 dpf to 14 dpf larvae, using a MATLAB (Mathworks, USA) script (see Fish Growth - methods section).

From the total length measurements made on Giant Danio and Zebrafish, it was possible to conclude that Giant Danio larvae had faster growth than Zebrafish (fig. 3.1). At 4 dpf Giant Danio larvae were almost 40 % bigger than Zebrafish larvae, and at 14 dpf they were more than 50 % bigger. This difference in size is even greater in adults, with Giant Danio being able to reach sizes up to 15 cm in total length [27], more than three times the size of an adult Zebrafish. Considering that Zebrafish can be found in the same habitat and share a similar diet with Giant Danio [28], this difference in size is most probably due to an evolutionary adaptation of both species to different water currents. It is possible that water current could, by itself, lead to major differences on body size and shape, and swimming ability, due to different selective pressures [126]. The major difference in the habitat conditions where both species were reported in the same place was the current, with Giant Danio occupying considerably faster current waters than Zebrafish, which remained in slow moving waters [28]. Studies in salmonids have shown that fish that habit arduous hydrodynamic conditions have a more fusiform body shape [8, 127], and that a deepening of the body to give a deep flat cross-section, together with a longer body, increases the mass of water displaced by the swimming motion of the fish, leading to greater thrust [128]. Therefore, the overall bigger size of the Giant Danio, along with a fusiform body and deeper body shape than Zebrafish, could provide similar advantages to the Giant Danio in faster moving waters.

The video recording technique applied to measure the fish has three mains advantages: being easy to apply – acquiring multiple figures for each fish is easy and not time consuming; not invasive – there is no need to anesthetize the fish and bring him out of the

water for measuring or further stress the fish with other equipment; and the measuring is automated. Even so, it carries some caveats. As the fish develops and becomes more active, a high-speed camera becomes necessary to capture images of fish without any tail bend. Then, multiple figures of each fish in every development stage are necessary in order to average the measurements of all of them. This is necessary because the fish will never be perfectly still and horizontal in the water column. In fact, the fish will often be tilted up or down, which would reduce considerably the total length being measured. Additionally, background luminance changes may create variations in pixel intensity that lead to mistakes during the computational measurement process. In those cases, measurement needs to be done by adjusting every parameter independently for every fish that was poorly measured and re-measure all the images with over or underestimated values. Despite these caveats, I believe this method gives accurate results, due to the large number of measurements that can be done to assess the total length of larvae, and the fact that often the measurements did not need to be manually corrected. Having established the overall growth rate of the fish, we wanted to get an understanding of the brain anatomy of the Giant Danio.

4.1.2 Brain Template

Brain templates are widely used nowadays as a spatial map reference for comparison and annotations of brain-wide information regarding cell morphology features, all the way to gene expression and physiological activity [116]. Furthermore, with such templates, bridging registrations to already existing Zebrafish standard atlases allows for importing information about the anatomical, functional, and molecular insights from Zebrafish.

Here, a shape-averaged brain template of the anti-tERK immunohistochemical stainings was made, for the first time, in Giant Danio (fig. 3.2). This template was made to be able to analyze the overall anatomy of the Giant Danio brain, so that it could eventually be bridged to a Zebrafish template and support the comparative approach. To build the template, a shape average image of the brain was generated from the registration of four Giant Danio immunohistochemical tERK stained brain confocal stacks into the same common space, using rigid, affine and non-rigid registration from the CMTK library. Furthermore, this registration process was shown to have good precision, through the landmark analysis (fig. 3.3, 3.4). Likewise, the originated template comes to show that, from the staining to the registration, the similarity of both fish goes beyond anatomy, allowing the same technique and protocol used for Zebrafish to be directly applied in the Giant Danio.

More than being the first time a brain template was made for Giant Danio, this template made clear how similar the Giant Danio and Zebrafish brains are. Comparing the anatomy of the brain with a tERK Zebrafish template from Zebrafish Brain Browser (ZBB) [116], the major anatomy of the brain is identical, with the Giant Danio brain being in general slightly more elongated and larger due to the bigger size of the fish. Some very

small differences in the shape can be noted, but these small differences could be due to the small amount of brains used for the registration of both the Giant template and the ZBB template. All the major structures are present, conserved in identical positions and clearly visible. Interestingly, while the two templates are generated from fish of similar age, the underlying motor circuits of the larvae, the reticulospinal neurons, are more visible in the Giant Danio than in the Zebrafish.

Even though it was possible to make the template, there are some limitations to the approach taken. During confocal imaging of the brains, the bigger volume of the Giant Danio makes it challenging to reach more ventral parts of the brain. For that reason, the Giant Danio template does not extend as ventral as the ZBB Zebrafish template. Regarding the registration process, the main weakness of the approach lies in the fact that there was a very limited number of brains to do the registration. Following on this, the landmark analysis for assessing the accuracy and precision of the registration would ideally be done with brains that were not used during the process of registration, thereby avoiding any bias due to the non-independence of the samples used for the statistical analysis.

Further improving the already existing template could be done by adding more brains and acquiring z-stacks that extend more ventrally in the brain. This would be key to get a more accurate and precise full spatial reference map of the Giant Danio, ready to use for mapping brain activity and bridging to Zebrafish templates. By doing so, I believe it will facilitate a better comparison of brain-wide information of both fish.

4.1.3 Backfills

Descending control signals sent from the brain to the spinal cord, often involving reticulospinal neurons, drive motor behaviors in vertebrates [129]. These neurons were initially classified and characterized in Zebrafish by Kimmel and his colleagues [117, 119, 122].

The retrograde labelling of the reticulospinal neurons on Giant Danio (fig. 3.5) was done by following already existing protocols for Zebrafish, with minor modifications to the protocol. The backfills were essential to analyze and characterize the underlying circuit structure of the descending motor system, considering that all visually evoked behavioral responses from the fish are expressed under the form of motor actions.

As was mentioned in the results, reticulospinal neurons in the Giant Danio are divided in a total of 7 clusters, arranged bilaterally and remaining approximately symmetrical in relation to the midline of the brain. The first and largest cluster lies in the nucleus of the Medial Longitudinal Fasciculus (nMLF), located in the midbrain, while the remaining 6 clusters are found in a segmental arrangement, regularly spaced, along the rostrocaudal axis of the hindbrain. This organization is identical to the one present in Zebrafish, in particular the arrangement found in the hindbrain [117, 119, 122]. Furthermore, this same organization of reticulospinal cells found in the hindbrain had previously been seen

in lampreys [130, 131] as well as in the adult eel *Anguilla*[1] [117], and was described as being considerably similar to the Zebrafish by Kimmel [122] and Metcalfe and colleagues [119]. This similarity, of the lamprey and *Anguilla* reticulospinal cells to the Zebrafish, has been referred as potentially homologous to the reticulospinal neurons of the Zebrafish by the same authors. In the same way and considering the phylogenetic proximity between the Giant Danio and the Zebrafish, such assumption could be made in this case as well.

Although no single-cell identification techniques like electroporation or sparse genetic labelling were used, cells that resemble the main cells found in every cluster on Zebrafish can be found in Giant Danio as well. For most of those cells, anatomy and location in the clusters is identical to the ones in Zebrafish, pointing towards them being homologs. In the midbrain – in the nMLF, a set of big cells resembling the MeL cells (MeLm, MeLr and MeLc in Zebrafish) can be found in the cluster, as well as a cell resembling the MeM1 cell in Zebrafish [122]. The same projections were seen in all cells, with exception for the homolog of the MeLc in the Giant Danio, which, additionally, presents a dendrite projecting contralaterally that is not present in the Zebrafish.

In the hindbrain, following the segmental arrangement (Ro1 to Ro7) – in Ro1, the sub-clusters of cells resemble the RoL1 and RoM1 cells in Zebrafish. Just like in the Zebrafish, between the Ro1 and Ro2 there is a division of the mlf into the dorsal mlf and ventral mlf. While in the Zebrafish the division begins in a similar position, in relation to the rostrocaudal axis, as the RoM1 cells [119], in the Giant Danio it was not possible to pinpoint the position where the division starts. In Ro2, a group of fusiform cells that resemble the RoM2 cells in Zebrafish could be identified [122]. Furthermore, one big cell found ventrally on the cluster showing an axonal projection that extends ventromedial and contralaterally to the cluster found on Ro3 is not present in the Zebrafish. In the same manner, the RoL2 and RoI2 cells present in the Zebrafish [119] were not seen in the Giant Danio backfills.

In Ro3, fusiform and rounded cells resembling the RoM3 and RoV3 cells in Zebrafish [122], respectively, can be found. More ventrally on the cluster, there are at least two cells that, unlike what is seen in the Zebrafish, seem to have contralateral projections to the opposite cluster. Moreover, in Zebrafish, there is one cell designated MiR1 [122]. In the Giant Danio, although not discarding the possibility that there exists a homolog cell to the Zebrafish MiR1, there wasn't any labelled cell resembling it.

The cluster of cells located in Ro4 is where we can see the Giant Danio Mauthner cell (M-cell), which highly resemble the ones in Zebrafish, as well as cells resembling the MiM1 and MiV1 cells of the Zebrafish [122]. Taking into account the fact that the M-cells are present in fish from all major groups of Gnathostoma (jawed craniates), and in one group of Agnatha (jawless craniate) – the lamprey [122], and considering the phylogenetic proximity between the Giant Danio and Zebrafish species, it would be expected for these

[1] data originally from Stefanelli, A., and Camposano, A. (1946). I Centri tegmentali dell'anguilla e le relazioni degli elementi giganti del tegmento dei ciclostomi, dei pesci e degli anfibi; ricerche sul sistema mauthneriano. Pub. Staz. Zool. Napoli 20:19-45; cited in Kimmel et al., 1982

cells to be highly homologous and similar. Such similarities, as well as the presence of the M-cell in various distinct groups of fish, is most likely due to the possibility that the M-cells arose in a common ancestor craniate to all known vertebrates [122]. Although they are very similar, one very distinctive characteristic of the M-cells in the Giant Danio, in relation to the ones found in Zebrafish, is the much larger diameter axon projection. This could be due to bigger size of fish and the behavioral responses where the M-cell is involved, like the startle response [87]. Increasing the cross-sectional area and volume of the neurons, translated into a bigger radius of the neuron, will reduce conduction time and increase the signal transmission speed, as well as the timing precision, which is key in regions where the time needs to be short and/or distance is great [132, 133], both of which can be applied to the M-cell, bearing in mind the larger size of the fish. Still in this cluster, some of the MiV1 resembling cells found in the Giant Danio have, apparently, contralateral projections from the medial aspect of the soma, which are not seen in Zebrafish. Notwithstanding the fact that the vestibular nucleus and its cells are not reticulospinal neurons, it is still worth to mention that its presence is clear in Ro4 and are identical to the Zebrafish [122], changing only the arrangement of the cells.

The cell clusters found in Ro5 and Ro6, excluding few exceptions, are identical to the Zebrafish ones in arrangement, anatomy and location [119, 122]. Ro5 cluster encompasses cells that resemble the MiD2 in Zebrafish, resembling them not only in anatomy and projections, but also in the number of cells that project contralaterally and ipsilaterally. More ventrally in the cluster, there is a clear group of cells that strongly resemble the MiV2 cells in Zebrafish. In this cluster, one clear difference to the Zebrafish was the absence of the MiR2 cells. Just like with the Zebrafish MiR1 cells, once again, although not discarding the possibility that there exists a homolog cell to the Zebrafish MiR1, no similar cells were labelled. Ro6 cells appear to be homologous to the MiD3 cells in Zebrafish, with the same number of cells projecting axons contralaterally and ipsilaterally.

The caudal region of the hindbrain, in Ro7, was the only segment of the hindbrain where in the Zebrafish there is a small cluster of cells [122], but no cluster was found in Giant Danio. Only some isolated cases of larger cells labelled in that region on the Giant Danio were found, but it was not conclusive whether they were homologous to the CaD or CaV cells of the Zebrafish cluster or not. Finally, in this region, like in Zebrafish, it is possible to see the ventral and dorsal divisions of the mlf merging [122].

Regarding the number of cells, even though no definitive cell count was done, and according to the definition of reticulospinal neuron given by Metcalfe and colleagues [119], cell numbers also seem to be very near the ones from the Zebrafish. In order to get a correct cell count, allying the already done backfills with nuclei stainings, like DAPI staining, of the labelled cells, would allow identification of different cells that may be tightly packed without clear definition of cell boundaries in the clusters.

In most of the cases where groups of cells present in the Zebrafish circuit weren't seen in the backfills, although the simplest explanation is that they don't exist in the Giant Danio, it remains quite likely that they exist but just weren't labelled. In previous

studies of the distribution of reticulospinal cells in higher fish groups, cells unique to any particular species were not identified [134], making it hard to believe that, between two very closely related fish species, unique cells or non-homologous cells would be present in the circuit. Furthermore, with the technique used in my experiment, more rostral injections (around the 5ft myomere) labeled more groups of cells that otherwise were rarely labelled, but at the same time lead to much lower survival rates of the larvae. Moreover, the lesion made in the spinal cord by the injection needs to be very localized, as well as capable of shearing the aimed projections, otherwise only partial labelling will be achieved. However, the bigger the lesion made, the higher the probability of the larvae not surviving. Further increasing the number of backfills done, with injections done in different regions of the spinal cord, will help clear this doubt. Additionally, registering these backfills into the brain template and bridging it to the zebrafish can reinforce the observations made or potentially lead to new insights regarding similarities or differences in the circuit.

The retrograde labelling worked in the Giant Danio with positive results, using a protocol and technique adapted directly from the Zebrafish. It is easy to employ, leading to the good labelling results obtained. But aside from the good results, the technique has some caveats to it. It is laborious to optimize, although once optimized it is very fast and a simple straightforward method to use. Furthermore, according to where in the rostrocaudal axis of the spinal cord the injections are done, as well as the extent of damage caused during the injection, different numbers of cells can be labeled, and different survival rates of larvae are achieved.

Overall, there is a striking resemblance of this circuit in both species, pointing towards a high homology of the circuit. Most of the major clusters of cells are found in the Giant Danio, with the general division and number of clusters being very well conserved, and with roughly similar organization. With such similarities in the underlying pathways, I wanted to see to what extent these similarities would translate into the different behavior assays used to test the larvae.

4.2 Behavior

4.2.1 Optomotor Response

The OMR is a visual stabilization behavior in response to whole-field motion where the larvae will turn and swim in the direction of the perceived motion [64]. In a laboratory experimental context, the OMR expressed by the larvae is an attempt to cancel the visual motion created by the stimuli presentation which ends up mimicking an illusory current [56]. In a wild habitat, the OMR showed by larvae is triggered by apparent motion of substrate underneath the fish or drifting particles passing by the fish [135]. The OMR has been studied in order to try and define a functional circuit and the sensorimotor transformations involved in the response [68], as well as in the context of psychophysical

and physiological characterization of vision [64, 136] and large-scale forward genetic screens for visuomotor defects [63, 137].

The Circular Optomotor Response behavior assay consists of a moving radial grating stimulus (fig. 2.6) projected in an arena with a circular track (Annex I.2). The stimulus was presented at different speeds. Every stimulus speed was projected 10 times, and every presentation lasted 1 min. The main difference and advantage of this assay in relation to other assays used to test the OMR in fish larva is that the fish are tested in a circular track without any opposition stopping them during stimulation. Thus, the long periods of stimulation would increase the probability of eliciting a response from the fish. That would ideally allow the fish to sustain the OMR for longer periods without finding a barrier to stop him, enabling him to fine tune the response the best it could to the perceived motion. This was used to compare the OMR in both species, as well as to look at the onset of the response, tracking vs non-tracking states and if the development of the larvae would bring a higher neural control of the response, leading to a more refined speed tuning to the perceived motion.

In response to the stimuli presented, the moving gratings, Zebrafish reliably elicited an OMR as early as 5 dpf (fig. 3.6, 3.7), as has been shown in [62]. Differently, Giant Danio, showed a reliable OMR as early as 4 dpf (fig. 3.6, 3.7). That earlier response from the Giant Danio is most likely due to their faster development.

In Zebrafish, no improvement in the OMR was seen with age (fig. 3.7). This result proved to be contradictory, since an improvement was expected. The prey-capture behavior in Zebrafish has been shown to improve as the larvae develop, since there is an improvement of the neural control of the predatory behavior [73]. Similarly, this has also been shown for the OKR [16]. The same was expected to be seen for the OMR. Ideally, the larvae would have shown a higher gain in their average speed and a better tune of the average speed to the stimulus speed as they developed. Contrasting this, the Giant Danio larvae did show some improvement with age, although this improvement was not seen all the way through to the older developmental stages tested (13 and 14 dpf) (fig. 3.7). In later developmental stages, it is possible that other sensory inputs start to aid the fish capacity to perceive what is happening in his surrounding environment and possibly even intervening as an inhibitory signal to the OMR.

During the behavior assay, the effects of the behavioral states of the larvae were very clear in their performance. There was a significant difference in the tracking state for all but one stimulus speed, 7 mm/s, in both species (fig. 3.8). In Zebrafish, larvae spent more time in a tracking state for lower stimulus speeds, especially for 7 mm/s. The non-tracking state of the Zebrafish followed the opposite trend to the tracking state. This was conserved in all three Zebrafish strains. In contrast, Giant Danio spent more time in a tracking state for speeds above 7 mm/s, while not really showing a stationary non-tracking state. Although not expected, there was no significant difference for the non-tracking state at any stimuli speed for both species(fig. 3.9). The differences from the tracking to the non-tracking state, particularly in Zebrafish, can be related to an

attempt to manage effort-expenditure. It has been shown that a prolonged stimulation that an animal cannot cope with, or that turns out to be inescapable, represents a stressful behavioral challenge and, in an attempt to best manage effort-expenditure in stressful scenarios, such challenges can lead the animals to change an active behavioral state to a passive coping behavioral state [138]. Once an action selected by the animal fails to counteract the challenge, it may choose to adaptively suppress the action. These transitions have been shown in Zebrafish, and a passive coping behavioral state response has been characterized by immobility [139]. Hence, at higher speeds that the fish struggles to keep up with, Zebrafish may be adopting a passive behavioral state. Furthermore, in a natural environment, motion at higher speeds may not have an ethological relevance, since Zebrafish are found in very slow moving waters [28], which would in turn promote a non-tracking state of the fish. This does not apply to the Giant Danio, considering that it is a fish used to faster currents than Zebrafish [28], which would allow the fish to remain far longer in a tracking state for the majority of the presented speeds.

Regarding speed tuning, Zebrafish larvae from the three strains tracked stimuli speeds up to 20 mm/s, although having higher probability of tracking lower speeds, and then plateaued (fig. 3.10). These observations are consistent with a previously published work where the authors suggested that the 20 mm/s represent an upper limit of what the fish may face in its natural environment [65]. From the Zebrafish strains, one of the wild-derived strains, the Anju, showed higher probability of tracking the projected stimuli at speeds of 20 mm/s and higher, which suggests that wilder fish may be able to show stronger and more reliable behavioral responses. The Giant Danio were able to track the motion of the projected gratings at higher speeds than Zebrafish (fig. 3.10). Per se, the ethological relevance in its natural environment supports the observations made for the Giant Danio, since the fish can be found in naturally faster flowing waters [28]. When it comes to slower speeds, up to 4 mm/s, the larvae show higher probability of swimming at higher speeds than the projected stimuli speed. Taking into account the natural ethological relevance and the larger size of the larvae, this suggests that the larvae do not modulate their swimming kinematics in order to reduce their swimming speed below what we consider to be their basal swimming speed (6 mm/s; observed when stimuli speeds were 0 mm/s). It is unknown whether the larvae grow in already fast-moving waters or if they face such slow currents, but this points towards the larvae being wired only to compensate waters above a baseline speed.

There were multiple times where larvae from both species swam in the opposite direction of the gratings (fig. 3.10). These events have not been addressed and remain as a question to why the fish apparently ignore the stimulation. Even though those events were very clear, they do not represent evidence that the larvae were purposely swimming against the gratings or ignoring the stimulation. If they were, more variation in their speed would be expected. The fact that whenever they are swimming in the opposite direction of the gratings, they have a higher probability of swimming at a constant speed,

independently of the projected stimuli speed, supports the idea of larvae being in a non-tracking behavioral state.

This novel behavior assay revealed itself to be an excellent tool for the study of speed tuning in the OMR, as well as the dissociation of tracking vs non-tracking behavioral states. The fact that it offers the fish an "infinite" track to swim in, during the entire course of a stimulus trial, remains as one of the main advantages that, coupled with a well-defined stimuli protocol and ease of data handling, allows for the acquisition of clean results that are consistent with already published data. Even so, it faces some limitations. It is highly specific for OMR and, applied in a set up like the one used here, does not allow for tracking the fish tail and acquisition of data from different kinematic parameters. Still, considering the limitations mentioned, it remains a valuable assay for the study of OMR.

A careful analysis of kinematic parameters would allow a better understanding and further support of the aforementioned results.

4.2.2 Swimming Kinematics

Zebrafish larvae swim by performing single locomotion events, consisting of specific patterns of body undulations – tail oscillations – in the horizontal plane. This locomotor pattern is characterized by swim bouts – short bursts of tail movement that propel the larvae – followed by interbout periods, where the larvae moves passively through the water [79]. The swimming kinematics of the Zebrafish have been thoroughly studied in the context of different behaviors [57, 70, 85, 88] and in different developmental stages [140].

Understanding how larvae swim and their basic swimming kinematics, for example bout duration and interbout interval (IBI), is a necessary step in order to compare larvae of both species. To do so, Tu Zebrafish and Giant Danio larvae were tested with the virtual open loop optomotor response assay, across multiple developmental stages – 4 dpf, 5 dpf, 6 dpf, 8 dpf and to 10 dpf for Giant Danio and 4 dpf, 5 dpf, 6 dpf, 8 dpf, 10 dpf, 12 dpf and 14 dpf for Zebrafish. With the high special resolution of the virtual open loop optomotor response assay, tracking the tail of the fish during each experiment allowed me to extract these kinematics.

Both species showed similar bout durations. While Tu Zebrafish show a clear and continuous shift towards shorter bouts as they develop (fig. 3.13), as was expected; in contrast, the Giant Danio only show a punctuated reduction of the bout duration from 4 dpf to 5 dpf, while after that it remains mostly unchanged (fig. 3.13). This could be due to a developmental switch, similar to the immature to mature locomotor pattern switch described for zebrafish from 3 dpf to 4 dpf [84].

It is possible that more than one switch in the locomotor pattern happens during development in the Giant Danio. For instance, Zebrafish larvae show a systematic development from 3 dpf where the fish maintains an immature locomotor pattern, to 4 dpf, where the fish can already sustain an active freely swimming behavior with a more

developed or mature locomotor pattern. Perhaps the Giant Danio larvae also show this switch from 3 dpf to 4 dpf as well as a switch from 4 dpf to 5 dpf, leading the fish to locomotor pattern characterized by shorter bouts. The combination of short swim bouts (fig. 3.13) with relatively short IBIs (fig. 3.12) allow the Giant Danio larvae to maintain a more continuous swimming style. Investigating if the same mechanisms involved in the Zebrafish 3 dpf to 4 dpf developmental switch are present and active on the Giant Danio, both from the 3 dpf to 4 dpf, and then from the 4 dpf to 5 dpf, would possibly allow us to understand if there is in fact another developmental switch happening and bring some light to how the swimming kinematics of different locomotor patterns from both species come to be and evolve with development.

As the larvae develop, they show a maturation in the length of their individual swim bouts. Similarly, the IBI in Giant Danio larvae (fig. 3.12) seems to also follow the mentioned developmental switch for the locomotion [84], again being visible from 4 dpf onwards. Although not varying much, specially from 5 dpf to 10 dpf, the difference of all those ages to the 4 dpf is that there is a higher probability of performing shorter IBIs. In comparison, Tu Zebrafish shows a clear and gradual reduction of the IBI as they develop (fig. 3.12). The developmental trajectory of the IBI follows the same trend that was observed for the bout duration in both species. Furthermore, Giant Danio, at all analyzed ages, generally perform shorter IBIs than Tu Zebrafish, even though the later can perform IBIs as short. This shorter IBIs performed by Giant Danio larvae reflect the natural conditions they habit in, as they will increase the overall locomotion by performing more bouts in a shorter period of time and compensate for faster moving waters.

Overall, Giant Danio appear to settle more rapidly into a stable mature locomotor swimming pattern, while zebrafish show a more gradual development, with clear changes as the larva gets older. This could reflect two different ways of coping with the habitat conditions that both species face. In the case of the Giant Danio, an earlier development of its swimming kinematics into a more mature form could bring advantages in dealing with the faster moving waters they inhabit [28], right from an early larval stage. For Zebrafish, the more forgiven slow moving waters they inhabit [28] may allow the larva to develop in a more gradual manner.

The priming of these swimming kinematics in both species are key for many innate behaviors that are expressed early on development from 4 dpf and 5 dpf onwards in Giant Danio and Zebrafish, respectively. A behavior where such developments of the swimming kinematics are crucial is prey capture, from which larvae depend on for their own survival and growth.

4.2.3 Prey Capture

Prey capture is, as the name implies, a behavior where larvae will hunt and catch live prey. It is also a behavior where, in early stages, larvae mostly rely on their vision [74]. Besides being a well-known behavior in Zebrafish, it has been analyzed in other larval fish,

like the Herring larvae (*Clupea harengus*) [141, 142], the Clownfish larvae (*Amphiprion perideraion*) [143], or the Carp larvae (*Cyprinus carpio*) [144], which show differences in the way they capture prey and the strategies used to do so [69]. In Zebrafish, the kinematics elements underlying an hunting event have already been described, from the initiation of an hunting event with the eye convergence response which last until after the prey has been captured [71], to the description of the approach swims and j-turns to maneuver and approach a prey, to the capture-swim to capture and swallow the prey [69, 70]. More recent works have been focusing on the visuomotor transformations and command systems involved in the prey capture behavior [145, 146].

The prey capture assay was used to assess the prey capture behavior of Tu Zebrafish and Giant Danio larvae, at 6 dpf and 5 dpf respectively. Larvae were recorded, one at a time, freely swimming while hunting rotifers, a common lab food for zebrafish larvae.

Giant Danio hunting routines closely resembled the ones from Zebrafish, as they were briefly described above. Hunting initiation, approach and orienting in relation to the prey to be at striking distance, and the maintenance of high vergence angle of the eyes even after capturing the prey, were extremely similar to what has been described for Zebrafish [69–71]. The only noticeable difference in the entire hunting routine lies in the capture strategy applied by the larvae. In the Giant Danio it was not evident that they performed capture-swims like described for Zebrafish, and they relied more on a strategy closer to a suction feeding. But considering that a suction feeding strategy has also been reported for Zebrafish [69, 85, 147], and the similarities in the entire hunting routine of both larva, I have a tendency to believe that a combination of a ram and suction feeding strategy, like the one used by Zebrafish, could in fact being used by the Giant Danio larvae.

In general, Giant Danio eat more rotifers than (fig. 3.14), and manage to capture more rotifers in shorter ICIs (fig. 3.15). The bigger size of the Giant Danio larvae, coupled with a faster development, would suggest that higher nutritional demands come into play and hence, the fact that they eat more rotifers was expected and add previously been observed when feeding the larvae during other experimental assays. The shorter ICIs don't necessarily have to do with the larger size of the larvae, or with the fact they can swim faster than the Zebrafish. Shorter ICI suggest that Giant Danio larvae have higher neural control of their swim bouts and, consequently, have higher maneuverability. This could be a consequence of a faster development.

The behavior assay used, although it allowed the observation of the hunting routines of the larva and acquisition of some basic parameters like number of eaten rotifers and the intercapture interval, has some limitations. The experiments, in case it was of interest to increase the time length of the assay, cannot be too long, otherwise water evaporation becomes a major issue and a stressing factor for the fish, invalidating all results. Furthermore, considering the larger size of the Giant Danio and more continuous swimming, the small arena used during the recordings may have been a constrain and inhibited their behavior. Devising a bigger arena for the assay will be a step further to try and optimize the assay.

4.2.4 Head-Restrained in Virtual Reality

Currently in neuroscience, head-restrained preparations and virtual reality environments are important tools for the study of animal behavior as a proxy for brain function and underlying neural circuits. The aim behind these tools is to convincingly replicate a subset of the stimuli that the animal would sense while freely moving with the recreation of that stimuli in a virtual environment [148]. Coupling a head-restrained preparation with a virtual reality environment offers the advantage of better controlling the stimulus used and allows the use of multiple high precision functional neural recording techniques [148]. These techniques could then be coupled with genetic reporters or photoactivated proteins with optogenetics, as well as neuron ablations and other perturbations [148–150]. All of those would be, although not impossible, extremely hard to apply in behavioral assays with freely moving animals. Furthermore, these preparations have been widely used in larval zebrafish where visual behaviors like OMR, OKR, prey capture, and visual escape responses have been reproduced with movement sequences closely resembling the ones observed in freely swimming larva [66, 75, 150, 151].

Bearing the above mentioned in mind, the Head-Restrained Closed Loop Virtual Reality Optomotor Response assay was used as "proof of concept" in order to see if the Giant Danio larvae would show any behavioral responses in such preparations. Head-embedded Giant Danio larvae at 4 dpf and 5 dpf were tested to see if they performed the OMR in a 3D virtual reality environment and were left embedded overnight. The goal was to observe if the larva would respond to the stimulation while showing naturalistic sequences of movements with swimming kinematics that would match the observed ones in freely swimming larvae. It was also important to test for their survival overnight when head-embedded, as some future behavioral experiments may require the larvae to be embedded overnight and used the next morning.

Giant Danio larvae showed a positive response to the Head-Restrained Closed Loop Virtual Reality Optomotor Response assay, with larvae performing the OMR at different stimuli speeds (fig. 3.16). These results allowed a comparative analysis of the head-restrained locomotor output with the freely swimming data obtained with other experiments. In the head-restrained larvae there was a clear modulation of the IBI and number of bouts performed according to the stimuli speed being projected, which was identical to what was already observed in freely swimming larvae during the Virtual Open Loop Optomotor Response assay, further supporting the fidelity of the acquired data. Furthermore, similar observations have been made in Zebrafish, with the larvae modulating various swimming kinematics according to the stimuli speed [65, 66]. Such observations support the positive results obtained.

Although there was a clear response, most of the larva had low locomotor activity (fig. 3.16). This low locomotor activity match observations made in Zebrafish larva in identical conditions, where the activity of the larvae was limited in head-restrained preparations, with larvae performing less bouts than in freely swimming assays [71, 145, 151, 152].

This reduced motor activity in a head-restrained preparation could be due to mechanical constrains or stress induced by the immobilization caused from being embedded, or due to a lack of sensory feedback from non-visual modalities [152].

Even though restraining an animal may not be the best method for studying behavior and locomotion, the experiments succeeded and validated the use of Giant Danio larvae in head-restrained preparations and in a 3D virtual reality environment. The way this behavior assay was conducted leaves space for improvement and optimization in some key aspects. Only one gain for the feedback of the closed loop was tested, without any clear notion if it would be the ideal or not. Adjusting the gain to better suit the Giant Danio response may lead to more consistent responses from the fish. It has been shown in Zebrafish that having a sub-optimal gain in virtual reality environments where the swim attempts do not lead to the expected visual flow can make the larva go into a passive coping behavior state and give up on its actions [153]. The selected stimuli speeds were based on other work from the lab and available literature from Zebrafish [65, 66], and can be fine-tuned to speeds more prone to elicit the desired response from the Giant Danio larvae. Only early larval stages were tested (4 dpf and 5 dpf), leaving the possibility of seeing better responses from older larva. In spite of the optimization that can be made to the assay, the obtained results still remain a hallmark, proving that Giant Danio can be a valid model for functional neural recordings and the study of brain function and underlying neural circuits, as well as for comparative studies with Zebrafish and validation of previous observations made with Zebrafish larva under similar conditions.

Chapter 5

Conclusions

The Giant Danio, although known to science, was an unknown model to behavioral neuroscience up until now. It is the largest danionin teleost fish [92] and stands phylogenetically close to the Zebrafish [89, 90]. Both models can be found sharing similar habitat and ecological niche, although the Giant Danio is found in faster water currents [28]. Furthermore, just like the Zebrafish, the Giant Danio possesses characteristics desirable in a research model (see section 1.6). Altogether, this makes the Giant Danio a strong candidate for a research model, both on its own strengths and for its potential as a comparative model for Zebrafish. Motivated by this, I applied a systematic analysis to the behavior and underlying motor system of the Giant Danio and the Zebrafish, to try to answer three main questions: i) do both species have similar locomotor characteristics; ii) do Zebrafish and Giant Danio have similar underlying motor system structure; iii) will differences in the underlying motor system structure reflect differences in visually guided behaviors?

Using already existing tools in the lab, paired with a simple method devised to facilitate and automate the measurement of larvae, the growth of the larvae from both species was studied. The results showed a faster development of the Giant Danio larva such that Giants had larger sizes than Zebrafish at the same times post-fertilization right from early developmental stages (fig. 3.1). This laid the foundation for the entirety of the remaining work to be developed during the project, by allowing me to set the specific ages that I wanted to work with the larvae. With this knowledge I adapted behavior set-ups accordingly, as well as building arenas scaled to fit the different sizes I knew to expect during development.

After comparing their growth and size in different developmental stages, it was necessary to see if basic tools developed to look at the brain structure and anatomy of the

Zebrafish could be directly applied to the Giant Danio. Using the tERK immunohistochemistry staining protocol applied to Zebrafish [113], I showed that the tERK immunohistochemistry staining works in Giant Danio, and that all the major brain structures are present and conserved in identical positions. I also made, for the first time, a brain template in this model organism (fig. 3.2). This supports the idea that already developed tools for Zebrafish can be directly applied or adapted to the Giant Danio.

Following on the brain template, a protocol and technique from Zebrafish for the retrograde labelling of the reticulospinal neurons [110, 153] was successfully adapted to be used in the Giant Danio. From these preparations, I compared the reticulospinal neurons of the Giant Danio (fig. 3.5) to the Zebrafish, which have already been fully characterized in published literature [117, 119, 122]. From this comparison came the conclusion that there is a high similarity of this circuit in both species, with the number of cell clusters, general division and organization being very well conserved, and indicating a high homology of the circuit. Such similarity of the circuits further adds evidence that the Giant Danio is a good model for comparative studies with Zebrafish.

Lastly, knowing how similar the motor circuits are, Giant Danio and Zebrafish were tested in multiple behavior assays in order to compare their locomotor behavior. Larvae were tested in their Optomotor response (OMR) and prey capture behavior. In order to look at the OMR for extended periods, a novel assay was devised, the circular OMR. The other assays used were adaptations from already existing protocols to provide further validation of the behavioral similarities and differences between the species. The Giant Danio showed both behaviors with clear responses and when compared to the Zebrafish, with better performance. When testing the OMR, the Giant Danio larvae have an earlier onset of the response (fig. 3.6), and show a more consistent response, following the stimuli for longer (fig. 3.8), with higher average speeds (fig. 3.7) and doing a better speed tuning at higher motion speeds than the Zebrafish (fig. 3.10). While Giant danio were observed to have a bout duration similar to Zebrafish (fig. 3.13), their interbout interval was shorter (fig. 3.12); these swimming kinematics allowed them to perform almost twice as many bouts as Zebrafish in the same time. Shorter IBIs and an apparent better maneuverability allowed the Giant Danio to have higher performance in the prey capture behavior assay, catching more rotifers (fig. 3.14) with shorter inter-capture intervals (fig. 3.15). Furthermore, the hunting routine observed for the Giant Danio was similar to the Zebrafish, with the initiation, approach, orientation and eye vergence being alike. Together, these results suggest that the Giant Danio has higher neural control of their swim bouts than Zebrafish. The Giant Danio was also tested in a head-restrained preparation and 3D virtual environment, where clear behavioral responses were observed, validating its use under such preparations which allow the use of fine techniques for functional imaging and neural recordings. Considering the observations of the locomotor behavior of both species, they represent strong evidence that the similarities in the underlying motor circuits structure reflect the behavior of the larvae. The differences found are most likely related to physiological differences at celular level in the circuits.

From this work, I have introduced the Giant Danio as a non-standard model organism for behavioral neuroscience that offers a rich behavioral repertoire, similar underlying motor circuits to the Zebrafish, larger neurons and faster development, making it a suitable model for comparative studies with Zebrafish as well as a promising model on its own.

Chapter 6

Future Perspectives

In this chapter, brief insight over future work and perspectives will be given.

6.1 Brain Template

The current Giant Danio brain template incorporated four brains into the template. Even though the achieved result is good, follow up to further increase the number of brain z-stacks up to 10 brains would be ideal. A necessary task will be to find ways to image deeper into the larger brain, possibly trying the RTF clearing method [154], in order to acquire the full extent of the ventral part of the Giant Danio brain to make a more reliable brain template. After that, a bridging registration to a Zebrafish template can be done. Furthermore, knowing that the tERK staining is already very good, it would be interesting to do stainings against neurotransmitters to add further richness of detail to the anatomy of the Giant Danio. Lastly, I would like to see how particular populations of interneurons are distributed in the fish central nervous system.

6.2 Reticulospinal neurons

Although it was possible to do a simple characterization of the reticulospinal neurons of the Giant Danio with the observed backfills, continuing this work to complete the characterizations of those circuits in the Giant Danio larvae is essential. To further improve the already good characterization achieved, performing nuclear stainings, perhaps using a DAPI conterstain, will allow a more correct and clear cell counts of each cluster of cells. Following, performing a more specific labelling of specific clusters or cells from the circuit may allow us to understand where do different cells or different clusters project their axons to. Understanding this may provide new insights towards understanding

how different bouts are generated and which clusters or cells may be directly involved in specific bout types. And so, two ways this could be achieved would be by injecting at different locations along Rostro-Caudal or Dorso-Ventral axes for more extensive retrograde lebelling and injecting in the brain at different rhombomeres for anterograde labelling. Finally, more specific backfills might allow for interesting filling with synthetic calcium indicators, and therefore allow a functional view of each cluster.

6.3 Behavior

Giant Danio larvae were tested for two behaviors: OMR and prey capture. The Giant Danio showed a robust response, following stimuli speeds up to 40 mm/s without apparent difficulty. Understanding their limit and capacity by increasing the stimuli speeds above 40 mm/s remains an experiment to be done, also as a way to fully understand and unveil their swimming kinematics. The prey capture assay needs to be optimized, possibly with a different arena and protocol that bring less constrains on the fish. Tracking the eyes and tail of the larvae during the prey capture behavior will be necessary, in order to be able to characterize their swimming kinematic parameters and compare them to the Zebrafish.

More behaviors remain to be tested in order to fully grasp their behavioral repertoire and further reveal the richness of their behavioral and locomotor repertoire. Behaviors like the OKR, phototaxis, looming escape response (visually evoked escape) and visual startle response are some of the behaviors that remain to be tested and characterized in the Giant Danio.

6.4 The Giant Danio Locomotor Repertoire

One of the major remaining goals is to classify and characterize the locomotor repertoire of the Giant Danio. A vast data-set with a wide variety of conditions and behaviors is mandatory in order to analyse all the kinematic parameters necessary and try to classify the entire locomotor repertoire of Giant Danio larvae. A large data-set is already being acquired and built so that we can have as many bouts as possible, in different conditions, to which we can then apply the lab existing tools to do the classification of the Giant Danio larval bouts. Here, the importance of having a large data-set that covers multiple conditions is stressed, since different behaviors will provide, in many cases, different and more specific bouts that the fish may only execute under special conditions. Such specific bouts have been classified in the Zebrafish, like the O-bend that the larvae perform during sudden luminance changes, or the SLC and LLC bouts performed during escape responses [79].

6.5 The Giant Danio and Neuroscience

The Giant Danio holds the potential to become a research model in neuroscience. Using behavior as a proxy to understand the brain, I believe that studying the Giant Danio visually guided behaviors and underlying neural circuits may shed some light on the current knowledge from Zebrafish as well as on how the brain interprets visual stimulation and converts that information into motor responses. More future work lies with the development of mutants and transgenic lines, and the use of cell ablation, brain functional imaging and neural recordings to further advance our understanding of the brain function.

Bibliography

[1] E. Marder. "Non-mammalian models for studying neural development and function." In: *Nature* 417 (2002), pp. 318–321.

[2] E Knudsen. "Early Auditory Experience Aligns the Auditory Map of Space in the Optic Tectum of the Barn Owl." In: *Advancement Of Science* 222 (1983), pp. 939–942.

[3] A. Feng, J. Simmons, and S. Kick. "Echo detection and target-ranging neurons in the auditory system of the bat Eptesicus fuscus." In: *Science* 202 (1978), pp. 645–648.

[4] M. M. Yartsev. "The emperor's new wardrobe: Rebalancing diversity of animal models in neuroscience research." In: *Science* 358 (2017), pp. 466–469. ISSN: 10959203.

[5] E. R. Kandel. "The Molecular Biology of Memory Storage: A Dialogue Between Genes and Synapses." In: *Science* 294 (2001), pp. 1030–1038.

[6] S. Grillner. "The motor infrastructure: From ion channels to neuronal networks." In: *Nature Reviews Neuroscience* 4 (2003), pp. 573–586.

[7] E. A. Brenowitz and H. H. Zakon. "Emerging from the bottleneck: Benefits of the comparative approach to modern neuroscience." In: *Trends in Neurosciences* 38 (2015), pp. 273–278.

[8] B. E. Riddell and W. C. Leggett. " Evidence of an Adaptive Basis for Geographic Variation in Body Morphology and Time of Downstream Migration of Juvenile Atlantic Salmon (Salmo salar)." In: *Canadian Journal of Fisheries and Aquatic Sciences* 38 (1981), pp. 308–320.

[9] H. Yang, T. A. Bell, G. A. Churchill, and F. Pardo-Manuel De Villena. "On the subspecific origin of the laboratory mouse." In: *Nature Genetics* 39 (2007), pp. 1100–1107.

[10] J. Keifer and C. H. Summers. "Putting the "biology" back into "neurobiology": The strength of diversity in animal model systems for neuroscience research." In: *Frontiers in Systems Neuroscience* 10 (2016), pp. 1–9.

[11] L. Shmuelof and J. W. Krakauer. "Are we ready for a natural history of motor learning?" In: *Neuron* 72 (2011), pp. 469–476.

[12] R. Gerlai. "Fish in behavior research: Unique tools with a great promise!" In: *Journal of Neuroscience Methods* 234 (2014), pp. 54–58.

[13] T. H. Bullock, K. Behrend, and W. Heiligenberg. "Comparison of the jamming avoidance responses in Gymnotoid and Gymnarchid electric fish: A case of convergent evolution of behavior and its sensory basis." In: *Journal of comparative physiology* 103.1 (1975), pp. 97–121.

[14] M. E. Hale. "Mapping circuits beyond the models: Integrating connectomics and comparative neuroscience." In: *Neuron* 83 (2014), pp. 1256–1258.

[15] Z. J. Hall, A. R. De Serrano, F. H. Rodd, and V. Tropepe. "Casting a wider fish net on animal models in neuropsychiatric research." In: *Progress in Neuro-Psychopharmacology and Biological Psychiatry* 55 (2014), pp. 7–15.

[16] J. C. Beck, E. Gilland, D. W. Tank, and R. Baker. "Quantifying the ontogeny of optokinetic and vestibuloocular behaviors in zebrafish, medaka, and goldfish." In: *Journal of Neurophysiology* 92 (2004), pp. 3546–3561.

[17] K. E. Fujimori. "Characterization of the regulatory region of the dopa decarboxylase gene in Medaka: An in vivo green fluorescent protein reporter assay combined with a simple TA-cloning method." In: *Molecular Biotechnology* 41 (2009), pp. 224–235.

[18] L. Schulze, J. Henninger, M. Kadobianskyi, T. Chaigne, A. I. Faustino, N. Hakiy, S. Albadri, M. Schuelke, L. Maler, F. Del Bene, and B. Judkewitz. "Transparent Danionella translucida as a genetically tractable vertebrate brain model." In: *Nature Methods* 15 (2018), pp. 977–983.

[19] N. J. Dingemanse, J. Wright, A. J. Kazem, D. K. Thomas, R. Hickling, and N. Dawnay. "Behavioural syndromes differ predictably between 12 populations of three-spined stickleback." In: *Journal of Animal Ecology* 76 (2007), pp. 1128–1138.

[20] W. H. Norton and H. C. Gutiérrez. "The three-spined stickleback as a model for behavioural neuroscience." In: *PLoS ONE* 14 (2019), pp. 1–18.

[21] L. A. O'Connell, M. R. Fontenot, and H. A. Hofmann. "Neurochemical profiling of dopaminergic neurons in the forebrain of a cichlid fish, Astatotilapia burtoni." In: *Journal of Chemical Neuroanatomy* 47 (2013), pp. 106–115.

[22] K. P. Maruska and R. D. Fernald. "Astatotilapia burtoni: A Model System for Analyzing the Neurobiology of Behavior." In: *ACS Chemical Neuroscience* 9 (2018), pp. 1951–1962.

[23] H. Hinaux, S. Rétaux, and Y. Elipot. "Social Behavior and Aggressiveness in Astyanax." In: *Biology and Evolution of the Mexican Cavefish*. Ed. by A. C. Keene, M. Yoshizawa, and S. E. McGaugh. Academic Press, 2016. Chap. 17, pp. 335 –359. ISBN: 978-0-12-802148-4.

[24] S. Rétaux, A. Alié, M. Blin, L. Devos, Y. Elipot, and H. Hinaux. "Neural Development and Evolution in Astyanax mexicanus: Comparing Cavefish and Surface Fish Brains." In: *Biology and Evolution of the Mexican Cavefish*. Ed. by A. C. Keene, M. Yoshizawa, and S. E. McGaugh. Academic Press, 2016. Chap. 12, pp. 227 –244. ISBN: 978-0-12-802148-4.

[25] M. Beltramo, M. Krieger, Y. Tillet, J. Thibault, A. Calas, V. Mazzi, and M. F. Franzoni. "Immunolocalization of aromatic L-amino acid decarboxylase in goldfish (Carassius auratus) brain." In: *Journal of Comparative Neurology* 343 (1994), pp. 209–227.

[26] C. Maximino, R. X.d. C. Silva, S. D.N. S. Da Silva, L. D.S.D. S. Rodrigues, H. Barbosa, T. S. De Carvalho, L. K.D. R. Leão, M. G. Lima, K. R. M. Oliveira, and A. M. Herculano. "Non-mammalian models in behavioral neuroscience: Consequences for biological psychiatry." In: *Frontiers in Behavioral Neuroscience* 9 (2015), pp. 1–21.

[27] P. K Talwar and A. G Jhingran. *Inland fishes of India and adjacent countries*. English. OCLC: 25796005. Rotterdam: A.A. Balkema, 1992. ISBN: 978-90-6191-164-7 978-90-6191-162-3.

[28] M. M. McClure, P. B. McIntyre, and A. R. McCune. "Notes on the natural diet and habitat of eight danionin fishes, including the zebrafish Danio rerio." In: *Journal of Fish Biology* 69 (2006), pp. 553–570.

[29] R. Spence, G. Gerlach, C. Lawrence, and C. Smith. "The behaviour and ecology of the zebrafish, Danio rerio." In: *Biological Reviews* 83 (2008), pp. 13–34.

[30] G. Sumbre and G. G. de Polavieja. "The world according to zebrafish: how neural circuits generate behavior." In: *Frontiers in neural circuits* 8 (2014), p. 91.

[31] G. Streisinger, C. Walker, N. Dower, D. Knauber, and F. Singer. "Production of clones of homozygous diploid zebra fish (Brachydanio rerio)." In: *Nature* 291 (1981), pp. 293–296.

[32] G. Streisinger, F. Coale, C. Taggart, C. Walker, and D. J. Grunwald. "Clonal origins of cells in the pigmented retina of the zebrafish eye." In: *Developmental Biology* 131 (1989), pp. 60–69.

[33] W. Driever, L. Solnica-Krezel, A. F. Schier, S. C. Neuhauss, J. Malicki, D. L. Stemple, D. Y. Stainier, F. Zwartkruis, S. Abdelilah, Z. Rangini, J. Belak, and C. Boggs. "A genetic screen for mutations affecting embryogenesis in zebrafish." In: *Development* 123 (1996), pp. 37–46.

[34] K. Howe et al. "The zebrafish reference genome sequence and its relationship to the human genome." In: *Nature* 496 (2013), pp. 498–503.

[35] A. M. Stewart, O. Braubach, J. Spitsbergen, R. Gerlai, and A. V. Kalueff. "Zebrafish models for translational neuroscience research: From tank to bedside." In: *Trends in Neurosciences* 37 (2014), pp. 264–278.

[36] D. L. McLean and J. R. Fetcho. "Ontogeny and innervation patterns of dopaminergic, noradrenergic, and serotonergic neurons in larval zebrafish." In: *Journal of Comparative Neurology* 480 (2004), pp. 38–56.

[37] A. Filippi, J. Mahler, J. Schweitzer, and W. Driever. "Expression of the paralogous tyrosine hydroxylase encoding genes th1 and th2 reveals the full complement of dopaminergic and noradrenergic neurons in zebrafish larval and juvenile brain." In: *Journal of Comparative Neurology* 518 (2010), pp. 423–438.

[38] A. V. Kalueff, A. M. Stewart, and R. Gerlai. "Zebrafish as an emerging model for studying complex brain disorders." In: *Trends in Pharmacological Sciences* 35 (2014), pp. 63–75.

[39] W. Y. Hwang, Y. Fu, D. Reyon, M. L. Maeder, S. Q. Tsai, J. D. Sander, R. T. Peterson, J. J. Yeh, and J. K. Joung. "Efficient genome editing in zebrafish using a CRISPR-Cas system." In: *Nature biotechnology* 31.3 (2013), p. 227.

[40] T. O. Auer, K. Duroure, A. De Cian, J.-P. Concordet, and F. Del Bene. "Highly efficient CRISPR/Cas9-mediated knock-in in zebrafish by homology-independent DNA repair." In: *Genome research* 24.1 (2014), pp. 142–153.

[41] M. B. Orger and G. G. de Polavieja. "Zebrafish behavior: opportunities and challenges." In: *Annual review of neuroscience* 40 (2017), pp. 125–147.

[42] P. McGonigle and B. Ruggeri. "Animal models of human disease: Challenges in enabling translation." In: *Biochemical Pharmacology* 87 (2014), pp. 162–171.

[43] A. M. Stewart, D. Desmond, E. Kyzar, S. Gaikwad, A. Roth, R. Riehl, C. Collins, L. Monnig, J. Green, and A. V. Kalueff. "Perspectives of zebrafish models of epilepsy: What, how and where next?" In: *Brain Research Bulletin* 87 (2012), pp. 135–143.

[44] A. M. Stewart, M. Nguyen, K. Wong, M. K. Poudel, and A. V. Kalueff. "Developing zebrafish models of autism spectrum disorder (ASD)." In: *Progress in Neuro-Psychopharmacology and Biological Psychiatry* 50 (2014), pp. 27–36.

[45] B. D. Fontana, N. J. Mezzomo, A. V. Kalueff, and D. B. Rosemberg. "The developing utility of zebrafish models of neurological and neuropsychiatric disorders: A critical review." In: *Experimental Neurology* 299 (2018), pp. 157–171.

[46] R. L. Vaz, T. F. Outeiro, and J. J. Ferreira. "Zebrafish as an animal model for drug discovery in Parkinson's disease and other movement disorders: A systematic review." In: *Frontiers in Neurology* 9 (2018).

[47] R. W. Friedrich, G. A. Jacobson, and P. Zhu. "Circuit Neuroscience in Zebrafish." In: *Current Biology* 20 (2010), pp. 371–381.

[48] M. B. Ahrens and F. Engert. "Large-scale imaging in small brains." In: *Current Opinion in Neurobiology* 32 (2015), pp. 78–86.

[49] M. B. Ahrens, J. M. Li, M. B. Orger, D. N. Robson, F Alexander, A. F. Schier, F. Engert, R. Portugues, and F Alexander. "Brain-wide neuronal dynamics during motor adaptation in Zebrafish." In: *Nature* 485 (2013), pp. 471–477.

[50] G. Nagel, D. Ollig, M. Fuhrmann, S. Kateriya, A. M. Musti, E. Bamberg, and P. Hegemann. "Channelrhodopsin-1: A light-gated proton channel in green algae." In: *Science* 296 (2002), pp. 2395–2398.

[51] A Nakai, Junichi and Ohkura, Masamichi and Imoto, Keiji. "A high signal-to-noise Ca2+ probe composed of a single green fluorescent protein." In: *Nature Biotechnology* 19 (2001), pp. 137–141.

[52] S. C. Neuhauss. "Behavioral genetic approaches to visual system development and function in zebrafish." In: *Journal of Neurobiology* 54 (2003), pp. 148–160.

[53] M. B. Orger. "The Cellular Organization of Zebrafish Visuomotor Circuits." In: *Current Biology* 26 (2016), pp. 377–385.

[54] S. S. Easter and G. N. Nicola. "The Development of Vision in the Zebrafish (Danio rerio)." In: 663 (1996), pp. 646–663.

[55] S. S. Easter and G. N. Nicola. "The Development of Eye Movements in the Zebrafish (Danio rerio)." In: *Developmental Psychobiology* 31 (1997), pp. 267–276.

[56] M. B. Orger and H. Baier. "Channeling of red and green cone inputs to the zebrafish optomotor response." In: *Visual neuroscience* 22.3 (2005), pp. 275–281.

[57] H. A. Burgess and M. Granato. "Modulation of locomotor activity in larval zebrafish during light adaptation." In: *Journal of Experimental Biology* 210 (2007), pp. 2526–2539.

[58] X. Chen and F. Engert. "Navigational strategies underlying phototaxis in larval zebrafish." In: *Frontiers in Systems Neuroscience* 8 (2014), pp. 1–13.

[59] H. A. Burgess, H. Schoch, and M. Granato. "Distinct Retinal Pathways Drive Spatial Orientation Behaviors in Zebrafish Navigation." In: *Current Biology* 20 (2010), pp. 381–386.

[60] J. D. Burrill and S. S. Easter. "Development of the retinofugal projections in the embryonic and larval zebrafish (Brachydanio rerio)." In: *Journal of Comparative Neurology* 346 (1994), pp. 583–600.

[61] R. Portugues, C. E. Feierstein, F. Engert, and M. B. Orger. "Whole-brain activity maps reveal stereotyped, distributed networks for visuomotor behavior." In: *Neuron* 81 (2014), pp. 1328–1343.

[62] R. Portugues and F. Engert. "The neural basis of visual behaviors in the larval zebrafish." In: (2009), pp. 644–647.

[63] A. Muto, M. B. Orger, A. M. Wehman, M. C. Smear, J. N. Kay, P. S. Page-McCaw, E. Gahtan, T. Xiao, L. M. Nevin, N. J. Gosse, W. Staub, K. Finger-Baier, and H. Baier. "Forward genetic analysis of visual behavior in zebrafish." In: *PLoS Genetics* 1 (2005), pp. 575–588.

[64] M. B. Orger, M. C. Smear, S. M. Anstis, and H. Baier. "Perception of Fourier and non-Fourier motion by larval zebrafish." In: *Nature Neuroscience* 3 (2000), pp. 1128–1133.

[65] K. E. Severi, R. Portugues, J. C. Marques, D. M. O'Malley, M. B. Orger, and F. Engert. "Neural Control and Modulation of Swimming Speed in the Larval Zebrafish." In: *Neuron* 83 (2014), pp. 692–707.

[66] R. Portugues and F. Engert. "Adaptive Locomotor Behavior in Larval Zebrafish." In: *Frontiers in Systems Neuroscience* 5 (2011), pp. 1–11.

[67] M. B. Orger, A. R. Kampff, K. E. Severi, J. H. Bollmann, and F. Engert. "Control of visually guided behavior by distinct populations of spinal projection neurons." In: *Nature neuroscience* 11.3 (2008), p. 327.

[68] E. A. Naumann, J. E. Fitzgerald, T. W. Dunn, J. Rihel, H. Sompolinsky, and F. Engert. "From Whole-Brain Data to Functional Circuit Models : The Zebrafish Optomotor Response." In: *Cell* 167 (2016), 947–947.e20.

[69] M. A. Borla, B. Palecek, S. Budick, and D. M. O'Malley. "Prey capture by larval zebrafish: Evidence for fine axial motor control." In: *Brain, Behavior and Evolution* 60 (2002), pp. 207–229.

[70] M. B. McElligott and D. M. O'Malley. "Prey tracking by larval zebrafish: Axial kinematics and visual control." In: *Brain, Behavior and Evolution* 66 (2005), pp. 177–196.

[71] I. H. Bianco, A. R. Kampff, and F. Engert. "Prey Capture Behavior Evoked by Simple Visual Stimuli in Larval Zebrafish." In: *Frontiers in Systems Neuroscience* 5 (2011), pp. 1–13.

[72] J. L. Semmelhack, J. C. Donovan, T. R. Thiele, E. Kuehn, E. Laurell, and H. Baier. "A dedicated visual pathway for prey detection in larval zebrafish." In: *eLife* 3 (2014), pp. 1–19.

[73] R. E. Westphal and D. M. O'Malley. "Fusion of locomotor maneuvers, and improving sensory capabilities, give rise to the flexible homing strikes of juvenile zebrafish." In: *Frontiers in Neural Circuits* 7 (2013).

[74] E. Gahtan, P. Tanger, and H. Baier. "Visual prey capture in larval zebrafish is controlled by identified reticulospinal neurons downstream of the tectum." In: *Journal of Neuroscience* 25.40 (2005), pp. 9294–9303.

[75] I. Temizer, J. C. Donovan, H. Baier, and J. L. Semmelhack. "A Visual Pathway for Looming-Evoked Escape in Larval Zebrafish." In: *Current Biology* 25 (2015), pp. 1823–1834.

[76] T. W. Dunn, C. Gebhardt, E. A. Naumann, C. Riegler, M. B. Ahrens, F. Engert, and F. Del Bene. "Neural Circuits Underlying Visually Evoked Escapes in Larval Zebrafish." In: *Neuron* 89 (2016), pp. 613–628.

[77] Y. Yao, X. Li, B. Zhang, C. Yin, Y. Liu, W. Chen, S. Zeng, and J. Du. "Visual Cue-Discriminative Dopaminergic Control of Visuomotor Transformation and Behavior Selection." In: *Neuron* 89 (2016), pp. 598–612.

[78] K. Bhattacharyya, D. L. McLean, and M. A. MacIver. "Visual Threat Assessment and Reticulospinal Encoding of Calibrated Responses in Larval Zebrafish." In: *Current Biology* 27 (2017), 2751–2762.e6.

[79] J. C. Marques, S. Lackner, R. Félix, and M. B. Orger. "Structure of the Zebrafish Locomotor Repertoire Revealed with Unsupervised Behavioral Clustering." In: *Current Biology* 28 (2018), pp. 181–195.

[80] S. A. Romano, T. Pietri, V. Pérez-Schuster, A. Jouary, M. Haudrechy, and G. Sumbre. "Spontaneous Neuronal Network Dynamics Reveal Circuit's Functional Adaptations for Behavior." In: *Neuron* 85 (2015), pp. 1070–1085.

[81] R. R. Buss and P. Drapeau. "Synaptic drive to motoneurons during fictive swimming in the developing zebrafish." In: *Journal of Neurophysiology* 86 (2001), pp. 197–210.

[82] T. W. Dunn, Y. Mu, S. Narayan, O. Randlett, E. A. Naumann, C. T. Yang, A. F. Schier, J. Freeman, F. Engert, and M. B. Ahrens. "Brain-wide mapping of neural activity controlling zebrafish exploratory locomotion." In: *eLife* 5 (2016), pp. 1–29.

[83] O. Mirat, J. R. Sternberg, K. E. Severi, and C. Wyart. "ZebraZoom: An automated program for high-throughput behavioral analysis and categorization." In: *Frontiers in Neural Circuits* 7 (2013), pp. 1–12.

[84] A. M. Lambert, J. L. Bonkowsky, and M. A. Masino. "The conserved dopaminergic diencephalospinal tract mediates vertebrate locomotor development in zebrafish larvae." In: *Journal of Neuroscience* 32 (2012), pp. 13488–13500.

[85] S. Budick and D. O'Malley. "Locomotor repertoire of the larval zebrafish: swimming, turning and prey capture." In: *The Journal of experimental biology* 203 (2000), pp. 2565–79.

[86] A. M. Fernandes, K. Fero, A. B. Arrenberg, S. A. Bergeron, W. Driever, and H. A. Burgess. "Deep brain photoreceptors control light-seeking behavior in zebrafish larvae." In: *Current Biology* 22 (2012), pp. 2042–2047.

[87] D. M. O'Malley, Y. H. Kao, and J. R. Fetcho. "Imaging the functional organization of zebrafish hindbrain segments during escape behaviors." In: *Neuron* 17 (1996), pp. 1145–1155.

[88] H. A. Burgess and M. Granato. "Sensorimotor gating in larval zebrafish." In: *Journal of Neuroscience* 27 (2007), pp. 4984–4994.

[89] F. Fang. "Phylogenetic Analysis of the Asian Cyprinid Genus Danio (Teleostei, Cyprinidae)." In: *Copeia* 2003 (2003), pp. 714–728.

[90] K. L. Tang, M. K. Agnew, M. V. Hirt, T. Sado, L. M. Schneider, J. Freyhof, Z. Sulaiman, E. Swartz, C. Vidthayanon, M. Miya, K. Saitoh, A. M. Simons, R. M. Wood, and R. L. Mayden. "Systematics of the subfamily Danioninae (Teleostei: Cypriniformes: Cyprinidae)." In: *Molecular Phylogenetics and Evolution* 57 (2010), pp. 189–214.

[91] S. O. Kullander, M. M. Rahman, M. Norén, and A. R. Mollah. "Devario in Bangladesh: Species diversity, sibling species, and introgression within danionin cyprinids (Teleostei: Cyprinidae: Danioninae)." In: *PLoS ONE* 12 (2017).

[92] S. Dey, S. M. Kharbuli, R. Chakraborty, S. P. Bhattacharyya, and U. C. Goswami. "Toxic effect of environmental acid-stress on the sperm of a hill-stream fish devario aequipinnatus: A scanning electron microscopic evaluation." In: *Microscopy Research and Technique* 72 (2009), pp. 76–78.

[93] Z. Lele and P. Krone. "The zebrafish as a model system in developmental, toxicological and transgenic research." In: *Biotechnology Advances* 14 (1996), pp. 57 –72.

[94] L. M. De Jesus-Silva, P. V. De Oliveira, C. Da Silva Ribeiro, A. Ninhaus-Silveira, and R. Veríssimo-Silveira. "Ovarian cycle in Devario aequipinnatus with emphasis on oogenesis." In: *Zygote* 26 (2018), pp. 168–176.

[95] C. Prakash, M. P. Singh Kohli, A. M. Kiran Dube, B. Rani, S. Dam Roy, K. D. Raju, and N. A. Pawar. "Studies on captive breeding and larval rearing of Danio aequipinnatus (McClelland, 1839)." In: *Indian Journal of Animal Research* 48 (2014), pp. 379–383.

[96] S Dey, S. N. Rananujam, and B. K. Mahapatra. "Breeding and development of ornamental hill stream fish Devario aequipinnatus (McClelland) in captivity." In: *International Journal of Fisheries and Aquatic Studies* 1 (2014), pp. 01–07.

[97] B. S. Vorbach, H. Chandasana, H. Derendorf, and R. P. Yanong. "Pharmacokinetics of Oxytetracycline in the Giant Danio (Devario aequipinnatus) following bath immersion." In: *Aquaculture* 498 (2019), pp. 12–16.

[98] B. Govindasamy, D. Paramasivam, A. Dilipkumar, K. R. Ramalingam, K. Chinnaperumal, and P. Pachiappan. "Multipurpose efficacy of the lyophilized cell-free supernatant of Salmonella bongori isolated from the freshwater fish, Devario aequipinnatus: toxicity against microbial pathogens and mosquito vectors." In: *Environmental Science and Pollution Research* 25.29 (2018), pp. 29162–29180.

[99] S. Arumugam and S. Ramaiah. "Concentrations of toxic metals (Pb, Cd, Cr) in the tissues and their effects on diversification of Devario aequipinnatus populations." In: *International Journal of Environmental Health Research* 28 (2018), pp. 379–390.

[100] A. R. Grubh and K. O. Winemiller. "Spatiotemporal variation in wetland fish assemblages in the Western Ghats region of India." In: *Knowledge & Management of Aquatic Ecosystems* 419 (2018), p. 35.

[101] O. Shifatu, S. Glasshagel, P. Patel, H. Nelson, W. Tomamichel, C. Higginbotham, and P. J. Lafontant. "Ventricular Growth and Coronary Vessel Development in the Giant Danio (Devario Aequipinnatus) Heart." In: *The FASEB Journal* 31 (2017), pp. 586.13–586.13.

[102] Y. Huang and D. M. Umulis. "Scale invariance of BMP signaling gradients in zebrafish." In: *Scientific reports* 9.1 (2019), p. 5440.

[103] A Dey, H Choudhury, S Basumatary, R. Bharali, and D Sarma. "Length–weight relationships of three freshwater fish species from the Kameng River (Brahmaputra basin) in Arunachal Pradesh, northeast India." In: *Journal of applied ichthyology* 34.4 (2018), pp. 1002–1003.

[104] P. J. Mekdara, M. A. B. Schwalbe, L. L. Coughlin, and E. D. Tytell. "The effects of lateral line ablation and regeneration in schooling giant danios." In: *The Journal of Experimental Biology* (2018), jeb.175166.

[105] K. Y. Wong, A. R. Adolph, and J. E. Dowling. "Retinal bipolar cell input mechanisms in giant danio. I. Electroretinographic analysis." In: *Journal of Neurophysiology* 93 (2005), pp. 84–93.

[106] K. Y. Wong, E. D. Cohen, and J. E. Dowling. "Retinal bipolar cell input mechanisms in giant danio. II. Patch-clamp analysis of ON bipolar cells." In: *Journal of Neurophysiology* 93 (2005), pp. 94–107.

[107] K. Y. Wong and J. E. Dowling. "Retinal bipolar cell input mechanisms in giant danio. III. ON-OFF bipolar cells and their color-opponent mechanisms." In: *Journal of Neurophysiology* 94 (2005), pp. 265–272.

[108] J. L. Sanders, V. Watral, M. F. Stidworthy, and M. L. Kent. "Expansion of the Known Host Range of the Microsporidium, Pseudoloma neurophilia." In: *Zebrafish* 13 (2016), pp. 102–106.

[109] S. Martins, J. F. Monteiro, M. Vito, D. Weintraub, J. Almeida, and A. C. Certal. "Toward an Integrated Zebrafish Health Management Program Supporting Cancer and Neuroscience Research." In: *Zebrafish* 13 (2016), pp. 47–55.

[110] L.-H. Ma, B. Punnamoottil, S. Rinkwitz, and R. Baker. "Mosaic hoxb4a neuronal pleiotropism in zebrafish caudal hindbrain." In: *PloS one* 4.6 (2009), e5944.

[111] R. Lu, W. Sun, Y. Liang, A. Kerlin, J. Bierfeld, J. D. Seelig, D. E. Wilson, B. Scholl, B. Mohar, M. Tanimoto, M. Koyama, D. Fitzpatrick, M. B. Orger, and N. Ji. "Video-rate volumetric functional imaging of the brain at synaptic resolution." In: *Nature Neuroscience* 20 (2017), pp. 620–628.

[112] K. Turner, T. Bracewell, and T. Hawkins. "Anatomical Dissection of Zebrafish Brain Development." In: *The Neurobiology of Brain and Behavioral Development* 1082 (2014), pp. 3–27.

[113] O. Randlett, C. L. Wee, E. A. Naumann, O. Nnaemeka, D. Schoppik, J. E. Fitzgerald, R. Portugues, A. M. B. Lacoste, C. Riegler, F. Engert, and A. F. Schier. "Whole-brain activity mapping onto a zebrafish brain atlas." In: *Nature Methods* 12 (2015), pp. 1039–1046.

[114] J. Schindelin, I. Arganda-Carreras, E. Frise, V. Kaynig, M. Longair, T. Pietzsch, S. Preibisch, C. Rueden, S. Saalfeld, B. Schmid, J.-Y. Tinevez, D. White, V. Hartenstein, K. Eliceiri, P. Tomancak, and A. Cardona. "Fiji: an open-source platform for biological-image analysis." In: *Nature methods* 9.7 (2012), p. 676.

[115] S. Preibisch, S. Saalfeld, and P. Tomancak. "Globally optimal stitching of tiled 3D microscopic image acquisitions." In: *Bioinformatics* 25.11 (2009), pp. 1463–1465.

[116] G. D. Marquart, K. M. Tabor, E. J. Horstick, M. Brown, A. K. Geoca, N. F. Polys, D. D. Nogare, and H. A. Burgess. "High-precision registration between zebrafish brain atlases using symmetric diffeomorphic normalization." In: *GigaScience* 6 (2017), pp. 1–15.

[117] C. B. Kimmel, S. L. Powell, and K. M. Walter. "Brain Neurons Which Project to the Spinal Cord in Larvae of Zebrafish." In: *Soc. Neurosci.* 6 (1982), p. 628.

[118] C. B. Kimmel, W. K. Metcalfe, and E. Schabtach. "T reticular interneurons: A class of serially repeating cells in the zebrafish hindbrain." In: *Journal of Comparative Neurology* 233 (1985), pp. 365–376.

[119] W. K. Metcalfe, B Mendelson, and C. B. Kimmel. "Segmental Homologies Among Reticulospinal Neurons in the Hindbrain of the Zebrafish Larvae." In: *Journal of Comparative Neurology* 6517 (1986), pp. 147–159.

[120] I. H. Bianco, L. H. Ma, D. Schoppik, D. N. Robson, M. B. Orger, J. C. Beck, J. M. Li, A. F. Schier, F. Engert, and R. Baker. "The tangential nucleus controls a gravito-inertial vestibulo-ocular reflex." In: *Current Biology* 22 (2012), pp. 1285–1295.

[121] L.-H. Ma, C. L. Grove, and R. Baker. "Development of oculomotor circuitry independent of hox3 genes." In: *Nature Communications* 5 (2014), pp. 1–12.

[122] C. B. Kimmel. "Reticulospinal and Vestibulospinal Neurons in the Young Larva of a Teleost Fish, Brachydanio rerio." In: *Progress in Brain Research* 57 (1982), pp. 1–23.

[123] R. C. Eaton, R. D. Farley, C. B. Kimmel, and E. Schabtach. "Functional development in the mauthner cell system of embryos and larvae of the zebra fish." In: *Journal of Neurobiology* 8 (1977), pp. 151–172.

[124] D. A. Prober, S. Zimmerman, B. R. Myers, B. M. McDermott, S. H. Kim, S. Caron, J. Rihel, L. Solnica-Krezel, D. Julius, A. J. Hudspeth, and A. F. Schier. "Zebrafish TRPA1 channels are required for chemosensation but not for thermosensation or mechanosensory hair cell function." In: *Journal of Neuroscience* 28 (2008), pp. 10102–10110.

[125] Y. C. Liu, I. Bailey, and M. E. Hale. "Alternative startle motor patterns and behaviors in the larval zebrafish (Danio rerio)." In: *Journal of Comparative Physiology A: Neuroethology, Sensory, Neural, and Behavioral Physiology* 198 (2012), pp. 11–24.

[126] C. Senay, D. Boisclair, and P. R. Peres-Neto. "Habitat-based polymorphism is common in stream fishes." In: *Journal of Animal Ecology* 84 (2015), pp. 219–227.

[127] D. P. Swain and L. B. Holtby. "Differences in morphology and behavior between juvenile coho salmon (Oncorhynchus kisutch) rearing in a lake and in its tributary stream." In: *Canadian Journal of Fisheries and Aquatic Sciences* 46.8 (1989), pp. 1406–1414.

[128] Q. Bone and R. Moore. *Biology of fishes*. Taylor & Francis, 2008.

[129] E. Gahtan and D. M. O'Malley. "Visually guided injection of identified reticulospinal neurons in Zebrafish: A survey of spinal arborization patterns." In: *Journal of Comparative Neurology* 459 (2003), pp. 186–200.

[130] C. Rovainen. "Physiological and anatomical studies on large neurons of central nervous system of the sea lamprey (Petromyzon marinus). I. Müller and Mauthner cells." In: *Journal of Neurophysiology* 30.5 (1967), pp. 1000–1023.

[131] C. M. Rovainen. "Müller cells,"Mauthner" cells, and other identified reticulospinal neurons in the lamprey." In: *Neurobiology of the Mauthner cell* (1978), pp. 245–269.

[132] R. Keynes. "J.Z. AND THE DISCOVERY OF SQUID GIANT NERVE FIBRES." In: *Journal of Experimental Biology* 208 (2005), 179 LP –180.

[133] J. A. Perge, J. E. Niven, E. Mugnaini, V. Balasubramanian, and P. Sterling. "Why do axons differ in caliber?" In: *Journal of Neuroscience* 32 (2012), pp. 626–638.

[134] J.-W. P. Kremers and R. Nieuwenhuys. "Topological analysis of the brain stem of the crossopterygian fish Latimeria chalumnae." In: *Journal of Comparative Neurology* 187.3 (1979), pp. 613–637.

[135] I. Rock and D. Smith. "The optomotor response and induced motion of the self." In: *Perception* 15 (1986), pp. 497–502.

[136] H. Maaswinkel and L. Li. "Spatio-temporal frequency characteristics of the optomotor response in zebrafish." In: *Vision research* 43.1 (2003), pp. 21–30.

[137] S. C. Neuhauss, O. Biehlmaier, M. W. Seeliger, T. Das, K. Kohler, W. A. Harris, and H. Baier. "Genetic disorders of vision revealed by a behavioral screen of 400 essential loci in zebrafish." In: *Journal of Neuroscience* 19.19 (1999), pp. 8603–8615.

[138] J. M. Koolhaas, S. M. Korte, S. F. De Boer, B. J. Van Der Vegt, C. G. Van Reenen, H. Hopster, I. C. De Jong, M. A. Ruis, and H. J. Blokhuis. "Coping styles in animals: Current status in behavior and stress- physiology." In: *Neuroscience and Biobehavioral Reviews* 23 (1999), pp. 925–935.

[139] A. S. Andalman, V. M. Burns, M. Lovett-Barron, M. Broxton, B. Poole, S. J. Yang, L. Grosenick, T. N. Lerner, R. Chen, T. Benster, P. Mourrain, M. Levoy, K. Rajan, and K. Deisseroth. "Neuronal Dynamics Regulating Brain and Behavioral State Transitions." In: *Cell* (2019), pp. 1–16.

[140] E. Fontaine, D. Lentink, S. Kranenbarg, U. K. Müller, J. L. Van Leeuwen, A. H. Barr, and J. W. Burdick. "Automated visual tracking for studying the ontogeny of zebrafish swimming." In: *Journal of Experimental Biology* 211 (2008), pp. 1305–1316.

[141] P. Munk and T Kiorboe. "Feeding behaviour and swimming activity of larval herring(Clupea harengus) in relation to density of copepod nauplii." In: *Marine ecology progress series* 24.1 (1985), pp. 15–21.

[142] R. Batty, J. Blaxter, and Q Bone. "The effect of temperature on the swimming of a teleost (Clupea harengus) and an ascidian larva (Dendrodoa grossularia)." In: *Comparative Biochemistry and Physiology Part A: Physiology* 100.2 (1991), pp. 297–300.

[143] D. Coughlin, J. Strickler, and B Sanderson. "Swimming and search behaviour in clownfish, Amphiprion perideraion, larvae." In: *Animal Behaviour* 44 (1992), pp. 427–440.

[144] M. Drost, J. Osse, and M Muller. "Prey capture by fish larvae, waterflow patterns and the effect of escape movements of prey." In: *Netherlands journal of zoology* 38.1 (1988), pp. 23–45.

[145] I. H. Bianco and F. Engert. "Visuomotor transformations underlying hunting behavior in zebrafish." In: *Current Biology* 25 (2015), pp. 831–846.

[146] P. Antinucci, M. Folgueira, and I. H. Bianco. "A pretectal command system controls hunting behaviour." In: *bioRxiv* (2019), p. 637215.

[147] L. Hernandez. "Intraspecific scaling of feeding mechanics in an ontogenetic series of zebrafish, Danio rerio." In: *Journal of Experimental Biology* 203.19 (2000), pp. 3033–3043.

[148] D. A. Dombeck and M. B. Reiser. "Real neuroscience in virtual worlds." In: *Current Opinion in Neurobiology* 22 (2012), pp. 3–10.

[149] Y. Kimura, C. Satou, S. Fujioka, W. Shoji, K. Umeda, T. Ishizuka, H. Yawo, and S. I. Higashijima. "Hindbrain V2a neurons in the excitation of spinal locomotor circuits during zebrafish swimming." In: *Current Biology* 23 (2013), pp. 843–849.

[150] C. E. Feierstein, R. Portugues, and M. B. Orger. "Seeing the whole picture: A comprehensive imaging approach to functional mapping of circuits in behaving zebrafish." In: *Neuroscience* 296 (2015), pp. 26–38.

[151] C. A. Trivedi and J. H. Bollmann. "Visually driven chaining of elementary swim patterns into a goal-directed motor sequence: A virtual reality study of zebrafish prey capture." In: *Frontiers in Neural Circuits* 7 (2013), pp. 1–18.

[152] A. Jouary, M. Haudrechy, R. Candelier, and G. Sumbre. "OPEN A 2D virtual reality system for visual goal-driven navigation in zebrafish larvae." In: *Nature Publishing Group* (2016), pp. 1–13.

[153] Y. Mu, D. V. Bennett, M. Rubinov, S. Narayan, C. T. Yang, M. Tanimoto, B. D. Mensh, L. L. Looger, and M. B. Ahrens. "Glia Accumulate Evidence that Actions Are Futile and Suppress Unsuccessful Behavior." In: *Cell* 178 (2019), 27–43.e19.

[154] T. Yu, J. Zhu, Y. Li, Y. Ma, J. Wang, X. Cheng, S. Jin, Q. Sun, X. Li, H. Gong, et al. "RTF: a rapid and versatile tissue optical clearing method." In: *Scientific reports* 8.1 (2018), p. 1964.

Annex I

I.1 Supplementary figures

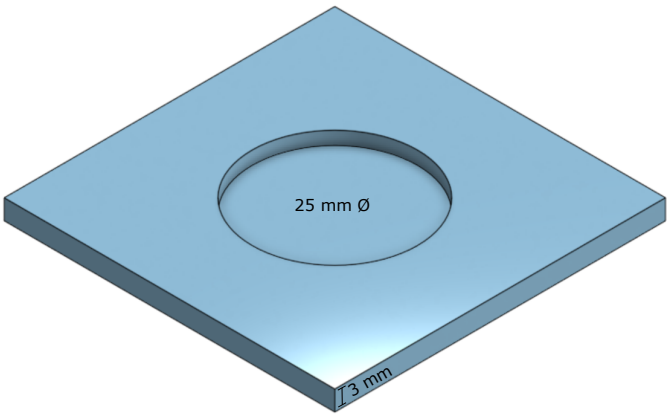

Figure I.1: Custom-made acrylic transparent circular arena with a 25 mm diameter and 2 mm depth used for taking pictures for measurements of Giant Danio and Zebrafish larvae.

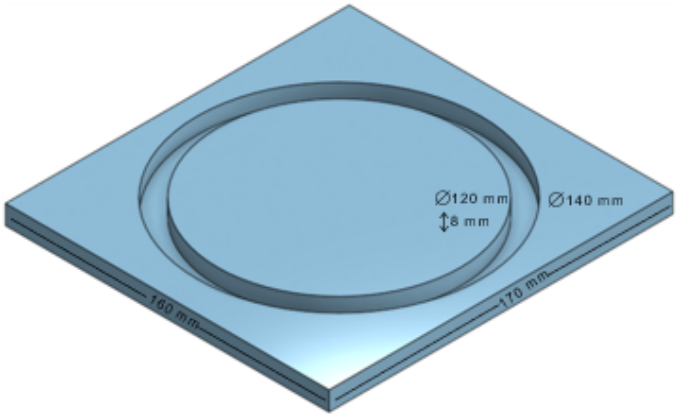

Figure I.2: Custom-made circular acrylic arena, used during the circular OMR experiments, consisting of a 10 mm wide circular track that had a 140 mm outer diameter, 120 mm inner diameter and 8 mm depth

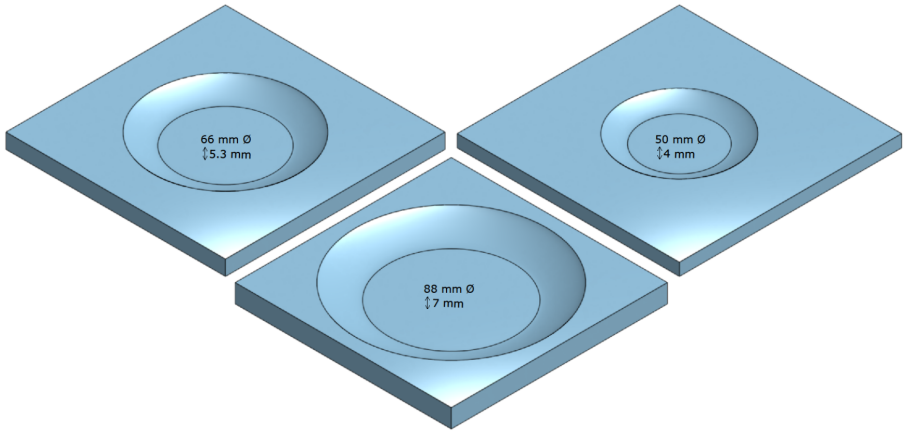

Figure I.3: Custom-made concave arenas used during behaviral experiments in the high-resolution behavioral set-up. The arena's dimensions were proportionally increased to use with larvae, of both Giant Danio and Zebrafish, in different developmental stages. There are three different arenas: a 50 mm diameter arena with a 4 mm depth; a 66 mm diameter arena with a 5.3 mm depth; and a 88 mm diameter arena with a 7 mm depth.

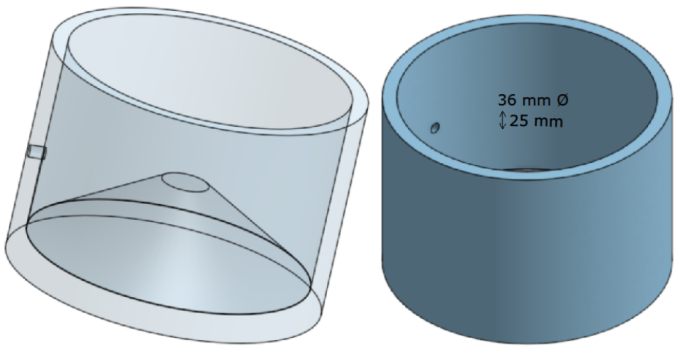

Figure I.4: Custom-made acrylic cylindrical arena with a 36 mm diameter and a 25 mm depth, used during the Head-Restrained Closed Loop Virtual Reality Optomotor Response assay experiments. A Sylgard cone is inserted inside the arena, and larvae are embedded on top of the cone. Left: Arena with sylgard cone inside ; Right: Schematic of the cylindrical arena.

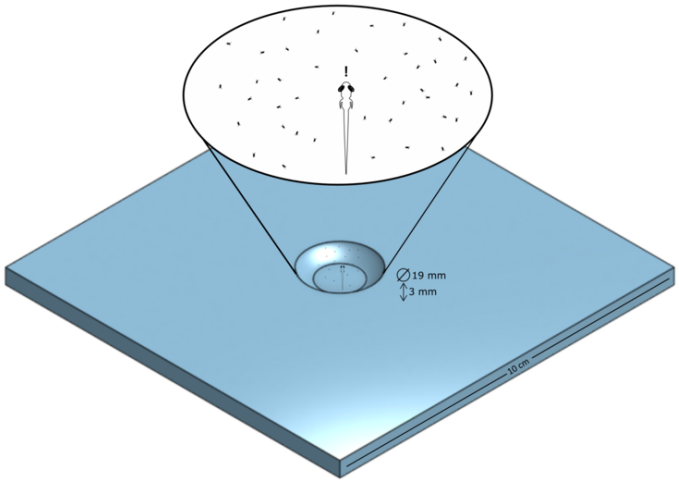

Figure I.5: Custom-made 19 mm diameter 3 mm deep acrylic concave arena used during the Prey Capture assay experiments. Inlet: Schematic representation of a larva and the rotifers inside the arena.

I.2 Suplementary Code

```
Algorithm Growth_Measurements (figures) is
    for i = youngest age to oldest age
        folder1 = folder where the ages are separated
        for k = number of figures in each age folder
            img = select image from folder
            binary_img = binarize (img) to find arena contours
            binary_img2 = find arena (binary_img) image
            stats = measure major and minor axis length of the arena (
                ↪ binary_img2) image
            center = find center of the arena (binary_img2) image
            radius = get the radius of the arena (binary_img2) image
            arenasize_diameter = measure major axis length in pixels of the
                ↪  arena (binary_img2)
            mask = create a mask around the circle of the arena
            Entropy = find pixel intensity variation (img) to find fish
            Binary_Img = binarize (Entropy) with (0.7) pixel selection
                ↪ threshold
            Binary_Img2 = extract fish from (Binary_Img)
            stats = measure major axis length of fish (Binary_Img2) in
                ↪ pixels
            calculated_size = (stats) of major axis length
            size_pixtomicrons = ((calculated_size * number of microns) /
                ↪ arenasize_diameter)
        end
    end
```

Figure I.6: Custom MATLAB script used for image analysis and total length measurements of Giant Danio and Zebrafish larvae.

Annex II

II.1 Current outcomes of the work presented

Poster and Oral Communication: Zebrafish Husbandry Workshop - Aquaculture 2019, New Orleans, USA

Date and Venue: 8-9 of March of 2019, New Orleans, USA

Title: Giant Danio: A Promising New Model for Neuroscience.

Authors: Ana Catarina Certal, Raquel Tomás, Sandra Martins, **Pedro Silva**, Adrien Jouary, Michael Orger

Affilitation: Champalimaud Center for the Unknown, Lisbon, Portugal

Abstract: Comparative biology allows us to understand what aspects of an animal's locomotor repertoire represent general features of motor organization, versus specialized adaptations for its anatomy and ecological niche.

Here we introduce the Giant Danio (*Devarius aequipinnatus*) as an emerging model for comparative studies with Zebrafish, a well-established animal model in neuroscience. We will present the husbandry and breeding optimization for this species in a laboratory setting and investigate the growth rate of Giant Danio, and the ontogeny of swimming behaviors, including the optomotor response (OMR), in larvae over several days of development. Compared with Zebrafish larvae, the Giant Danio larvae display faster growth and development. While both species show a clear OMR, starting around 5 days post fertilization, the behavior appears to be more consistent and reliably evoked in Giant Danio,

with larvae tracking gratings for longer periods, presenting shorter interbout intervals, and able to track motion at higher speeds.

With a faster development, combined with larger neurons that facilitate physiological studies, and variations in innate behaviors compared with Zebrafish, Giant Danio is a promising model for comparative behavioral neuroscience.

Poster Communication: Edin Fish Tech 2019, Royal College of Physicians of Edinburgh, Edinburgh

Date and Venue: 28-30 of August of 2019, Edinburgh

Title: Comparative analysis of the locomotor repertoire and descending motor system anatomy of larval fish

Authors: Pedro Silva, Adrien Jouary, Michael Orger

Affilitation: Champalimaud Center for the Unknown, Lisbon, Portugal

Abstract: A major challenge for comparative biology is understanding what aspects of an animal locomotor repertoire represent general features of motor organization, versus specialized adaptations for its anatomy and ecological niche. We have investigated the Giant Danio (*Devarius aequipinnatus*) as a potential model for comparative studies with Zebrafish, a well-established animal model in neuroscience. We investigate the locomotor repertoire and how its differences are reflected in the underlying neural circuit structure. First, we compared visually guided behaviours in Giant Danio to different Zebrafish strains. Giant Danio show a stronger optomotor response than Tübingen strain zebrafish. The optomotor response first appears around 4 days post fertilization and can be consistently and reliably evoked. During optomotor tracking Giant Danio show shorter interbout intervals and are able to track motion at higher speeds than zebrafish larvae of the same size. We also observed that the higher manoeuvrability of Giant Danio was also reflected during prey capture. Interestingly, Zebrafish strains derived from more recently wild-caught fish showed more robust optomotor behaviour, closer to Giant Danio. Second, we are currently comparing the anatomy of the descending pathways controlling locomotion in both species using retrograde labelling of reticulospinal neurons.

Combined with the potential for comparative approaches with Zebrafish, the faster development, larger neurons, and rich behavioural repertoire of Giant Danio make it a promising model for neuroscience.

Poster Communication: Edin Fish Tech 2019, Royal College of Physicians of Edinburgh, Edinburgh

Date and Venue: 28-30 of August of 2019, Edinburgh

Title: Giant Danio – Establishment of a New Model for Neuroscience

Authors: Sandra Martins, Mariana Sampaio, **Pedro Silva**, Adrien Jouary, Joana Monteiro, Michael Orger, Ana Catarina Certal

Affilitation: Champalimaud Center for the Unknown, Lisbon, Portugal

Abstract: Comparative biology allows us to understand what aspects of animals' locomotor repertoire represent general features of motor organization, versus specialized adaptations for its anatomy and ecological niche. Here we introduce the Giant Danio (*Devarius aequipinnatus*) as an emerging model for comparative studies with Zebrafish, a well-established animal model in neuroscience. We will present the husbandry optimization for this species in a laboratory setting, including water parameters, feeding, housing systems and breeding preferences.

We are also investigating the development and growth rate of Giant Danio, and the ontogeny of swimming behaviors, including the optomotor response (OMR), in larvae. Compared with Zebrafish larvae, the Giant Danio larvae display faster growth and development. While both species show a clear OMR, starting around 5 days post fertilization, the behavior appears to be more consistent and reliably evoked in Giant Danio, with larvae tracking gratings for longer periods, presenting shorter interbout intervals, and able to track motion at higher speeds. To help understanding the organization and function of the neural circuits underlying these visually guided behaviors, we are working on the generation of Giant Danio transgenic lines for assessing neuronal activity.

With a faster development, combined with larger neurons that facilitate physiological studies, and variations in innate behaviors compared with Zebrafish, Giant Danio is a promising model for comparative behavioral neuroscience.

Poster Communication: 2nd CONGENTO Annual Meeting, Champalimaud Center for the Unknown, Lisbon, Portugal

Date and Venue: 21 of October of 2019, Lisbon

Title: Giant Danio – Establishment of a New Model for Neuroscience

Authors: Sandra Martins, Mariana Sampaio, **Pedro Silva**, Adrien Jouary, Joana Monteiro, Michael Orger, Ana Catarina Certal

Affilitation: Champalimaud Center for the Unknown, Lisbon, Portugal

Abstract: We introduce Giant Danio (*Devarius aequipinnatus*) as an emerging model for comparative studies with Zebrafish, a well-established animal model in neuroscience. Comparisons between both species will improve our understanding on which aspects of animals' locomotorrepertoire represent general features of motor organization and which are species-specific adaptations. We will present the husbandry optimization for this species in a laboratory setting, including water parameters, feeding, housing systems and breeding. We are also investigating the development and growth rate of Giant Danio, and the ontogeny of swimming behaviours, including the optomotor response (OMR), in larvae. Giant Danio larvae grow and develop faster than Zebrafish. While both species show a clear OMR, starting around 5 days post fertilization, the behaviour appears to be more consistent and reliably evoked in Giant Danio, with larvae tracking gratings for longer periods, presenting shorter interbout intervals, and able to track motion at higher speeds.

To help understanding the organization and function of the neural circuits underlying these visually guided behaviours, we are working on the generation of the firstGiant Danio transgenic lines, for assessing neuronal activity.